



# **Physical bone ablation: 'Will less be more?'**

Hendricus Nijland

## Colofon

Physical bone ablation: ‘will less be more?’  
PhD thesis, University of Groningen, the Netherlands.

Copyright © 2025 - Hendricus Nijland 2025

All rights reserved. No part of this publication may be reproduced or transmitted in any form or by any means without written permission of the author and the publisher holding respective copyrights of the published articles, if applicable.

Printing: Ridderprint | [www.ridderprint.nl](http://www.ridderprint.nl)





rijksuniversiteit  
 groningen

# **Physical bone ablation: ‘will less be more?’**

## **Proefschrift**

ter verkrijging van de graad van doctor aan de  
 Rijksuniversiteit Groningen  
 op gezag van de  
 rector magnificus prof. dr. ir. J.M.A. Scherpen  
 en volgens besluit van het College voor Promoties.

door

**Hendricus Nijland**

geboren op 26 september 1992

**Promotores**

Prof. dr. P.C. Jutte

Dr. T.C. Kwee

**Beoordelingscommissie**

Prof. dr. R.A.J.O. Dierckx

Prof. dr. J.J. Fütterer

Prof. dr. S. Misra



# Contents

|                      |          |
|----------------------|----------|
| <b>Chapter 1</b>     | <b>9</b> |
| General introduction |          |

---

## **Part 1 – looking back**

### **How far are we in minimally invasive treatment?**

---

|  |           |
|--|-----------|
| <b>Chapter 2</b>   | <b>31</b> |
| Evaluation of accuracy and precision of CT-guidance in Radiofrequency Ablation for osteoid osteoma in 86 patients. |           |

|   |           |
|---|-----------|
| <b>Chapter 3</b>  | <b>51</b> |
| Radiofrequency Ablation for Atypical Cartilaginous Tumors is safe and effective: analysis of 189 consecutive cases. |           |

|  |           |
|--|-----------|
| <b>Chapter 4</b>   | <b>77</b> |
| Long-Term Halo Follow-Up Confirms Less Invasive Treatment of Low-Grade Cartilaginous Tumors with Radiofrequency Ablation to Be Safe and Effective. |           |

---

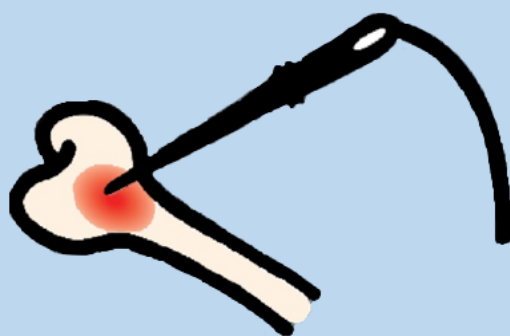
## **Part 2 – looking ahead**

### **Towards safe, reliable and effective treatment**

---

|  |            |
|--|------------|
| <b>Chapter 5</b>   | <b>95</b>  |
| Experiments on physical ablation of long bone using microwave ablation; defining optimal settings using ex- and in-vivo experiments. |            |
| <b>Chapter 6</b>   | <b>115</b> |
| Animal experiments show that minimally invasive microwave ablation of bone is not safe enough for clinical application.              |            |
| <b>Chapter 7</b>   | <b>131</b> |
| Mechanical bone strength decreases considerably after microwave ablation-ex-vivo and in-vivo analysis in sheep long bones.           |            |
| <b>Chapter 8</b>   | <b>153</b> |
| Safety assessment of microwave ablation in sheep vertebral bodies.   |            |
| <hr/>  |            |
| <b>Chapter 9</b>   | <b>171</b> |
| General discussion   |            |
| <b>Chapter 10</b>  | <b>185</b> |
| English summary  |            |
| Nederlandse samenvatting   |            |
| <b>Appendices</b>  | <b>195</b> |
| Dankwoord  |            |
| List of lectures   |            |
| Curriculum Vitae   |            |





# Chapter 1

General introduction

## **Introduction**

Orthopedic oncology is the medical field concerning cancer of the bone and the surrounding soft tissue. Bone sarcoma can be divided into primary and secondary tumors. Primary tumors originate from bone-derived cells; secondary tumors are metastases from other sites (1).

### **Primary bone tumors**

Primary bone cancer is a relatively rare type of cancer, accounting for less than 1% of the total amount of diagnosed cancers every year (2). The three main types of primary bone sarcomas are osteosarcoma, Ewing sarcoma and chondrosarcoma (figure 1-3). Osteosarcoma is the most common type. It typically occurs in children and young adults, with peak incidence at 10-14 years (2-4). Most cases of osteosarcoma originate around the knee (figure 4). Sometimes a typical sunburst periosteal reaction can be seen on radiography as a result of aggressive periosteal growth (figure 5) (4).

Ewing sarcoma (figure 6) is the most lethal type given its frequent tendency to metastasize (often within weeks after the onset of symptoms). It originates from the bone medulla and grows into the surrounding soft tissue (2,3). It typically occurs in teenagers (peak 15-19 years) and predominates in the pelvis, lower leg and shoulder. On radiography there is a typical aggressive appearance, often with permeative (moth-like) appearance or with periosteal reaction (5). Survival rates for both osteosarcoma and Ewing sarcoma are around 80% in case of no metastatic disease at presentation. When metastasized five-year survival drops to 20-30% (2,3).

The third type of primary bone cancer is chondrosarcoma. This type develops in the cartilage cells. Contrary to the other two types it

normally develops in middle-aged or older adults and has better survival rates (1). In radiography it can present with endosteal scalloping (focal resorption of the inner cortex) as a result of its slow growing (6). Chondrosarcoma can be divided into three grades based on histology combined with macroscopic imaging features. Grade-1 tumors (ACTs) and are usually asymptomatic (7). These tumors can show locally aggressive growth, but metastases are very uncommon. Prognosis of ACT is favorable, with 3-year overall survival of 96% and 5-year overall survival of 93%. Intermediate and high grade chondrosarcoma (grade 2-3) show more frequent metastases and have an overall 5-year survival of 79% (8).

The most common symptom in all three types of sarcoma is local pain, especially at night. Sometimes a growing lump or area of swelling is seen. In case of localization close to a joint a decreased range of motion may present (1-3).

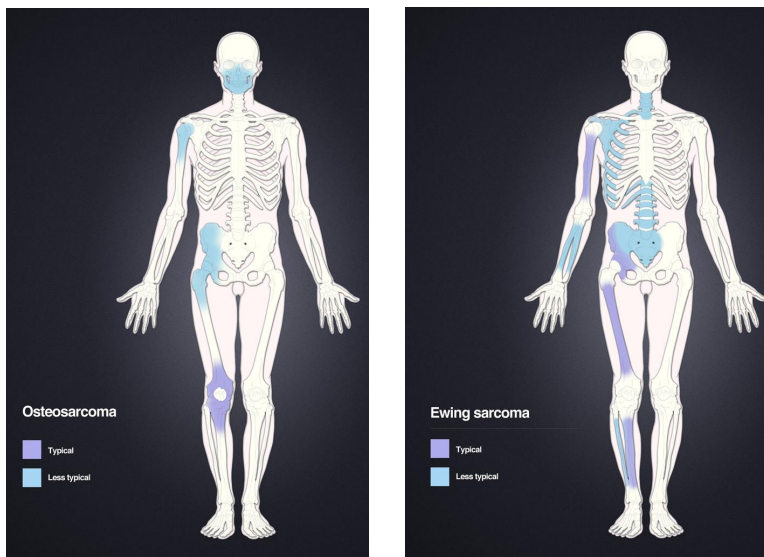


**Figure 1-2.** Preferred locations for osteosarcoma and Ewing sarcoma and chondrosarcoma (9-10)

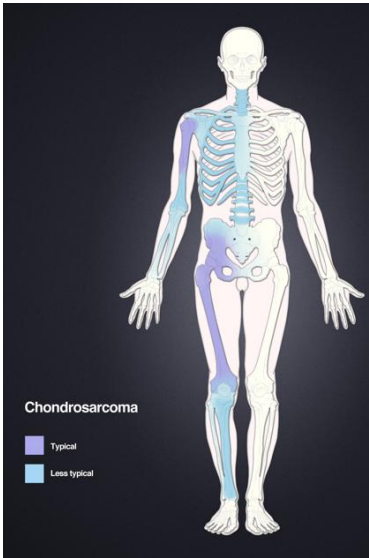


**Figure 3.** Preferred locations for chondrosarcoma (11)

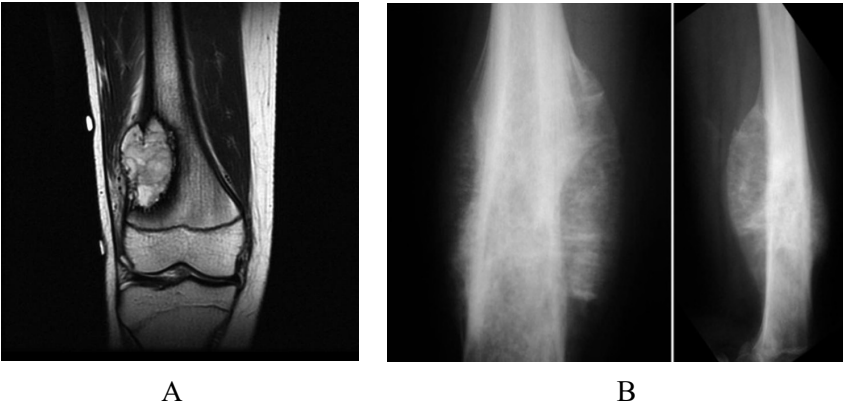


**Figure 4** A. Osteosarcoma of the distal femur (12) B. Sunburst periosteal reaction in fast growing osteosarcoma (13)





**Figure 5** *Ewing sarcoma of the right proximal tibia. A typical sharp transition zone can be seen. (14)*

## **Secondary bone tumors**

The secondary bone tumors comprise metastases from different primary tumors. Nearly all types of cancer can metastasize to the bone (15). However, breast- and prostate carcinoma are the most common types to lead to skeletal metastases. These tumors metastasize in up to 70% of cases. Primary locations of these metastases include the proximal part of the long bones, ribs, pelvis, skull and vertebrae, which is due to their high red marrow content (figure 6a). The main type metastatic spread of primary tumors into the bone is hematogenous. However, lymphatic spread is also seen (15-16). Direct extension of tumor into the bone, for instance with Pancoast tumors, is not considered metastatic disease (15).

Bone metastases can lead to both resorption and formation of new bone. In osteolytic metastases there is destruction of bone matrix and therefore an increased risk of pathologic fractures. In sclerotic metastases new bone is formed. This can be stromal bone (within the tumor tissue) or reactive bone formation. Clinical presentation can be

asymptomatic for a long time. The most frequently reported symptom is local bone pain. Furthermore, compression of adjacent structures (e.g. the spinal cord) and pathologic fractures have been reported. Skeletal metastases typically demonstrate a pattern of increased uptake (15).

When skeletal metastases are found, treatment typically is no longer aimed at cure. With multiple osseous metastases there is a shift towards palliative treatment.

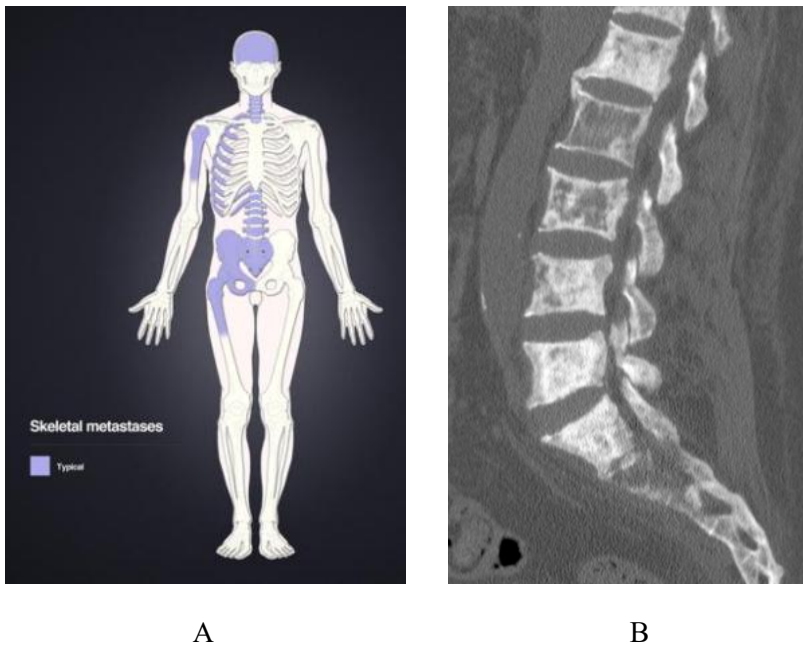


**Figure 6** A. Preferred locations of skeletal metastases (17) B. Skeletal metastases in lumbar spine (18).

## **Treatment**

Dependent on tumor characteristics (e.g. size, grade and location) either amputation or limb-salvage surgery can be performed (19). In case of osteosarcoma and Ewing sarcoma this is combined with radiation- and chemotherapy. Chondrosarcomas are relatively resistant to these forms of therapy. Examples of limb-salvage surgery are en-bloc resection followed by reconstruction and intralesional curettage followed by consolidation with a prophylactic plate (20-22). However, these forms of treatment are relatively invasive and come with a risk of complications including infection, non-union, pseudarthrosis, tumor recurrence and fractures (19-22). A minimally invasive approach could be a good alternative. With minimally invasive treatment expected functional outcome is better, especially when soft tissues, limbs and joints can be preserved. Furthermore, minimally invasive procedures come with higher patient satisfaction, lower complication risk, shorter hospitalization periods and only a short period of weight bearing restriction (23-25). In case of metastasized disease a minimally invasive approach could offer a low-impact treatment to counter symptoms like pain and thereby prevent immobilization.

### **Minimally invasive approach**

In recent years local tumor ablation has gained interest as a good and minimally invasive alternative to the classical surgical approaches described above. With these percutaneous forms of treatment, a tract is drilled towards a tumor based on CT guidance and a needle is brought up. Subsequently the tumor is thermally destroyed using either heat ( $>60^{\circ}\text{C}$ ) or cold ( $<-40^{\circ}\text{C}$ ) (26). The most common methods for local tumor ablation are radiofrequency ablation (RFA) and microwave ablation (MWA) (heat-based) and cryoablation (cold-based). In soft tissue, ablation is a generally accepted form of treatment, for instance for liver metastases (27-30). Use in bone tumors is promising, though application has mainly been limited to benign lesions and low-grade

cartilaginous tumors (especially ACT) (31-33). Literature on effectiveness and safety in ACT is limited, especially for larger tumors (25,34).

#### *Effect of hyperthermia on cells*

Effects of temperatures outside the normal homeostatic range of the body (36-42°C) at cell level mainly originate from membrane dysfunction (35). With increased temperature the fatty acid tails of phospholipids become less rigid and thereby allow more movement of proteins and other molecules into the cell. As a result permeability changes, allowing harmful molecules to enter the cell. With further increase of temperature proteins denature and the membrane melts, leading to necrosis and cell death. The area of dead cells is called the 'halo' (ablation area) and can be seen on MRI as an ellipse around the ablated tumor tissue (figure 7B). The elliptic line of the halo around the tumor consists of granulation tissue as a response to ablation. All tissue within this halo can be considered completely destroyed (31).

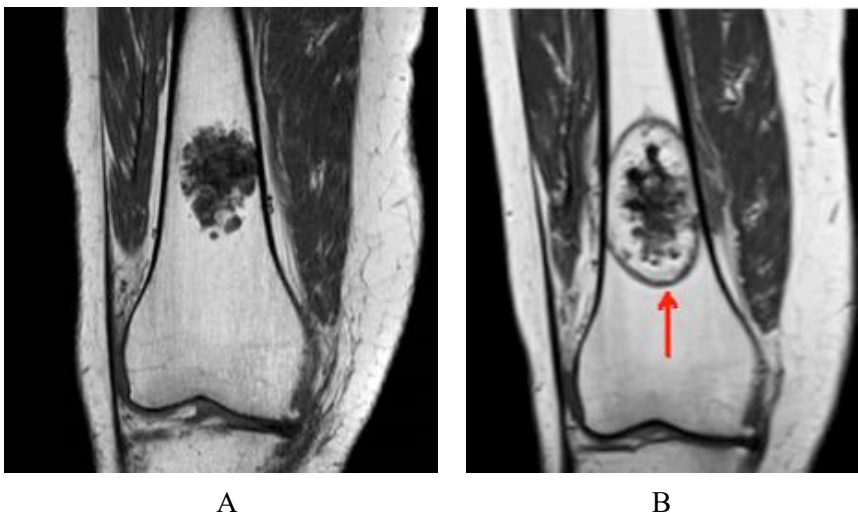


**Figure 7** *A. Atypical cartilaginous tumor before radiofrequency ablation. B. 3 months after radiofrequency ablation. The 'halo' is indicated by the arrow. All tissue within this halo is considered to be completely destroyed.*

Instant cell death occurs at temperatures over 60°C. Between 50-60°C it takes 1-6 minutes to reach complete cell death (36-39). To ensure complete ablation, a target temperature of >60°C should be reached up to the edge of the tumor. At temperatures >100°C vaporization of water (leading to desiccation of the cell) and carbonization occur, potentially limiting heat conduction (26,35,40). Therefore, the ideal ablation range is between 60-95°C. To ensure sufficient temperatures up to the tumor edge, target temperature at the tip of the needle is assumed to be 85-90°C. In figure 8, a model is shown depicting the tissue reaction to hyperthermia as described above.

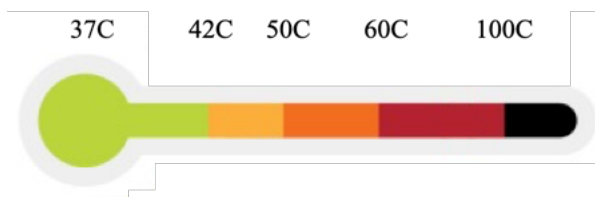


**Figure 8** *Tissue reaction to heat. Ideal temperature for ablation is 60-95°C since instant cell death is the aim. Above 100°C carbonization occurs, limiting distribution of heat.*

### *Radiofrequency ablation*

In RFA an electromagnetic current of 300-500 KHz is used. Heat is the result of molecular friction movements by ionic agitation caused by changes in current phase (41). With high temperatures coagulation necrosis occurs leading to (irreversible) cell death. RFA is already used for an array of indications in bone tumors (e.g. osteoid osteoma and atypical cartilaginous tumors).

### *Microwave ablation*

In MWA electromagnetic waves in the microwave energy spectrum (300MHz – 300GHz) are used. The principle of MWA is production of heat by means of dielectric hysteresis: polar molecules (especially H<sub>2</sub>O) continuously realign with an oscillating electric field, thereby

increasing kinetic energy leading to increased temperature and ultimately tissue necrosis due to apoptosis (42-43). From application in liver tissue it is known that the effect of MWA is harder to plan and control compared to RFA (42). In clinical use this potentially results in excessively large margins or incomplete ablation. Regardless of the above-mentioned limitations MWA is already widely used in treatment of liver, kidney, and lung tumors. Experience in bone tissue is still limited (44-47).

## **Procedure planning**

Based on the model in figure 8, a temperature of  $>60^{\circ}\text{C}$  is sufficient for instant cell death. To ensure complete ablation with a small margin we need to examine the heat distribution for different ablation settings. When the required settings to reach temperatures  $>60^{\circ}\text{C}$  at different distances are known, more accurate procedure planning can be performed. Other factors to account for are heat sink (thermal flow from areas with high temperature towards areas with lower temperature, e.g. fluid- or air containing bodies) and tissue impedance. They potentially lead to lower temperatures than aimed for. MWA is hypothesized to be less susceptible to effects of heat sink and tissue impedance due to its higher heat intensity (42,43,48,49).

With regard to the possibility of incomplete ablations, planning a procedure with small margins is a risk. However, using larger margins increases the risk of damage to nerves, cartilage and skin. Literature on the plannability and predictability of minimally invasive treatments is still very limited. This needs to be expounded first before being able to perform effective and safe ablations.

### *Safety of surrounding structures*

Since the extent of heat distribution is unknown, there is a risk of damage to fragile structures like the spinal cord, vessels and nerve roots. In literature an insulating effect of cortical bone protecting extra-osseous structures against high temperatures has been described (cortical insulation), however its exact degree of protection is unknown (44,50-54). Wallace et al. compared spinal cord histology after RFA, MWA and cryoablation. In MWA and cryoablation they described white matter necrosis in the spinal cord (52).

According to clinical experience in long bone, the expected halo will be elliptical around the active part of the needle as illustrated in figure 9a and 9b. The part of the halo closest to the ablation needle is the result of electrical current from the needle into the tissue (depicted as green waves in figure 9a) (55). The remnant of the halo results from thermal conduction through the tissue. In figure 9b and 9c an ablation close to the cortex of a vertebral body is depicted. In case of no cortical insulation the halo reaches to the spinal canal (figure 9b), while cortical insulation potentially protects the spinal canal (figure 9c).

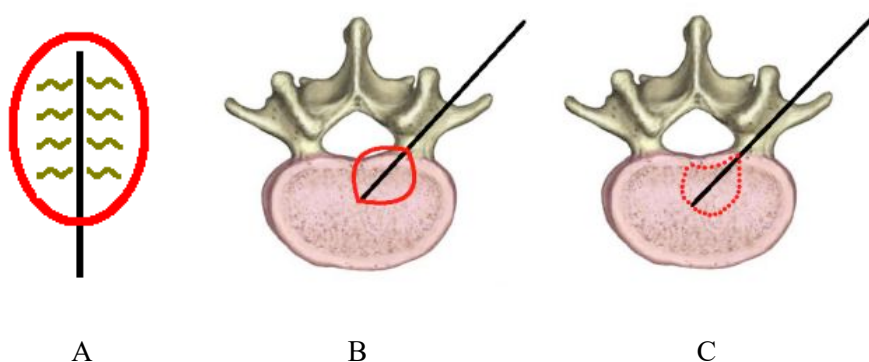


**Figure 9** *Illustration of expected ablation halo shape. A. Distribution of electrical current from the needle into the tissue. B. Elliptical halo as expected without cortical insulation. C. Halo with an estimation of the effect of cortical insulation.*

## **Basis for this thesis and key concepts**

Given the low incidence of primary bone tumors and the fact that minimally invasive treatment options are still limited and infrequently studied, there is insufficient knowledge to expand the technique to a larger scale and wider range of indications. Diagnosis of bone tumors is difficult and is based on clinical symptoms and radiological imaging. After this tissue sampling and histological examination can be performed, to diagnose the type of tumor. Given the potential of rapid growth and risk of metastatic disease, and the often young age of patients, timely diagnosis and treatment are vital. To reduce the risk of incomplete eradication and subsequent tumor spill it is important to completely destroy the tumor. However, given the proximity of the bone to structures like nerves and vessels there is only a small margin for error. In this thesis we evaluated clinical data on RFA procedures to form recommendations on future use. Furthermore we performed experiments on the use of MWA in bone to explore its effectiveness and safety, both in- and ex-vivo.

## **Aim of this thesis**

The overall aim of this thesis was to assess and evaluate the options for minimally invasive treatment of bone tumors. First, we evaluated the clinical utility of RFA in this setting. Second, we examined the effects of a less well known technique in bone, MWA, on a cellular level. We looked at both effectiveness as well as safety. With the results and recommendations from this study we hope to contribute to the development of less invasive and more patient-friendly methods of treatment.



# Contents of this thesis

## Part 1: looking back –

### How far are we in minimally invasive treatment?

In the first part of this thesis we are looking back at what has already achieved in the field of minimally invasive treatment of bone tumors. We focus on RFA, the technique that as thus far most frequently been used. This technique has mainly been used for treatment of small, benign tumors, for example osteoid osteoma (OO) and ACTs. The data for this first part was obtained from a prospectively kept database at the University Medical Center Groningen (UMCG). In **chapter 2** the accuracy and precision of probe placement in RFA procedures for OO are evaluated. Given the small range of error in minimally invasive treatment, the first step in predictable and reproducible ablation procedures is probe placement. **Chapter 3** describes our study on the effects of RFA for ACT. Data of 189 procedures carried out between 2007-2018 were evaluated on effectiveness (complete ablation or not) and safety. Furthermore, we looked deeper into procedure settings like temperature, ablation time per position and the number of needle positions. In **chapter 4** we looked at follow-up after RFA. For the patients treated with RFA in chapter 3 we measured the volume of the ablation halo on MRI at time intervals three months, one-, two-, five- and seven years after the procedure. Furthermore we looked into recurrences over time.

## **Part 2: looking ahead - Towards safe, reliable and effective treatment**

In the second part we look ahead on the future options of minimally invasive treatment. RFA has proven itself as an effective and safe alternative to open treatment. However, achievable ablation halos are relatively small. Therefore, this technique is less suitable for treatment of larger tumors. In this second part we looked at microwave ablation (MWA) as an alternative to RFA. Given the limited data in literature and limited experience of this technique in bone, this part of the thesis is of a more experimental nature. **Chapter 5** describes our results of MWA in both ex-vivo as well as in-vivo sheep long bone. We used different time intervals and different wattage levels to determine the effects of these parameters on resulting halo size (measured on histology). **Chapter 6** describes our in-vivo study on MWA in sheep long bone. We performed MWA with different settings and measured halo size both on histology as well as on MRI. Furthermore, the comparison was made between 1 and 6 weeks follow-up. After sacrifice the bones were harvested and samples were made for biomechanical analysis. Furthermore an ex-vivo ablation group was created. The results of this analysis are described in **chapter 7**.

In **chapter 8** the effectiveness and safety of MWA for treatment in spine are examined. Given the fact that the spine is a main location for bone metastases, leading to immobilization and pain, more knowledge of ablation effects is needed. There is a small margin of error with the proximity of the spinal cord. In this study we also examined the phenomenon of cortical insulation as possible protection of the spinal canal from excess heat. In **chapter 9** the results of our studies, clinical implications and future possibilities/limitations of minimally invasive treatment are discussed. Finally, **chapter 10** provides summaries of this thesis in English and Dutch.

## References

1. Gelderblom H, Hogendoorn PC, Dijkstra SD, van Rijswijk CS, Krol AD, Taminiau AH et al. The clinical approach towards chondrosarcoma. *Oncologist* 2008 Mar;13(3):320-329.
2. Ferguson JL, Turner SP. Bone Cancer: Diagnosis and Treatment Principles. *Am Fam Physician*. 2018 Aug 15;98(4):205-213.
3. Keil L. Bone Tumors: Primary Bone Cancers. *FP Essent*. 2020 Jun;493:22-26.
4. Website: [https://radiopaedia.org/articles/osteosarcoma?lang=us#image\\_list\\_item\\_1602362](https://radiopaedia.org/articles/osteosarcoma?lang=us#image_list_item_1602362)
5. Website: [https://radiopaedia.org/articles/ewing-sarcoma?lang=us#image\\_list\\_item\\_1602677](https://radiopaedia.org/articles/ewing-sarcoma?lang=us#image_list_item_1602677)
6. Website: [https://radiopaedia.org/articles/chondrosarcoma?lang=us#image\\_list\\_item\\_1602369](https://radiopaedia.org/articles/chondrosarcoma?lang=us#image_list_item_1602369)
7. Kim JH, Lee SK. Classification of Chondrosarcoma: From Characteristic to Challenging Imaging Findings. *Cancers (Basel)*. 2023 Mar 10;15(6):1703.
8. Fromm, J., Klein, A., Baur-Melnyk, A. et al. Survival and prognostic factors in conventional central chondrosarcoma. *BMC Cancer* 18, 849 (2018)
9. Case courtesy of Frank Gaillard, Radiopaedia.org, rID: 7529
10. Case courtesy of Hani Makky Al Salam, Radiopaedia.org, rID: 7876
11. Case courtesy of Frank Gaillard, Radiopaedia.org, rID: 6175
12. Case courtesy of Frank Gaillard, Radiopaedia.org, rID: 7527
13. Website: <https://www.orthobullets.com/pathology/8016/periosteal-osteosarcoma>
14. Kasalak Ö, Overbosch J, Adams HJ, Dammann A, Dierckx RA, Jutte PC, Kwee TC. Diagnostic value of MRI signs in differentiating Ewing sarcoma from osteomyelitis. *Acta Radiol*. 2019 Feb;60(2):204-212
15. Website: <https://radiopaedia.org/articles/bone-metastases-1>
16. O'Sullivan GJ, Carty FL, Cronin CG. Imaging of bone metastasis: An update. *World J Radiol*. 2015 Aug 28;7(8):202-11
17. Case courtesy of Frank Gaillard, Radiopaedia.org, rID: 16311
18. Case courtesy of David Cuete, Radiopaedia.org, rID: 29404

19. Campanacci DA, Scoccianti G, Franchi A, Roselli G, Beltrami G, Ippolito M et al. Surgical treatment of central grade 1 chondrosarcoma of the appendicular skeleton. *J Orthop Traumatol.* 2013 Jun;14(2):101-7
20. Hickey M, Farrokhyar F, Deheshi B, Turcotte R, Ghert M. A systematic review and meta-analysis of intralesional versus wide resection for intramedullary grade I chondrosarcoma of the extremities. *Ann Surg Oncol* 2011 Jun;18(6):1705-1709.
21. Chen YC, Wu PK, Chen CF, Chen WM. Intralesional curettage of central low-grade chondrosarcoma: A midterm follow-up study. *J Chin Med Assoc.* 2017 Mar; 80(3):178-182.
22. Dierselhuis EF, Goulding KA, Stevens M, Jutte PC. Intralesional treatment versus wide resection for central low-grade chondrosarcoma of the long bones. *Cochrane Database Syst Rev.* 2019 Mar 7;3:CD010778.
23. Zou T, Li Q, Zhou X, Yang Z, Wang G, Liu W et al. Remove orthopedic fracture implant with minimal invasive surgery is good for the patient's early rehabilitation. *Int J Clin Exp Med.* 2015 Dec 15;8(12):22377-81.
24. Reeves RA, DeWolf MC, Shaughnessy PJ, Ames JB, Henderson ER. Use of minimally invasive spine surgical instruments for the treatment of bone tumors. *Expert Rev Med Devices.* 2017 Nov;14(11):881-890.
25. Dierselhuis EF, Overbosch J, Kwee TC, Suurmeijer AJH, Ploegmakers JJW, Stevens M et al. Radiofrequency ablation in the treatment of atypical cartilaginous tumours in the long bones: lessons learned from our experience. *Skeletal Radiol.* 2019; 48(6): 881–887
26. Brace CL. Thermal Tumor Ablation in Clinical Use. *IEEE Pulse* 2011;2(5):28-38.
27. Rhim H, Dodd GD. Radiofrequency thermal ablation of liver tumors. *J Clin Ultrasound.* 1999 Jun;27(5):221-9.
28. Stoltz A, Gagnière J, Dupré A, Rivoire M. Radiofrequency ablation for colorectal liver metastases. *J. Visc Surg.* 2014 Apr;151 Suppl 1:S33-44
29. Tanigawa N, Arai Y, Yamakado K, Aramaki T, Inaba Y, Kanazawa S et al. Phase I/II Study of Radiofrequency Ablation for Painful Bone Metastases: Japan Interventional Radiology in Oncology Study Group 0208. *Cardiovasc Intervent Radiol.* 2018 Jul;41(7):1043-1048.
30. Ma Y, Wallace AN, Waqar SN, Morgensztern D, Madaelil TP, Tomasian A et al. Percutaneous Image-Guided Ablation in the Treatment of Osseous Metastases from Non-small Cell Lung Cancer. *Cardiovasc Intervent Radiol.* 2018 May;41(5):726-733.

31. Dierselhuis EF, van den Eerden PJ, Hoekstra HJ, Bulstra SK, Suurmeijer AJ, Jutte PC. Radiofrequency ablation in the treatment of cartilaginous lesions in the long bones: results of a pilot study. *Bone Joint J* 2014 Nov;96-B(11):1540-1545.
32. Rosenthal DI, Alexander A, Rosenberg AE, Springfield D. Ablation of osteoid osteomas with a percutaneously placed electrode: a new procedure. *Radiology* 1992 Apr;183(1):29-33.
33. Callstrom MR, Charboneau JW. Percutaneous Ablation: Safe, Effective Treatment of Bone Tumors. *Oncology (Williston Park)*. 2005 Oct;19(11 Suppl 4):22-6.
34. Nakatsuka A, Yamakado K, Uraki J, Takaki H, Yamanaka T, Fujimori M et al. Safety and Clinical Outcomes of Percutaneous Radiofrequency Ablation for Intermediate and Large Bone Tumors Using a Multiple-Electrode Switching System: A Phase II Clinical Study. *J Vasc Interv Radiol*. 2016 Mar;27(3):388-94.
35. Lavergne T, Sebag C, Ollitrault J, Chouari S, Copie X, Le Heuzey JY et al. Radiofrequency ablation: physical bases and principles. *Arch Mal Coeur Vaiss* 1996 Feb;89 Spec No 1: 57-63.
36. Eriksson AR, Albrektsson T: Temperature threshold levels for heat-induced bone tissue injury: A vital-microscopic study in the rabbit. *J Prosthet Dent*. 1983 Jul;50(1):101-7.
37. Eriksson A, Albrektsson T, Grane B, McQueen D. Thermal injury to bone A vital microscopic description of heat effects. *Int J Oral Surg*. 1982 Apr;11(2):115-21.
38. Feldman L, Fuchshuber P, Jones DB. The SAGES Manual on the Fundamental Use of Surgical Energy (FUSE). *Springer* 2012.
39. Dewhirst MW, Viglianti BL, Lora-Michiels M, Hanson M, Hoopes PJ. Basic principles of thermal dosimetry and thermal thresholds for tissue damage from hyperthermia. *Int. J. Hyperth.*, vol. 19, no. 3, pp. 267–294, 2003.
40. Book: Issa ZF, Miller JM, Zipes DP. Clinical Arrhythmology and Electrophysiology. Chapter 7: Ablation energy sources. 2nd ed. *Elsevier* 1983.
41. Palussière J, Pellerin-Guignard A, Descat E, Cornélis F, Dixmérias F. Radiofrequency ablation of bone tumours. *Diagn Interv Imaging*. 2012 Sep;93(9):660-4.
42. Brace CL: Microwave Tissue Ablation: Biophysics, Technology and Applications. *Crit Rev Biomed Eng*. 2010; 38(1): 65–78.

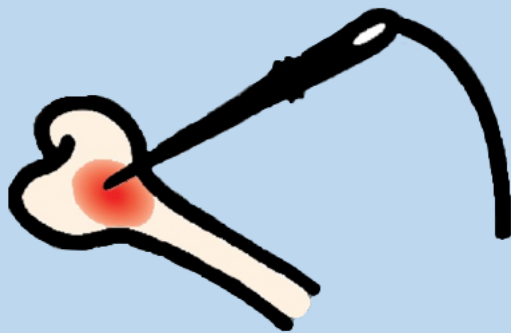
43. Lubner MG, Brace CL, Hinshaw JL, Lee FT. Microwave tumor ablation: mechanism of action, clinical results and devices. *J vasc interventional radiology*. 2010 Aug; 21(8 suppl)
44. Fan QY, Zhou Y, Zhang M, Ma B, Yang T, Long H et al. Microwave ablation of malignant extremity bone tumors. *Springerplus*. 2016 Aug 20;5(1):1373.
45. Kastler A, Alnassan H, Aubry S, Kastler B. Microwave thermal ablations of spinal metastatic bone tumors. *J vasc interv Radiol* 2014; 25:1470-1475
46. Khan MA, Deib G, Delbar B, Patel AM, Barr JS. Efficacy and Safety of Percutaneous Microwave Ablation and Cementoplasty in the Treatment of Painful Spinal Metastases and Myeloma. *AJNR Am J Neuroradiol*. 2018 Jul;39(7):1376-1383.
47. Fan QY, Zhou Y, Zhang M, Ma B, Yang T, Long H et al. Microwave Ablation of Primary Malignant Pelvic Bone Tumors. *Front Surg*. 2019 Mar 5;6:5.
48. Hinshaw JL, Lubner MG, Ziemlewicz TJ, Lee FT, Brace CL. Percutaneous Tumor Ablation Tools: Microwave, Radiofrequency, or Cryoablation—What Should You Use and Why? *Radiographics*. September-October 2014; 34(5): 1344–1362.
49. Laeseke PF, Lee FT, Sampson LA, van der Weide DW, Brace CL. Microwave ablation versus radiofrequency ablation in the kidney: high-power triaxial antennas create larger ablation zones than similarly sized internally cooled electrodes. *J Vasc Interv Radiol*. 2009 Sep;20(9):1224-9.
50. Rachbauer F, Mangat J, Bodner G, Eichberger P, Krismer M. Heat distribution and heat transport in bone during radiofrequency catheter ablation. *Arch Orthop Trauma Surg* (2003) 123 : 86–90
51. Zhao W, Peng ZH, Chen JZ, Hu JH, Huang JQ, Jiang YN et al. Thermal effect of percutaneous radiofrequency ablation with a clustered electrode for vertebral tumors: In vitro and vivo experiments and clinical application. *Journal of bone oncology* 12 (2018) 69-77.
52. Wallace AN, Hillen TJ, Friedman MV, Zohny ZS, Stephens BH, Greco SC et al. Percutaneous spinal ablation in a sheep model: protective capacity of an intact cortex, correlation of ablation parameters with ablation zone size, and correlation of postablation MRI and pathologic findings (2017). *AJNR Am J Neuroradiology* 2017 Aug; 38(8): 1653-1659.
53. Dupuy DE, Hong R, Oliver B, Goldberg SN. Radiofrequency ablation of spinal tumors: temperature distribution in the spinal canal. *AJR Am J Roentgenol* 2000; 175:1263-66

54. Zhang C, Han X, Douglas P, Dai Y, Wang G. Bipolar Radiofrequency Ablation of Spinal Tumors: The Effect of the Posterior Vertebral Cortex Defect on Temperature Distribution in the Spinal Canal. *AJNR Am J neuroradiol.* 2018 Jan; 39(1)
55. Schramm W, Yang D, Wood BJ, Rattay F, Haemmerich D. Contribution of Direct Heating, Thermal Conduction and Perfusion During Radiofrequency and Microwave Ablation. *Open Biomed Eng J.* 2007; 1: 47–52.





**Part 1: looking back –  
How far are we in minimally  
invasive treatment?**



# Chapter 2

## Evaluation of accuracy and precision of CT-guidance in Radiofrequency Ablation for osteoid osteoma in 86 patients

H Nijland<sup>1</sup>, JG Gerbers<sup>1</sup>, SK Bulstra<sup>1</sup>, J Overbosch<sup>2</sup>, M Stevens<sup>1</sup>, PC Jutte<sup>1</sup>

1. Department of orthopaedics, University of Groningen, University Medical Center Groningen (UMCG)
2. Department of radiology, University of Groningen, University Medical Center Groningen (UMCG)

*PLoS One. 2017 Apr 6;12(4)*

# **Abstract**

## **Background**

Osteoid osteoma is a benign skeletal tumour that accounts for 2-3% of all bone tumours. The male-to-female ratio is around 4:1 and it predominates in children and young adults. The most common symptom is pain, frequently at night-time. Historically the main form of treatment has been surgical excision. With the development of Radiofrequency Ablation (RFA) there is a percutaneous alternative. Success rates of RFA are lower but the main advantage is the minimal invasive character of the therapy and the low complication rate. As a result of the minimal invasiveness the hospitalization- and rehabilitation periods are relatively short. However, in current literature no values for accuracy and precision are known for the CT-guided positioning.

## **Methods**

Accuracy and precision of the needle position are determined for 86 procedures. Furthermore the population is divided into groups based on tumor diameter, location and procedure outcome.

## **Results**

The clinical success rate was 81.4%. In 79% of procedures complete ablation was achieved. Accuracy was 2.84 mm on average, precision was 2.94 mm. Accuracy was significantly lower in more profound lesions. Accuracy in tibia and fibula was significantly higher compared to the femur. No significant difference was found between different tumor diameters.

## **Interpretation**

The accuracy and precision found are considered good. Needle position is of major importance for procedure outcomes. The question however rises how the results will turn out in treatment of larger tumors.

## Introduction

Osteoid osteoma is a benign skeletal tumour that accounts for 2-3% of all bone tumours [1] and 10-12% of all benign bone tumors [2,3]. This tumour has low growth potential and usually a diameter less than 15mm [2]. Osteoid osteoma can develop on multiple locations, but are most frequently seen in the long bones of the lower extremity, i.e. femur, tibia and fibula [1]. Osteoid osteoma is characterized by a radiolucent nidus surrounded by a variable degree of sclerosis. The male-to-female ratio is around 4:1 and it predominates in children and young adults [3]. The most common symptom is pain localized in the bone which is most frequent during night-time. This pain can be relieved by using non-steroidal anti-inflammatory drugs (NSAID's) [1].

The main form of treatment of these tumors has, for a long time, been classical surgery. Hereby the options are curettage, en bloc resection and wide resection (with grafting). The success rate of classical surgery ranges from 88-100% [4]. However, the main point of concern is the occurrence of complications like avascular necrosis of the femoral head and fractures [4,5]. According to Cantwell et al. complications occur in 20-45% of procedures. Besides these complications mean surgery time is longer and tissue damage, scarring and morbidity are higher compared to minimally invasive therapies [4].

Minimal invasive treatment for osteoid osteoma can be done with Radiofrequency Ablation (RFA). RFA as a treatment for osteoid osteoma was first described by Rosenthal et al. in 1992 [6]. In RFA therapy a tumor is thermally ablated by a needle-shaped electrode. This needle is placed through a drilled tract based on CT-images (i.e. CT-guidance) [1]. The position of the needle is essential for optimal destruction without complications. When the tumor is within 15mm of a neurovascular structure classical surgery is the treatment of first-choice [4]. The main advantage of RFA compared to other forms of treatment is the minimal invasive character of the therapy in

combination with the corresponding low complication rate [7]. As a result of the minimal invasive character the hospitalization- and rehabilitation periods are relatively short [8].

Success rates for RFA range from 76-100% [4]. Although this success rate is lower compared to classical surgery (88-100%), RFA is currently considered to be the main treatment option mainly due to the low invasiveness of the treatment [5]. It is likely that the success rate of RFA can be improved by (more) accurate positioning of the needle. Complication rates can potentially be reduced by (more) precise positioning [5]. In current literature no values for accuracy and precision of CT guided RFA needle placements are known, although they are likely to be a major factor in success rates. Therefore, the main purpose of this paper is to determine and evaluate the accuracy and precision of freehand positioning under CT-guidance, the current standard technique for RFA needle guidance. The accuracy and precision are also determined for subgroups based on diameter and location of the tumor. Besides this, the typical use of CT-guidance is analyzed by means of secondary parameters (i.e. placement time, angulation, tumor depth, number of RFA tempi, number of runs, number of residues, complications, and the clinical success rate)

## **Methods**

All data is obtained from a prospectively kept bone tumor database of University Medical Center Groningen (UMCG) on the criteria of having had a RF-ablation for osteoid osteoma. Data of patients treated with RFA in the last 10 months is analyzed with Orthomap 3D software (Stryker, MahWah, United States) and added to the database. In accordance to regulations of the Medical Ethical Review Board of University Medical Center Groningen, patients were informed about the fact that data of the procedure could be used for scientific research. If patients had objections to the use of their data these data were not included in the study.

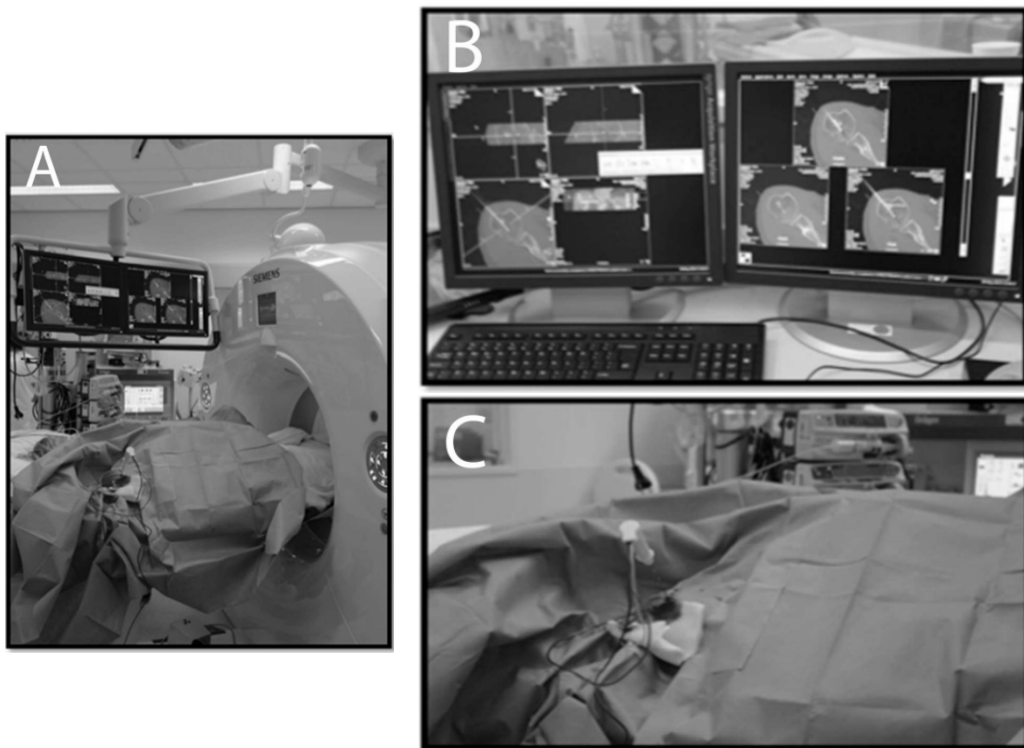


**Figure 1** RFA procedure. *A: Procedure set-up. B: Planning needle position. C: Needle in situ during ablation.*

### *Measurements*

In this study accuracy and precision are defined in accordance with the ISO 5725-1 norm [9]. Accuracy is formulated as the minimal distance between the needle and the nidus of the tumour and expressed in mm. The precision is formulated as the closeness of agreement of this distance between different patients and is measured as the standard deviation of the accuracy and expressed in mm. These measures are depicted in figure 2.

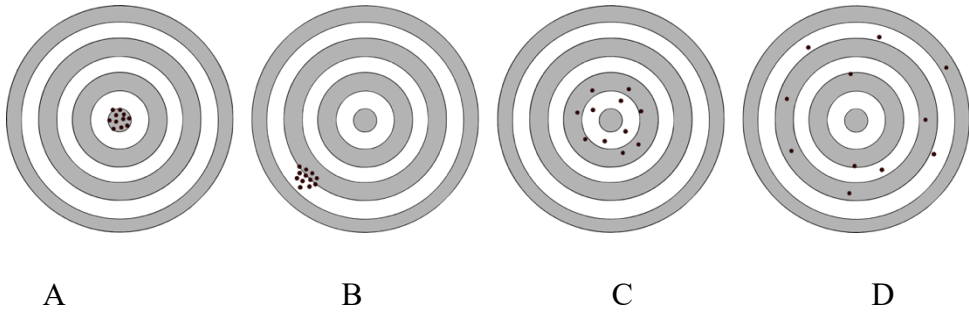


**Figure 2** *Formulation of accuracy and precision. A: high accuracy, high precision, B: high accuracy, low precision, C: low accuracy, high precision, D: low accuracy, low precision.*

In order to obtain more information about the accuracy and precision on different tumor sizes, the population has been separated into 2 groups based on the diameter of the tumor. Group 1 comprised tumors with a diameter of  $\leq 10$  mm and group 2 contained tumors of  $>10$  mm. The purpose of this separation is to evaluate the effect of tumor size on ablation effect rate. To compare the course and effects of the RFA procedure between different locations, patients are divided into 3 separated groups based on location (table 3).

After identifying the accuracy and precision for the entire population as well as for subgroups based on diameter and location, we evaluated whether there is a difference in accuracy, precision and procedure outcomes between the subgroups. By means of possible variances in these outcomes we look at the importance of accurate positioning. Secondary parameters are placement time, angulation, tumor depth, number of RFA tempi, number of runs, number of residues, complications, and the clinical success rate. The placement time is the period between the first and last run. The angulation is formulated as the angle between the true path of the needle and the shortest possible route from the chosen entry point to the nidus. RFA tempi is defined as



the number of ablations during a procedure and the clinical success rate is defined as being free of pain 2 weeks after the procedure.

### *Statistical analysis*

All data is analyzed with SPSS Statistics v20 (IBM). For the comparison between the groups based on diameter a Mann-Whitney U test is used. For locations a Kruskal-Wallis test is used. Fisher's exact test is used for the variables on an ordinal scale (i.e. residue, complications, clinical success) for the diameter groups. For these variables in the location groups a Chi-square test is used. For tests on precision Levene's test is used. Pearson's test is used to determine correlations. For all tests an alpha of 0.05 was chosen. To control alpha for multiple group comparisons (for locations) it is divided by the number of comparisons, in this case by 3 [10].

## **Results**

### *Demographics*

Table 1 displays the demographics of the patient population and the basic data about the tumors (i.e. diameter, depth, side, location). A number of 59 from 86 patients were male (2.2:1 ratio). The mean age of patients was 26.1 years. In 5 of the 86 analyzed procedures, a complication occurred. In 2 cases this comprised a skin burn, in 2 cases an infection occurred and finally 1 patient had a fracture.

**Table 1** *Demographics & basic tumor data*

|  |                    |
|--|--------------------|
| <b>Number of procedures</b>                | 86                 |
| <b>Sex (m/v)</b>                           | 59/27              |
| <b>Follow-up (months)</b>                  | 54.1 ( $\pm$ 30.6) |
| <b>Age (years)</b>                         | 26.1 ( $\pm$ 10.7) |
| <b>Diameter nidus (mm)</b>                 | 8.6 ( $\pm$ 4.5)   |
| <b>Depth (mm)</b>                          | 43.9 ( $\pm$ 24.3) |
| <b>Side (left/right)</b>                   | 40/46              |
| <b>Location (femur/tibia/fibula/other)</b> | 31/29/9/17*        |

*Mean values ( $\pm$  deviation) (\* = number of cases per group)*

#### *Accuracy & precision*

Table 2 shows the accuracy, precision and angulation for group 1 ( $\leq$ 10mm) compared to group 2 ( $>$ 10mm). The accuracy of the needle position appeared to be 2.84 mm on average for all patients together. The precision was found to be 2.94 mm. There was a mean angulation of 4.9° compared to the shortest route from entry point to nidus. Nine Patients (10.5%) had a residue. From the 86 included patients 70 no longer reported pain 2 weeks after the procedure. Therefore, the clinical success rate was 81.4%.

Values for accuracy, precision were smaller for group 1, but the outcomes show no significant differences with P values of 0.161 for accuracy and 0.266 for angulation. From the evaluated secondary parameters, only the depth turned out to be significantly different between the groups (P = 0.035) with the larger tumors situated more profound. The number of RFA tempi and runs did not differ between the different tumor sizes. In the small diameter group the number of residues was distinctly higher, but with regard to group sizes no significant difference was found (P = 0.223).

**Table 2** Population separated in groups based on tumor size

|                                      | <i>Diameter group</i> |                              |                              |         |
|--------------------------------------|-----------------------|------------------------------|------------------------------|---------|
|                                      | Total<br>(N=86)       | Group 1<br>(N=62):<br>≤10 mm | Group 2<br>(N=24):<br>>10 mm | P-value |
| <b>Distance needle to tumor (mm)</b> | 2.84 (±2.94)          | 2.5 (±2.8)                   | 3.7 (±3.3)                   | 0.161   |
| <b>Placement time (min)</b>          | 36.0 (±17.4)          | 35.5 (±17.8)                 | 37.3 (±16.9)                 | 0.350   |
| <b>Angulation (degrees)</b>          | 4.9 (±3.31)           | 4.8 (±3.5)                   | 5.1 (±2.8)                   | 0.266   |
| <b>Depth (mm from entry)</b>         | 43.9 (±24.3)          | 40.2 (±22.8)                 | 54.0 (±25.9)                 | 0.035   |
| <b>Number of RFA tempi</b>           | 2.35 (±0.68)          | 2.35 (±0.75)                 | 2.35 (±0.49)                 | 0.612   |
| <b>Number of runs</b>                | 7.85 (±2.93)          | 8.1 (±3.0)                   | 7.3 (±2.8)                   | 0.176   |
| <b>Number of residues</b>            | 9                     | 8                            | 1                            | 0.223   |
| <b>Number of complications</b>       | 5                     | 3                            | 2                            | 0.537   |
| <b>Free of pain** (y/n)</b>          | 70/16                 | 49/13                        | 21/3                         | 0.283   |

*Mean values (± deviation) (\*\* 2 weeks after procedure)*

In table 3 the population is separated based on tumor location. First, the distance between needle and tumor (i.e. the accuracy) differs between the locations (P = 0.018) although non-significant ( $\alpha = 0.017$  after correction). Second the depth of tumors in the femur (almost) doubles the average depth of tumors in tibia and fibula (P < 0.001). The correlation between depth and needle-tumor distance is 0.395. Furthermore the average diameter of tumors in the femur is significantly larger compared to the diameters on the other locations (P = 0.014). Finally no significant differences can be found in precision, placement time, angulation, the number of RFA tempi, runs, residues, complications and the clinical success rates.

**Table 3** Population separated in groups on location

|                                      | <i>Location</i> |              |              |         |
|--------------------------------------|-----------------|--------------|--------------|---------|
|                                      | Femur (N=31)    | Tibia (N=29) | Fibula (N=9) | P-value |
| <b>Distance needle to tumor (mm)</b> | 3.9 (±3.5)      | 1.8 (±2.1)   | 2.9 (±1.7)   | 0.018   |
| <b>Placement time (min)</b>          | 37.8 (±17.6)    | 32.7 (±14.2) | 33.1 (±14.1) | 0.439   |
| <b>Diameter (mm)</b>                 | 10.1 (±5.0)     | 7.5 (±4.8)   | 7.6 (±2.6)   | 0.014   |
| <b>Angulation (degrees)</b>          | 3.8 (±2.3)      | 5.4 (±3.3)   | 6.1 (±4.5)   | 0.098   |
| <b>Depth (mm from entry)</b>         | 61.7 (±25.6)    | 29.9 (±10.8) | 39.1 (±18.7) | <0.001  |
| <b>Number of RFA tempi</b>           | 2.45 (±0.57)    | 2.14 (±0.71) | 2.67 (±0.71) | 0.119   |
| <b>Number of runs</b>                | 7.6 (±3.0)      | 7.2 (±2.0)   | 7.8 (±2.9)   | 0.920   |
| <b>Number of residues</b>            | 2               | 4            | 2            | 0.317   |
| <b>Number of complications</b>       | 2               | 1            | 2            | 0.165   |
| <b>Free of pain (y/n)</b>            | 24/7            | 22/7         | 8/1          | 0.702   |

*Mean values (± deviation) P<sub>1-2</sub> = Femur/Tibia P<sub>2-3</sub> = Tibia/Fibula P<sub>1-3</sub> = Femur/Fibula*

In figure 3 the position of the needle and the halo around it are depicted for 4 groups dependent on the outcomes of the procedure. These groups are the ablation success categories. In table 4 it can be seen that 68 of 86 procedures resulted in complete ablation (79.1%) of the tumor with 10 of these procedures with the needle placed within the nidus of the tumor (11.6%). The diameter of the nidus in lesions with incomplete ablation is significantly larger than the diameter of the nidus in lesions with complete ablation ( $P < 0.001$ ). The Pearson correlation between diameter and ablation success categories is 0.63. Finally, even though

it looks like tumors with incomplete ablation are located deeper under the skin, the depth of the tumor is not significantly different between the 4 groups (P 0.053).

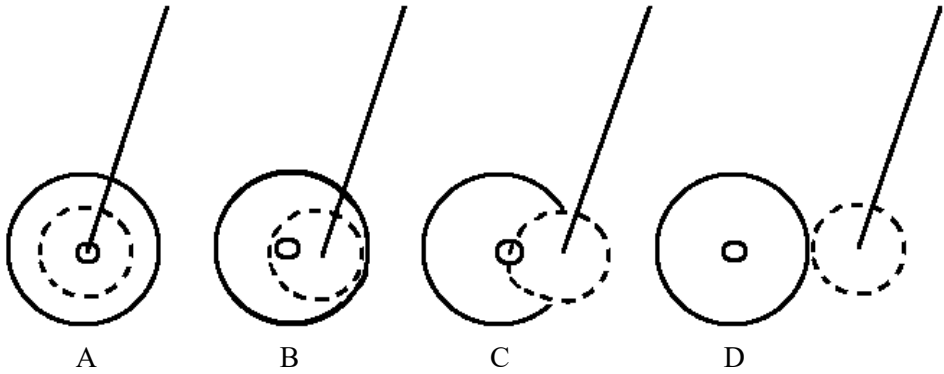


**Figure 3** The ablation success categories. A: In nidus, complete. B: In center, complete. C: In center, incomplete. D: Not in center, incomplete

**Table 4:** Population separated in groups on procedure accuracy and outcome

|                                     | Ablation success categories |                          |                            |                               |         |
|-------------------------------------|-----------------------------|--------------------------|----------------------------|-------------------------------|---------|
|                                     | In nidus, complete (10)     | In center, complete (57) | In center, incomplete (15) | Not in center, incomplete (4) | P-value |
| <b>Distance needle - tumor (mm)</b> | 0,0 ( $\pm$ 0,0)            | 2,3 ( $\pm$ 2,0)         | 5,6 ( $\pm$ 3,6)           | 8,3 ( $\pm$ 4,0)              | <0.001  |
| <b>Diameter nidus (mm)</b>          | 7,2 ( $\pm$ 3,3)            | 7,1 ( $\pm$ 2,6)         | 12,3 ( $\pm$ 4,4)          | 22,7 ( $\pm$ 2,50)            | <0.001  |
| <b>Placement time (min)</b>         | 30,0 ( $\pm$ 12,7)          | 36,2 ( $\pm$ 18,0)       | 39,7 ( $\pm$ 19,0)         | 33,7 ( $\pm$ 11,5)            | 0.481   |
| <b>Angulation (degrees)</b>         | 3,3 ( $\pm$ 2,0)            | 4,8 ( $\pm$ 3,4)         | 6,1 ( $\pm$ 3,6)           | 6,2 ( $\pm$ 1,7)              | 0.066   |
| <b>Depth (mm from entry)</b>        | 32,4 ( $\pm$ 15,9)          | 41,0 ( $\pm$ 22,8)       | 55,1 ( $\pm$ 24,8)         | 80,9 ( $\pm$ 30,8)            | 0.053   |
| <b>Number of RFA tempi</b>          | 2,5 ( $\pm$ 0,5)            | 2,3 ( $\pm$ 0,8)         | 2,4 ( $\pm$ 0,50)          | 2,0 ( $\pm$ 0,0)              | 0.575   |
| <b>Number of runs</b>               | 7,3 ( $\pm$ 1,8)            | 8,2 ( $\pm$ 3,2)         | 7,0 ( $\pm$ 2,6)           | 6,7 ( $\pm$ 0,6)              | 0.341   |

|                                |     |       |      |     |       |
|--------------------------------|-----|-------|------|-----|-------|
| <b>Number of residues</b>      | 1   | 7     | 0    | 1   | 0.414 |
| <b>Free of pain (y/n)</b>      | 7/3 | 46/11 | 15/0 | 2/2 | .075  |
| <b>Number of complications</b> | 0   | 3     | 1    | 1   | 0.345 |

*Mean values ( $\pm$  deviation)*

## **Discussion**

The goal of the current study was to identify and evaluate the accuracy and precision of needle position in freehand CT-guided radiofrequency ablation for the treatment of osteoid osteoma. The accuracy and precision of CT-guidance in RFA needle placement were found to be 2.84 mm and 2.94 mm respectively. The expected treatment radius is 5mm (ablation halo = 10 mm). Since this value exceeds the accuracy we found, tumor ablation can be expected for most patients. However, when considering the accuracy together with tumor diameter the treatment radius is no longer enough for large tumors, resulting in incomplete ablation.

Clinical results were in accordance with the findings in other studies on the results of RFA [4] as mentioned in the introduction. A number of 70 patients from the 86 included (81.4%) no longer reported pain 2 weeks after the procedure. The major advantage of RFA compared to classical surgery is the low number of complications and residues. In the current study we faced 5 complications in 86 procedures (5.8%) and 10.5% of the patients had a residue. This low rate of complications is indeed in contrast with classical surgery, since in classical surgery complications occur in 20-45% of procedures [4]. Furthermore the complications in this study were of low impact, for example the infections comprised cellulitis and the fracture were a small fibula fracture with no long-term immobilization. The number of runs was

7.85 on average. To minimize the drawbacks of ionizing radiation it is beneficial for both patient and surgeon to limit the number of needed scans [11]. Another advantage is the short placement time of 36 minutes on average (as this is only placement, patient positioning time should be added to this) in combination with the limited invasiveness of the procedure, thus making it appropriate for day treatment.

Factors that can potentially influence procedural accuracy, such as lesion depth and diameter have been investigated. With regard to the low correlation of 0.395 between depth and needle-tumor distance it cannot be stated that the accuracy is lower as a result of tumor depth. Furthermore this data is not due to an increase in the number of runs to reach more profound lesions. As can be seen in table 2 there is no significant difference in the accuracy of needle position between tumors with a small and large diameter. The P-value of 0.161 however indicates a (non-significant) decrease of accuracy with increases in diameter. This finding is in accordance with the differences in diameter between the different ablation success categories in table 4. As can be seen the diameter is significantly larger in tumors where the result of the procedure was incomplete ablation. Most likely this is the result of the limited size of the ablation halo, which is around 10mm in cortical bone [12]. More data is necessary to examine this decrease. The precision of needle placement seems to be better in smaller tumors as well, although not significant.

Location of the lesion is another potential factor in procedural accuracy. From the data the number of RFA tempi in the fibula is prominent compared to the other locations, although no significant difference can be found ( $P = 0.119$ ). There is no difference in size between lesions in the fibula compared to the other locations and the distance of the needle to the tumor is not significantly smaller in the fibula compared to the femur. An explanation for the high amount of tempi might be the lower risk of severe complications since the fibula is not a primary weight

supporting structure. On the other hand a consequence of multiple tempi might be damage to the peroneus nerve, which could lead to the development of a drop foot. Another prominent observation regarding the tumors in the fibula is the relatively high incidence of residues, moreover with the high number of tempi in mind.

In the data of table 4 it is notable that the number of patients reporting pain 2 weeks after the procedure is higher in the category 'needle in nidus' compared to the categories with the needle into the center (but not in the nidus). For procedures with the needle placed outside the center of the tumor the percentage of patients reporting pain 2 weeks after the procedure is higher compared to the other groups. With regard to the small amount of procedures with the needle outside the center however, no significant connection could be made ( $P = 0.075$ ). This observation however indicates it is necessary to position the needle within the center of the tumor to obtain elimination of the pain. Since pain is the main problem in osteoid osteoma this position should be the hallmark of treatment.

The essence of the RFA procedure is the need to accurately place the needle in or directly next to the tumor. To accomplish this position CT-imaging is used, which exposes the patient to ionizing radiation every placement run. With inaccuracies there is a chance of affecting surrounding tissues. The overall damage however is small compared to classical surgery. The chance of damage to surrounding tissue emphasizes the importance of accurate position of the needle within the center or nidus of the tumor. The accuracy and precision found are good enough for single point treatments, even on more profound lesions.

The importance of accurate positioning is even more emphasized in the treatment of larger tumors, with diameters exceeding the treatment radius around the needle (e.g. atypical cartilaginous tumors). In the treatment of these tumors multiple ablation points are necessary [12]. In this type of procedures RFA needles are placed on different locations



in the tumor, resulting in overlapping halos. When the needle is not in accurate position in such procedures the result is incomplete ablation and possibly vital tumor residue.

A remaining question is whether CT-guidance, with these results, is accurate and precise enough for multiple point ablations. Alternative techniques can be the use of fluoroscopy, image fusion, Computer assisted surgery (CAS) or guides. Not many studies have been published in this field [2,8]. An experimental study on 5 patients using (live guidance) fluoroscopy overlaying on CT data achieved a median accuracy of 0.6 mm [8].

The strength of the current study is the large patient population and the long follow-up of 54.1 months on average. Only in comparing locations the N became considerably smaller, mainly for the fibula. This is the first study to investigate the positional accuracy and precision of CT-guidance in RFA procedures. This data can be used to plan and perform safer (multiple point) ablations by compensating for known inaccuracy. For further research it is recommended to evaluate the accuracy of RFA procedures on larger tumors using multiple ablation points. The current study is however of retrospective nature and not powered.

As this study proves that accuracy is essential in RFA procedures, future research should focus on more accurate positioning (e.g. pre-planning, image fusion, and guidance), especially to enable multiple ablation points.

## **Conclusion**

The mean accuracy of CT-guidance was 2.84 mm between the needle and tumor. The precision turned out to be a deviation of 2.94 mm. Since the ablation halo is 10 mm and the diameter of the nidus is usually smaller than 15mm (in our data on average 8.57 mm), an accuracy of 2.84 is sufficient for (partial) destruction of most tumors. However with

larger tumors the ablation halo will not be sufficient for complete destruction. Therefore multiple ablations are necessary. These ablations need to overlap to ensure complete destruction of the tumor. When using multiple ablations one needs to account for the average deviation (i.e. accuracy) between needle and nidus for all ablation points. With regard to the relatively small ablation halo the question rises how many ablations are required for destructing large tumors. When using a large number of ablations the rate of complications might rise, taking away one of the major advantages of RFA compared to classic surgery. Therefore it is crucial to further increase accuracy. Furthermore our results make clear accuracy and precision differ between tumor locations. For locations with lower accuracy this technique might not be the optimal form of treatment, especially for large tumors.

Concluding, both the assessment of the technique and the clinical results in this series support the use of CT-guided RFA in osteoid osteoma treatment. With regard to the ablation halo of 10 mm it is of major importance to achieve a position in the center of the tumor to obtain complete ablation. The question remains if CT-guidance is good enough for multiple ablation procedures.

### **Conflict of interest and funding**

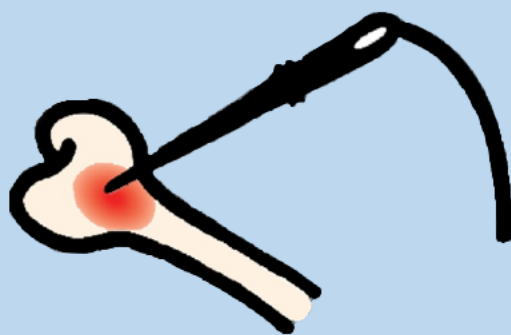
The authors have no financial or other interest that might bias the results of this research.

## References

1. Widmann, G., Schullian, P., Fasser, M., Niederwanger, C., & Bale, R. (2013). CT-guided stereotactic targeting accuracy of osteoid osteoma. *The International Journal of Medical Robotics + Computer Assisted Surgery : MRCAS*, 9(3), 274-279.
2. Busser, W. M., Hoogeveen, Y. L., Veth, R. P., Schreuder, H. W., Balguid, A., Renema, W. K., & Schultzekool, L. J. (2011). Percutaneous radiofrequency ablation of osteoid osteomas with use of real-time needle guidance for accurate needle placement: A pilot study. *Cardiovascular and Interventional Radiology*, 34(1), 180-183.
3. Kransdorf, M. J., Stull, M. A., Gilkey, F. W., & Moser, R. P., Jr. (1991). Osteoid osteoma. *Radiographics : A Review Publication of the Radiological Society of North America, Inc*, 11(4), 671-696.
4. Cantwell, C. P., Obyrne, J., & Eustace, S. (2004). Current trends in treatment of osteoid osteoma with an emphasis on radiofrequency ablation. *European Radiology*, 14(4), 607-617.
5. Ghanem, I. (2006). The management of osteoid osteoma: Updates and controversies. *Current Opinion in Pediatrics*, 18(1), 36-41.
6. Rosenthal, D. I., Alexander, A., Rosenberg, A. E., & Springfield, D. (1992). Ablation of osteoid osteomas with a percutaneously placed electrode: A new procedure. *Radiology*, 183(1), 29-33.
7. Rosenthal, D. I., Hornicek, F. J., Torriani, M., Gebhardt, M. C., & Mankin, H. J. (2003). Osteoid osteoma: Percutaneous treatment with radiofrequency energy. *Radiology*, 229(1), 171-175.
8. Okada, K., Myoui, A., Hashimoto, N., Takenaka, S., Moritomo, H., Murase, T., & Yoshikawa, H. (2014). Radiofrequency ablation for treatment for osteoid osteoma of the scapula using a new three-dimensional fluoroscopic navigation system. *European Journal of Orthopaedic Surgery & Traumatology : Orthopedie Traumatologie*, 24(2), 231-235.
9. Website:  
[http://www.iso.org/iso/catalogue\\_detail.htm?csnumber=11833](http://www.iso.org/iso/catalogue_detail.htm?csnumber=11833)
10. Toothaker LE. (1991) Multiple comparisons for researchers. *Newbury Park: Sage Publications, The International Professional Publishers. P.37*

11. Tselikas, L., Joskin, J., Roquet, F., Farouil, G., Dreuil, S., Hakime, A., Deschamps, F. (2015). Percutaneous bone biopsies: Comparison between flat-panel cone-beam CT and CT-scan guidance. *Cardiovascular and Interventional Radiology*, 38(1), 167-176.
12. Rachbauer, F., Mangat, J., Bodner, G., Eichberger, P., & Krismer, M. (2003). Heat distribution and heat transport in bone during radiofrequency catheter ablation. *Archives of Orthopaedic and Trauma Surgery*, 123(2-3), 86-90.





# Chapter 3

## Radiofrequency Ablation for Atypical Cartilaginous Tumors is safe and effective: analysis of 189 consecutive cases

H Nijland<sup>1</sup>, J Overbosch<sup>2</sup>, JJW Ploegmakers<sup>1</sup>, TC Kwee<sup>2</sup>, PC Jutte<sup>1</sup>

1. Department of Orthopaedic Surgery, University Medical Center Groningen, The Netherlands

2. Department of Radiology, University Medical Center Groningen, The Netherlands

*Open Access Journal of Oncology and Medicine. 2020 June 29;5(3)*

## **Abstract**

### *Objective*

The purpose of this study was to investigate the efficacy and safety of radiofrequency ablation (RFA) as a less invasive treatment alternative for atypical cartilaginous tumors.

### *Materials and methods*

Data of all consecutive RFA procedures for atypical cartilaginous tumors between 2007-2018 were analyzed, including temperature, amount of needle positions and ablation time per position. Tumor volume was measured on pre-operative MRI and ablation zone was assessed on 3-month postprocedural MRI. RFA outcome parameters were ablation result (R0: complete with margin ( $\geq 2\text{mm}$ ), R1: complete without margin ( $< 2\text{mm}$ ) and R2: incomplete) and occurrence of complications.

### *Results*

In 84.4% of cases complete ablation was achieved (66.7% R0, 17.7% R1). In 15.6% of procedures ablation was incomplete (R2). No recurrences were seen after R0/1 ablations (with minimum two years follow-up). R0 was achieved significantly more frequent in smaller tumors ( $p = .027$ , odds ratio (OR) = 1.04 (per  $\text{cm}^3$ ) and with longer ablation time per needle ( $p = .048$ , OR = .894). Temperature  $> 80^\circ\text{C}$  ( $p = .026$ , OR = 7.57) resulted in more complete (R0 or R1) ablations without increasing complication rate ( $p = .579$ ) compared to temperature of  $71\text{-}80^\circ\text{C}$ . In 15 procedures (7.9%) a complication occurred.

### *Conclusion*

RFA provides promising results for treatment of atypical cartilaginous tumors with complete ablation (R0, R1) in 84.4% of procedures. Complication rates are comparable with open surgery and the amount of fractures is lower. These encouraging data support the potential of RFA to replace more invasive surgical approaches.



## Introduction

Chondrosarcoma is the second most commonly diagnosed primary bone tumor in adults (after osteosarcoma), with a reported incidence of 8.78 per 1 million people [1-2]. They are often found coincidentally by MR, X-ray or CT imaging for unrelated musculoskeletal symptoms [3]. Incidence increases proportionally with the amount of imaging that is performed in the population [4]. They can be divided into three grades based on histology combined with macroscopic imaging features. Grade-1 central chondrosarcomas in long bone are called atypical cartilaginous tumors (ACTs) and are usually asymptomatic [3]. These tumors can show locally aggressive growth, but metastases are very uncommon. Prognosis of ACT is favorable, with 3-year overall survival of 96% and 5-year overall survival of 93% [2].

Since ACTs are resistant to both radiotherapy and chemotherapy, the first choice of treatment for these tumors has been surgical, either by curettage or wide resection [5-6]. Recent literature showed wide resection to be necessary only for tumors with local aggressive growth [3]. A systematic review analyzing 214 curettage procedures for ACT reported a success rate (i.e. no recurrent or residual tumor) of 90.2%, with a complication rate of 4.8% (6 out of 126, of which five fractures) [5]. For wide resection complications reportedly occurred in 24 out of 76 cases (= 31.6%) [5]. In a large Cochrane analysis, a success rate of 93.2% was found for curettage and 94.6% for wide resection [7]. In our center we found comparable results in 108 patients, as described by Dierselhuis et al. [3]. Recently, a wait- and see policy with radiological follow-up has also been advocated [8].

With less invasive treatment functional outcome is better, especially when limbs and joints can be preserved. Furthermore, overall patient satisfaction is better, complication risk lower, weight bearing is often not restricted, and hospitalization period is shorter for minimally invasive procedures [9-10].

Radiofrequency ablation (RFA) has already been used in soft tissue, primarily liver, for a long time. Application to bone tissue has so far mainly been in treatment of osteoid osteoma [11-14]. In RFA tumor tissue is destroyed by local application of electricity, causing motion, friction and heat and thereby causing coagulative necrosis. The principle is based on the fact that (irreversible) tissue damage starts at a temperature of 47°C and instantaneous protein denaturation starts at 60°C (figure 1).

Literature on RFA for treatment of bone malignancies is limited and mainly focused on metastases [15-17]. Knowledge on safety and efficacy of RFA treatment for ACTs, especially for larger tumors, needs to be expounded. The aim of the current paper is to present the data that were acquired over the last 12 years in the treatment of ACT using RFA. Recommendations regarding safety and effectivity of RFA for ACTs are provided.

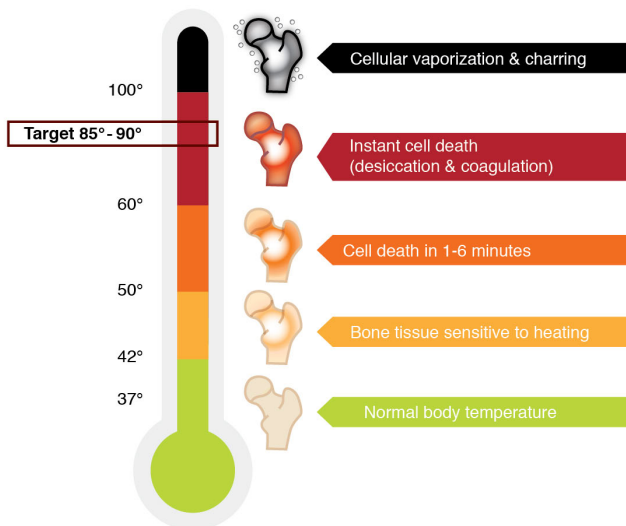


**Figure 1** Tissue reaction to heat. [18-20] Ideal temperature for ablation is 60-95°C because instant cell death is the aim. Above 100°C charring occurs, limiting conduction of heat and thereby limiting the slow cooking effect of slow heat flow into the surrounding [21].

## **Method**

### **Procedure**

Pre-RFA diagnosis of ACT was made based on imaging. On MR images they typically appear as a completely intramedullary located, popcorn-like lesion, with septonodular and peripheral enhancement after gadolinium-based contrast agent administration and limited scalloping. On T2-weighted imaging the chondroid components of an ACT appear as areas of high signal intensity. Perilesional edema and cortical breakthrough are signs of higher grade [22]. RFA was carried out in the department of radiology using CT guidance or in the operation room (OR) using fluoroscopy guidance or computer assisted surgery (CAS). This decision was dependent on tumor localization, size and comorbidities. Tumors with diameter over 6 cm were generally treated in the OR because of the possibility to place a prophylactic osteosynthesis to prevent fracture. Procedures were carried out under anesthesia. First a tract was drilled towards the tumor and a histological biopsy was performed to confirm the radiological diagnosis. Then an RFA needle was brought up towards the tumor and ablation was carried out. For the ablations from 2007-2014 a Boston Scientific RF3000 needle was used, from 2015-2019 a Cooltip needle (Medtronic). Parameters like ablation time per position and temperature were pre-operatively determined for every single procedure based on location in the bone, proximity to sensitive structures (cartilage, nerves, vessels) and volume of the tumor. After the procedure these parameters were documented in the electronic patient file. Immobilization was only advised after procedures in the pelvic region. For all other procedures three months sports restriction (contact- and indoor sports) was advised.

At three months, baseline MR (consisting of unenhanced T1-weighted, fat-suppressed T2-weighted and gadolinium-enhanced sequences in two perpendicular planes with 4-mm slice thickness) was made to determine the exact ablation area. Subsequent follow-up MR scans

were planned one, two, five and seven years after the procedure. For assessment of long-term effectivity only the data of the 85 patients with at 20 months follow-up was used.

### **Data collection**

Data, including histology results, from all consecutive RFA procedures carried out in our center in a 12-year period (2007-2018) were retrospectively collected from the prospectively kept local bone tumor database and the patient files. In accordance with regulations of the Medical Ethical Review Board of University Medical Center Groningen (UMCG), patients were informed by means of written information about the fact that anonymized data of the procedure could be used for scientific research in case they did not object. On pre-RFA MR images the tumor dimensions were measured on T1- and T2-weighted scans. The observer was blinded for final outcome during measurement. In three cases there was no pre-RFA MR. These cases were excluded from the tumor volume analysis. Treatment success (i.e. tumor completely within the RFA halo on all MR sequences and slices) was determined on MR images three months after RFA by a radiologist. Furthermore, the location in the bone (diaphysis, metaphysis, epiphysis) and whether the tumor completely covered the distance between the medial and lateral cortices (i.e wall to wall) was determined. From the tumor dimensions the volume was calculated using the following formula:

$$V = (\pi \cdot r^2) \cdot h$$

V = volume

r = radius

h = height

Since most tumors were elliptical (see figure 2) the formula was split up:

$$V = (\pi \cdot \frac{1}{2} \cdot a \cdot \frac{1}{2} \cdot b) \cdot h$$

a = width

b = depth

Which could be abbreviated to:

$$V = \frac{1}{4} \cdot \pi \cdot a \cdot b \cdot h$$

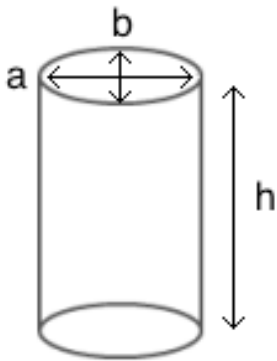


**Figure 2** animation of tumor dimensions for calculating volume.

This formula describes the volume of an elliptical cylinder in mm<sup>3</sup>; values were divided by 10<sup>3</sup> to be converted to cm<sup>3</sup>.

### Data analysis

Outcome parameters were technical success and complications. We divided the technical success into three groups, according to Dierselhuis et al. [23]. Group 1 comprised complete ablations with a margin  $\geq 2$ mm and was called R0, group 2 (R1) comprised complete ablations with a margin  $< 2$ mm, and group 3 (R2) comprised of incomplete ablations (tumor visible outside the ablation zone or halo) (figure 3). In our analysis we looked at the influence of peri-procedural parameters, including tumor volume, age, ablation time per position,

temperature, amount of needle positions, wall to wall filling (i.e. from cortex to cortex), type of bone and location within the bone. Evaluation of tumor volume was preferred over maximum diameter because we think volume provides a better approximation of actual tumor size when determining if a tumor is suitable for RFA treatment. Maximum diameter possibly underestimates tumor size, especially for round tumors.

In case of an R0 result, the ablation was considered technically successful, in case of R2 unsuccessful. R1 can be considered successful as well in case there is no local recurrence within two years (research with prolonged follow-up is ongoing). However, treatment aim was initially set at R0. Therefore, analysis was done for both R0 vs R1/2 and R0/R1 vs R2.

We also analyzed the association between the peri-procedural parameters and a complication in general to occur, as well as between these parameters and a fracture (which was the most frequent complication). Applied temperature was divided into three groups (60-70, 71-80, 81-90°C).

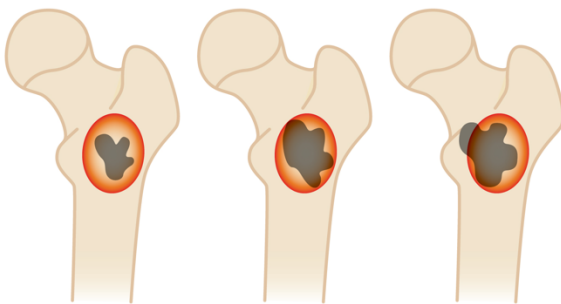


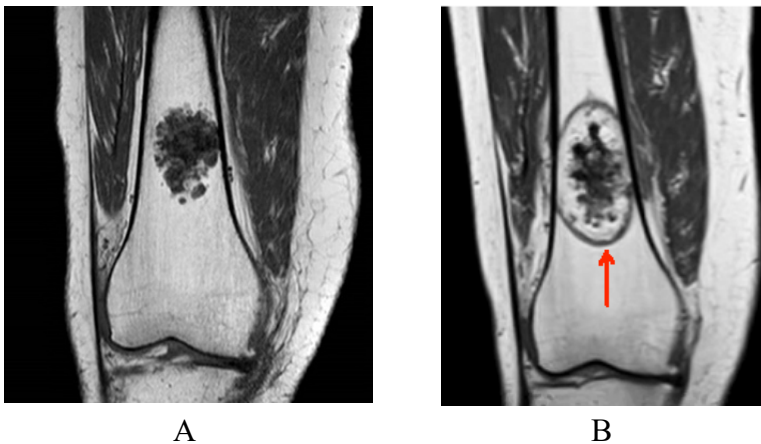
**Figure 3** The 3 post-RFA result groups. R0 = complete ablation with  $\geq 2$ mm margin, R1 = complete ablation with  $< 2$ mm margin, R2 = incomplete ablation.

### Statistical analysis

Data were analyzed using SPSS Statistics v20 (IBM, Armonk, United States). Data were tested on normality of distribution and for correlation between variables. Analysis on the influence of periprocedural variables on result and complications was done using univariate logistic regression. Odds ratios, confidence intervals and p-values were reported. For temperature we compared the 81-90°C group to the other two groups.

Variables with p-value  $<.10$  were included in a multivariate logistic regression. Furthermore, the odds ratios from logistic regression were used to look for a cut-off point for tumor volume (to determine if there is a maximum tumor volume from which the result is significantly worse). For all tests an alpha of .05 was chosen.

In figure 4 the RFA procedure is illustrated as well as images of an ACT with and without needles in situ and a 3-month post-RFA baseline T1-weighted MR.



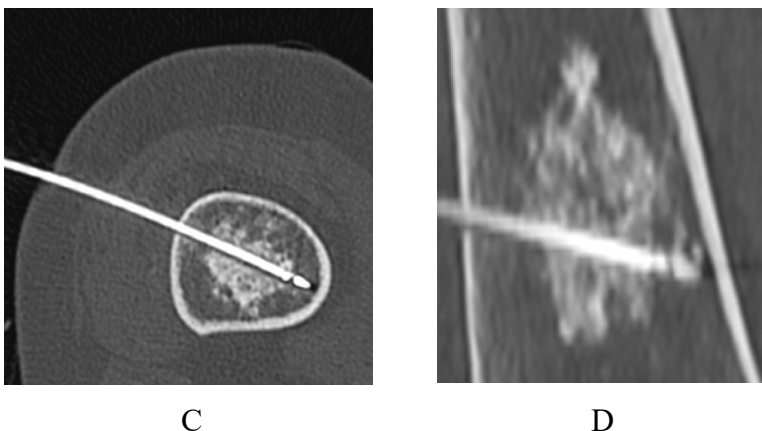


**Figure 4:** *Radiofrequency ablation of an atypical cartilaginous tumor. A: MR image of an ACT in distal femur. B: MR baseline, 3 months after RFA procedure. The red arrow indicates the ablation halo. C: Transverse oblique CT image with RF needle in situ. D: Sagittal oblique CT image with RF needle in situ.*

## Results

Since 2007, 189 RFA procedures (in 187 patients) were carried out as treatment for ACT at the UMCG. Of these procedures 163 were performed percutaneously (using CT-guidance) and 26 open. For three procedures baseline MRI was lacking for various reasons (explained in more detail later). Between 2009 and 2014 a pilot was carried out in which 44 patients received a combination of RFA treatment followed by MRI after three months and intralesional curettage two to six weeks later [11,23]. These patients are included in the current analysis as well. Of the 189 procedures, 129 were in the femur, 39 in the humerus, 19 in the tibia, one in the fibula and one in the acetabulum. Table 1 gives a summary of the most important peri-procedural parameters.



**Table 1:** Summary of most important peri-procedural parameters

|   |                           |
|---|---------------------------|
| <b>Procedures</b>                                   | 189                       |
| <b>Male/Female</b>                                  | 58 / 131                  |
| <b>Follow-up time (months)*</b>                     | 17.1 (3.88-32.6)          |
| <b>Age (years)**</b>                                | 53.3 ( $\pm$ 12.3)        |
| <b>Tumor volume (cm<sup>3</sup>)*</b>               | 8.69 (4.51-16.4)          |
| <b>Maximum diameter (mm)*</b>                       | 29.0 (23.0-40.5)          |
| <b>Result (R0 / R1 / R2)</b>                        | 124 / 33 / 29             |
| <b>Complications</b>                                | 15                        |
| <b>Recurrences after R0 / R1</b>                    | 0                         |
| <b>Needle positions*</b>                            | 2.00 (2.00-3.00)          |
| <b>Temperature (°C)**</b>                           | 83.3 ( $\pm$ 9.13)        |
| <b>Total ablation time (minutes)**</b>              | 20.0 ( $\pm$ 15.0)        |
| <b>Ablation time / position**</b>                   | 9.10 ( $\pm$ 3.05)        |
| <b>CT / fluoroscopy / CAS***</b>                    | 163 / 18 / 8              |
| <b>Location****<br/>(D / DM / M / ME / E / DME)</b> | 40 / 32 / 82 / 29 / 3 / 2 |
| <b>Wall to wall (yes/no)</b>                        | 70 / 118                  |

\* Median (inter quartile range)

\*\* Mean (SD)

\*\*\* CAS: computer assisted surgery

\*\*\*\* Location: Diaphysis (D), Diaphysis/Metaphysis (DM), Metaphysis (M) Metaphysis/Epiphysis (ME), Epiphysis (E), Diaphysis/Metaphysis/Epiphysis (DME)

### Treatment result

In 124 procedures (=66.7%) R0 was achieved. In 33 procedures (=17.7%) the result was R1 and 30 procedures (15.6%) were R2. In six patients 3-month post-RFA baseline MR was not made due to debilitating amyotrophic lateral sclerosis (n=1), death from another disease (n=1), or complications (n=4: one avascular necrosis (AVN), two fractures (which necessitated surgical intervention with curettage and a plate) and one thermal skin injury (which necessitated surgical intervention)). The RFA result of these latter three cases was determined based on pathology at the time of surgical re-interventions.

For the minimally invasive procedures 107 resulted in R0 (66.5%), 29 in R1 (18.0%) and 25 in R2 (15.5%).

In four of the patients with R2 result a re-ablation was carried out. In three cases this led to complete ablation (three times R0), one patient still had a small residue. Considering the size (15x10x8mm) of this residue a wait and see policy was chosen. Follow-up showed no progression at 5 years after the procedure.

Table 2 depicts the effects of peri-procedural parameters between the three different treatment outcomes (R0, R1, R2). No correlations of  $>.50$  were found between any variables. Based on univariate logistic regression for R0 vs R1/2, tumor volume ( $p = .033$ ), time per position ( $p = .048$ ), location on the transition of diaphysis to metaphysis ( $p = .036$ ) and tumors reaching from wall to wall ( $p = .072$ ) were included for multivariate analysis. In multivariate analysis only volume ( $p = .0450$ ) and mean time per position ( $p = .013$ ) had a significant effect. Larger tumor volume and shorter time per position lead to more incomplete (R1/2) ablations. The  $R^2$  of this multivariate model is .153, indicating only 15.3% of variance in result R0 vs R1/2 is due to the variables in the model.

From the ablations with temperature between 60-70°C 68.4% resulted in R0, for 71-80°C this was 70.0% and for 81-90°C 75.0%. Only 5.4% of ablations over 80°C resulted in R2, compared to 17.2% for ablations up to 80°C. Based on univariate analysis for R0/1 vs R2 a temperature of 71-80°C (compared to  $>80^\circ\text{C}$ ) ( $p = .026$ ) and mean time per position ( $p = .063$ ) were included for multivariate analysis. No variables had a significant effect on R0/1 vs R2. The multivariate model had an  $R^2$  of .171. For the 85 procedures (R0 or R1) with minimum 20 months follow-up no signs of residual tumor or recurrence were seen on MRI (median: 32.5 months, range: 20.0-115.4 months).

**Table 2 A.** *Effect of peri-procedural parameters on treatment result (R0 vs R1/2).*

| <b>R0 vs R1/2</b>                           | <b>Univariate OR (95% CI)</b> | <b>P-value</b> | <b>Multivariate OR (95% CI)</b> | <b>P-value</b> |
|---|-------------------------------|----------------|---------------------------------|----------------|
| <b>Tumor volume<sup>∅</sup></b>             | 1.03 (1.00-1.07)              | <b>.033</b>    | 1.04 (1.00-1.09)                | <b>.045</b>    |
| <b>Age<sup>∅∅</sup></b>                     | 1.00 (.977-1.03)              | .900           |                                 |                |
| <b>Mean time per position<sup>∅∅∅</sup></b> | .894 (.800-1.00)              | <b>.048</b>    | .841 (.734-.964)                | <b>.013</b>    |
| <b>Temperature (60-70°C)*</b>               | 1.39 (.442-4.33)              | .576           |                                 |                |
| <b>Temperature (71-80°C)*</b>               | 1.29 (.292-5.66)              | .740           |                                 |                |
| <b>Needle positions</b>                     | 1.19 (.944-1.49)              | .143           |                                 |                |
| <b>Wall to wall</b>                         | .561 (.299-1.05)              | .072           | .580 (.247-1.36)                | .211           |
| <b>Bone (humerus)**</b>                     | .983 (.450-2.15)              | .963           |                                 |                |
| <b>Bone (tibia)**</b>                       | .945 (.336-2.66)              | .915           |                                 |                |
| <b>Location DM***</b>                       | .312 (.105-.926)              | <b>.036</b>    | .328 (.103-1.04)                | .059           |
| <b>Location MET***</b>                      | .615 (.280-1.35)              | .225           |                                 |                |
| <b>Location ME***</b>                       | .827 (.311-2.20)              | .703           |                                 |                |

OR = odds ratio, CI = confidence interval

\* Temperature: compared to temperature 81-90C.

\*\* Bone: compared to femur

\*\*\* Location: all compared to diaphysis (DM = transition diaphysis/metaphysis, MET = metaphysis, ME = transition metaphysis/epiphysis)

∅ Tumor volume: OR per cm<sup>3</sup> in volume

∅∅ Age: OR per year in age

∅∅∅ Mean time per position: OR per minute

**Table 2B.** *Effect of peri-procedural parameters on treatment result (R0/1 vs R2).*

| <b>R0/1 vs R2</b>                            | <b>Univariate OR (95% CI)</b> | <b>P-value</b> | <b>Multivariate OR (95% CI)</b> | <b>P-value</b> |
|--|-------------------------------|----------------|---------------------------------|----------------|
| <b>Tumor volume</b> <sup>∅</sup>             | 1.03 (.991-1.06)              | .149           |                                 |                |
| <b>Age</b> <sup>∅∅</sup>                     | 1.01 (.973-1.04)              | .771           |                                 |                |
| <b>Mean time per position</b> <sup>∅∅∅</sup> | .866 (.745-1.01)              | .063           | .735 (.499-1.08)                | .118           |
| <b>Temperature (60-70°C)*</b>                | 2.08 (.320-13.5)              | .443           |                                 |                |
| <b>Temperature (71-80°C)*</b>                | 7.57 (1.27-45.1)              | <b>.026</b>    | 4.98 (.778-31.8)                | .090           |
| <b>Needle positions</b>                      | 1.20 (.910-1.59)              | .196           |                                 |                |
| <b>Wall to wall</b>                          | 1.12 (.489-2.58)              | .782           |                                 |                |
| <b>Bone (humerus)**</b>                      | .844 (.293-2.43)              | .753           |                                 |                |
| <b>Bone (tibia)**</b>                        | 1.01 (.270-3.80)              | .985           |                                 |                |

OR = odds ratio, CI = confidence interval

\* Temperature: compared to temperature 81-90C.

\*\* Bone: compared to femur

\*\*\* Location: all compared to diaphysis (DM = transition diaphysis/meta- physis, MET = metaphysis, ME = transition metaphysis/epiphysis)

∅ Tumor volume: OR per cm<sup>3</sup> in volume

∅∅ Age: OR per year in age

∅∅∅ Mean time per position: OR per minute

## **Complications**

In 189 procedures a total of 15 complications (7.9%) occurred (table 3). The most frequent complication was a fracture (nine cases, 4.8%), followed by AVN (four cases, 2.1%). Seven out of nine fractures were found in the femur, the other two in the humerus. One case of thermal injury involved damage to the radial nerve, leading to loss of both sensory and motoric function. During four years of follow-up only partial motor function returned.

**Table 3** *Complications*

| Complication       | Frequency |
|--------------------|-----------|
| Fracture           | 9         |
| Avascular necrosis | 4         |
| Thermal injury     | 2         |
| Total              | 15 (7.9%) |

There were no significant associations between peri-procedural variables and a complication in general- or a fracture (table 4). Only age had a possible correlation with risk of a complication in general ( $p = .090$ ) or a fracture ( $p = 0.070$ ) on univariate analysis.

**Table 4** *Effect of peri-procedural parameters on complication risk (general and fracture)*

| Complication yes/no    | Univariate OR (95% CI) | P-value | Fracture               | Univariate OR (95% CI) | P-value |
|------------------------|------------------------|---------|------------------------|------------------------|---------|
| Tumor volume           | 1.01 (.956-1.06)       | .823    | Tumor volume           | 1.02 (.961-1.08)       | .543    |
| Age                    | 1.04 (.994-1.09)       | .090    | Age                    | 1.06 (.995-1.14)       | .070    |
| Mean time per position | 1.06 (.902-1.25)       | .475    | Mean time per position | 1.04 (.848-1.29)       | .686    |
| Temperature (60-70°C)* | .963 (.178-5.21)       | .965    | Temperature (60-70°C)* | 2.04 (.315-13.2)       | .455    |
| Temperature (71-80°C)* | 2.17 (.371-12.7)       | .391    | Temperature (71-80°C)* | 2.04 (.190-21.8)       | .556    |
| Needle positions       | .875 (.565-1.35)       | .549    | Needle positions       | 1.08 (.668-1.75)       | .750    |
| Wall to wall           | .489 (.169-1.41)       | .186    | Wall to wall           | .730 (.189-2.82)       | .648    |
| Bone (humerus)**       | 1.96 (.616-6.24)       | .254    | Bone (humerus)**       | .818 (.166-4.02)       | .392    |
| Bone (tibia)**         | .741 (.089-6.20)       | .782    | Bone (tibia)**         |                        | .998    |
| Location DM***         | 1.67 (.408-6.80)       | .476    | Location DM***         | 1.76 (.365-8.52)       | .481    |
| Location MET***        | .342 (.073-1.61)       | .174    | Location MET***        | .308 (.015-1.51)       | .108    |
| Location ME***         | .667 (.114-3.91)       | .653    | Location ME***         | .440 (.043-4.46)       | .488    |

OR = odds ratio, CI = confidence interval

\* Temperature: compared to temperature 60-70°C.

\*\* Bone: compared to femur. There were no fractures in tibia.

\*\*\* Location: all compared to diaphysis (DM = transition diaphysis/metaphysis, MET = metaphysis, ME = transition meta/epiphysis)

The frequency distribution of the complications over the different bones is shown in table 5. Almost all fractures occurred in the femur and three out of four AVNs were in the humerus. Four out of nine fractures occurred on the transition diaphysis/metaphysis, three were in the diaphysis. All AVNs occurred in the proximal metaphysis/epiphysis.

**Table 5** *Distribution of complications over the different bones*

| <b>Bone</b>            | <b>Femur</b>                 | <b>Humerus</b>              | <b>Tibia</b>                | <b>Fibula</b>             | <b>Acetabulum</b>         | <b>Total</b>                 |
|------------------------|------------------------------|-----------------------------|-----------------------------|---------------------------|---------------------------|------------------------------|
| <b>Complication</b>    | 9<br>(7.0%)                  | 5 (12.8%)                   | 1 (5.3%)                    | 0 (0%)                    | 0 (0%)                    | 15<br>(7.9%)                 |
| Fracture               | 8                            | 1                           | 0                           | 0                         | 0                         | 9                            |
| Avascular necrosis     | 1                            | 3                           | 0                           | 0                         | 0                         | 4                            |
| Nerve injury           | 0                            | 1                           | 0                           | 0                         | 0                         | 1                            |
| Thermal injury         | 0                            | 0                           | 1                           | 0                         | 0                         | 1                            |
| <b>No complication</b> | <b>120</b><br><b>(93.0%)</b> | <b>34</b><br><b>(87.2%)</b> | <b>18</b><br><b>(94.7%)</b> | <b>1</b><br><b>(100%)</b> | <b>1</b><br><b>(100%)</b> | <b>174</b><br><b>(92.1%)</b> |
| <b>Total</b>           | <b>129</b>                   | <b>39</b>                   | <b>19</b>                   | <b>1</b>                  | <b>1</b>                  | <b>189</b>                   |

## Discussion

The current study represents a large series of 189 RFA procedures for ACT, of which 163 were carried out minimally invasive. No other studies on minimal invasive treatment of ACTs/chondrosarcoma grade 1 have been published other than the smaller series of our group by Dierselhuis et al. [11,23].

### Treatment result

With regard to effective ablation our aim was to achieve ablation with at least 2mm margin around the tumor. Therefore the success rate of treatment could be calculated as  $R0/(R0 + R1 + R2)$ , which was 66.7% (124/186) in this study. This result is lower than results for surgical treatment by curettage or wide resection (90 to 95%) [3-5]. Nevertheless, a margin <2mm may be sufficient as well, since the tumor still appears completely ablated. However, a small margin might result in more local recurrences. Therefore, a separate R1 group was created. When defining success to be a complete ablation, the success rate could be calculated as  $(R0 + R1) / R2 = 157/186 = 84.4\%$ , which is close to that of curettage of ACT. For the CT-guided percutaneous procedures the success rate would be  $136/161 = 84.5\%$ . To determine if R1 is a good result on the long term, extensive follow-up period is required. In our series, none of the R1 cases showed local residual disease activity on MRI during a minimum follow-up period of two years.

RFA result was dependent on tumor volume. A larger volume leads to a significantly higher risk of R1 or R2 ablation ( $p = .033$ ). For every  $\text{cm}^3$  increase in volume risk of R1/2 ablation increases by 4.4% (OR = 1.044). Therefore, risk of an R1/2 ablation is double for tumors over  $16\text{cm}^3$  and threefold for tumors over  $25\text{cm}^3$ . However, larger tumor volume does not significantly increase risk of an incomplete ablation (R2) compared to a complete ablation (R0/1) ( $p = .149$ ). Therefore,

larger tumors are also eligible for RFA. However, given these findings more caution is advised in deciding between minimal invasive- and open treatment for larger tumors over 20cm<sup>3</sup>. Switching to open treatment however, leads to a higher risk of complications, especially fractures (4-11% risk of a fracture in curettage vs 10.5% in (wide) resection vs 4.8% in minimally invasive RFA) [5][25].

Our results show that ablations at lower temperature result in more incomplete ablations ( $p = .026$  for 71-80°C vs 81-90°C). Ablations with 81-90°C result in 75% of cases in R0. Since all ablations were carried out with temperature over 60°C, this finding is contrary to the perception of instantaneous protein coagulation to occur with temperatures over 60°C as presented in figure 1. However, temperature measurement is done at the tip of the probe. The ablation zone is larger than only the electrical zone as it is formed by electrical conduction around the active zone of the needle tip and the subsequent heat distribution with a certain gradient within the surrounding tissue. With this distribution temperature decreases at longer distance from the needle tip. Relatively low ablation temperatures result in smaller ablation zones and more chance of incomplete ablation. Since higher temperatures do not significantly increase the risk of complications ( $p = .965$  for temperature >80°C compared to 60-70°C,  $p = .391$  for temperature >80°C compared to 71-80°C), safety is not compromised in high temperature ablations (81-90°C). A point of consideration is that for R0/1 vs R2, result is significantly different between 71-80°C and 81-90°C, but not between 60-70°C and 81-90°C ( $p = .443$ ). A possible explanation is the fact that there were relatively a lot of R1 ablations in the 60-70°C group (21.1%). The fact that only for R0/1 vs R2 a significant effect was found is due to the relatively high amount of R1 ablations in the 81-90°C group (19.6%). Another point of consideration is that temperature was only recorded in the patient files in 88 procedures (=46.6%). With more data differences might become more evident.



Shorter time per position leads to more R1/2 ablations (OR = .894,  $p = .048$ ), so longer ablation per position results in more R0. This could be explained by the fact that temperature slowly distributes through the bone during the ablation. Immediately after finishing the ablation, tissue temperature starts to cool again. The amount of needle positions does not affect the ablation result ( $p = .143$  for R0 vs R1/2,  $p = .196$  for R0/1 vs R2) and the complication risk is not dependent of increased time per position ( $p = .475$ ). Therefore, in the perspective of safe and effective ablation, it is recommendable to perform ablations with longer time per position instead of a large number of positions for large tumors. Experiments are designed to confirm this hypothesis.

Ablations of ACTs with location on the transition from diaphysis to metaphysis result in R0 significantly more often compared to other locations. In 81.2% of cases R0 was reached, compared to 57.5% in diaphysis, 68.8% in metaphysis and 62.1% on the transition between metaphysis and epiphysis. There was no difference in tumor volume, amount of needle positions, ablation time per position or temperature between the different locations.

### **Complications**

Temperature ( $p = .965$  for temperature  $>80^{\circ}\text{C}$  compared to  $60-70^{\circ}\text{C}$ ,  $p = .391$  for temperature  $>80^{\circ}\text{C}$  compared to  $71-80^{\circ}\text{C}$ ), amount of needle positions ( $p = .549$ ) and tumor volume ( $p = .823$ ) have no significant effect on complication occurrence. Therefore, our data do not indicate the complications were caused by overaggressive treatment.

None of the peri-procedural variables affected the risk of a fracture. The average age of the patients with a fracture was 60.8 years, compared to 53.0 years for patients without a fracture. However, this difference was not significant ( $p = .070$ ) and is most likely due to the increasing incidence of fractures with age in the population in general [24]. A possible solution could be to plan a DEXA-scan before RFA-treatment in patients over 60 years old.

The amount of complications after RFA of ACT (7.9%) was similar to curettage surgery (5-11%) and low compared to wide resection (31.6%) [5,25]. To further reduce the risk of complications our recommendation is to evaluate proximity to structures particularly prone to heat damage (e.g. nerves, cartilage, epiphyseal plate) carefully before the procedure. If the tumor is not close to such a structure it may be safe to use more aggressive ablation (longer time and higher temperature). Furthermore, since a fracture (4.8% of cases) was the most frequent complication it could be an option to introduce an immobilization period after treatment, especially in femur, giving the bone better opportunity to recover.

### **Points of consideration**

A possible weakness of the current study is the fact that the parameter ablation time is hard to describe. Dependent on the shape and volume of the tumor, ablation is done using single- or multiple positions. In the current analysis ablation time is described as the time per position. Since positions are normally close to each other, an area is already (partially) preheated when ablation on the next position starts. Furthermore, the peri-procedural parameters evaluated in this study only account for a small portion of variance in treatment result ( $R^2 = .153$  for R0 vs R1/2 and  $R^2 = .171$  for R0/1 vs R2). In future evaluations more variables should be included to form a stronger model. Also, longer follow-up is necessary to be able to evaluate long-term effect of RFA treatment. A final point for consideration is the unpredictability of treatment result (i.e. the fact we encountered 17.7% R1 ablations). The aim is to be able to use this technique more accurately in the future as a result of increased experience and research, hereby guarantying complete ablation with the desired safety margin. To further expand the value of RFA for ACTs and to improve treatment result it would be interesting to use real-time feedback on halo size during the procedure. Option for this are MRI thermometry and dual energy CT [26-28]. However, so far these methods come with limitations like motion artefacts and unpredictability and need to be examined in further detail.

## **Conclusion**

RFA provides promising results for the treatment of ACT with complete ablation (R0, R1) in 84.4% of procedures. Complication rate (7.9%) is comparable with open surgery. This is similar to results and complication rates as described in literature on surgical treatment [3-5]. There is less damage to surrounding tissue, costs are lower and it is more patient friendly because of the minimal invasive character. More research is needed to determine the optimal procedure parameters for ablation duration, needle positions and temperature. However, these encouraging data support the potential of RFA to replace more invasive surgical approaches for ACT treatment.

## References

1. Primary bone cancer. [Internet]. US National cancer institute; 2019 Nov 20. Available from: <https://www.cancer.gov/types/bone/bone-fact-sheet>
2. Van Praag V, Rueten-Budde AJ, Ho V, Dijkstra PDS, Fiocco M, van de Sande MAJ. Incidence, outcomes and prognostic factors during 25 years of treatment of chondrosarcomas. *Surg Oncol.* 2018 Sep;27(3):402-408
3. Dierselhuis EF, Gerbers JG, Ploegmakers JJ, Stevens M, Suurmeijer AJ, Jutte PC. Local Treatment with Adjuvant Therapy for Central Atypical Cartilaginous Tumors in the Long Bones: Analysis of Outcome and Complications in One Hundred and Eight Patients with a Minimum Follow-up of Two Years. *J Bone Joint Surg Am.* 2016 Feb 17;98(4):303-13
4. Stomp W, Reijnierse M, Kloppenburg M, de Mutsert R, Bovée JV, den Heijer M et al. Prevalence of cartilaginous tumours as an incidental finding on MRI of the knee. NEO study group. *Eur Radiol.* 2015 Dec;25(12):3480-7.
5. Chen X, Yu LJ, Peng HM, Jiang C, Ye CH, Zhu SB et al. Is intralesional resection suitable for central grade 1 chondrosarcoma: A systematic review and updated meta-analysis. *Eur J Surg Oncol.* 2017 Sep;43(9):1718-1726
6. Campanacci DA, Scoccianti G, Franchi A, Roselli G, Beltrami G, Ippolito M. Surgical treatment of central grade 1 chondrosarcoma of the appendicular skeleton. *J Orthop Traumatol.* 2013 Jun;14(2):101-7
7. Dierselhuis EF, Goulding KA, Stevens M, Jutte PC. Intralesional treatment versus wide resection for central low-grade chondrosarcoma of the long bones. *Cochrane Database Syst Rev.* 2019 Mar 7;3:CD010778.
8. Deckers C, Schreuder BH, Hannink G, de Rooy JW, van der Geest IC. Radiologic follow-up of untreated enchondroma and atypical cartilaginous tumors in the long bones. *J Surg Oncol.* 2016 Dec; 114(8): 987-991.
9. Reeves RA, DeWolf MC, Shaughnessy PJ, Ames JB, Henderson ER. Use of minimally invasive spine surgical instruments for the treatment of bone tumors. *Expert Rev Med Devices.* 2017 Nov;14(11):881-890.
10. Zou T, Li Q, Zhou X, Yang Z, Wang G, Liu W et al. Remove orthopedic fracture implant with minimal invasive surgery is good for the patient's early rehabilitation. *Int J Clin Exp Med.* 2015 Dec 15;8(12):22377-81.
11. Dierselhuis EF, Overbosch J, Kwee TC, Suurmeijer AJH, Ploegmakers JJW, Stevens M et al. Radiofrequency ablation in the treatment of atypical cartilaginous tumours in the long bones: lessons learned from our experience. *Skeletal Radiol.* 2019; 48(6): 881–887.

12. Callstrom MR, Charboneau JW: Percutaneous Ablation: Safe, Effective Treatment of Bone Tumors. *Oncology (Williston Park)*. 2005 Oct;19(11 Suppl 4):22-6.
13. Rosenthal DI, Alexander A, Rosenberg AE, Springfield D. Ablation of osteoid osteomas with a percutaneously placed electrode: a new procedure. *Radiology* 1992 Apr;183(1):29-33.
14. Nijland H, Gerbers JG, Bulstra SK, Overbosch J, Stevens M, Jutte PC. Evaluation of accuracy and precision of CT-guidance in Radiofrequency Ablation for osteoid osteoma in 86 patients. *PLoS One*. 2017 Apr 6;12(4):e0169171.
15. Nakatsuka A, Yamakado K, Uraki J, Takaki H, Yamanaka T, Fujimori M et al. Safety and Clinical Outcomes of Percutaneous Radiofrequency Ablation for Intermediate and Large Bone Tumors Using a Multiple-Electrode Switching System: A Phase II Clinical Study. *J Vasc Interv Radiol*. 2016 Mar;27(3):388-94.
16. Ma Y, Wallace AN, Waqar SN, Morgensztern D, Madaelil TP, Tomasian A et al. Percutaneous Image-Guided Ablation in the Treatment of Osseous Metastases from Non-small Cell Lung Cancer. *Cardiovasc Intervent Radiol*. 2018 May;41(5):726-733.
17. Tanigawa N, Arai Y, Yamakado K, Aramaki T, Inaba Y, Kanazawa S et al. Phase I/II Study of Radiofrequency Ablation for Painful Bone Metastases: Japan Interventional Radiology in Oncology Study Group 0208. *Cardiovasc Intervent Radiol*. 2018 Jul;41(7):1043-1048.
18. Eriksson AR, Albrektsson T: Temperature threshold levels for heat-induced bone tissue injury: A vital-microscopic study in the rabbit. *J Prosthet Dent*. 1983 Jul;50(1):101-7.
19. Eriksson A, Albrektsson T, Grane B, McQueen D. Thermal injury to bone A vital microscopic description of heat effects. *Int J Oral Surg*. 1982 Apr;11(2):115-21.
20. Feldman L, Fuchshuber P, Jones DB. The SAGES Manual on the Fundamental Use of Surgical Energy (FUSE). *Springer* 2012.
21. Issa ZF, Miller JM, Zipes DP: Ablation energy sources. Book: Advances in Radiation Biology 1983
22. Soldatos T, McCarthy EF, Attar S, Carrino JA, Fayad LM. Imaging features of chondrosarcoma. *J Comput Assist Tomogr*. 2011 Jul-Aug;35(4)
23. Dierselhuis EF, van den Eerden PJ, Hoekstra HJ, Bulstra SK, Suurmeijer

AJ, Jutte PC. Radiofrequency ablation in the treatment of cartilaginous lesions in the long bones: results of a pilot study. *Bone Joint J.* 2014 Nov;96-B(11):1540-5

24. Curtis EM, van der Velde R, Moon RJ, van den Bergh JP, Geusens P, de Vries F et al. Epidemiology of Fractures in the United Kingdom 1988-2012: Variation with age, sex, geography, ethnicity and socioeconomic status. *Bone.* 2016 June; 87: 19-26

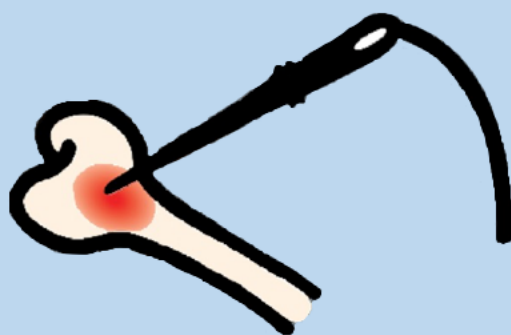
25. Gerbers JG, Dierselhuis EF, Stevens M, Ploegmakers JJW, Bulstra SK, Jutte PC. Computer-assisted surgery compared to fluoroscopy in curettage of atypical cartilaginous tumors / chondrosarcoma grade 1 in the long bones. *PLoS One.* 2018 May 17;13(5);e0197033.

26. Zhu M, Sun Z, Ng CK: Image-guided thermal ablation with MR-based thermometry. *Quant imaging med surg.* 2017 Jun; 7(3):356-368.

27. Zhou Y. Noninvasive Thermometry in High-intensity focused ultrasound ablation. *Ultrasound Q.* 2017 Dec; 33(4):253-260.

28. Paul J, Vogl TJ, Chacko A: Dual energy computed tomography thermometry during hepatic microwave ablation in an ex-vivo porcine model. *Phys Med.* 2015 Nov;31(7):683-91.







# Chapter 4

Long-term halo follow-up confirms less  
invasive treatment of low-grade cartilaginous  
tumors with radiofrequency ablation to be safe  
and effective

H Nijland<sup>1</sup>, J Overbosch<sup>2</sup>, JJW Ploegmakers<sup>1</sup>, TC Kwee<sup>2</sup>, PC Jutte<sup>1</sup>

1. Department of Orthopaedic Surgery, University Medical Center  
Groningen, The Netherlands

2. Department of Radiology, University Medical Center Groningen,  
The Netherlands

*J Clin Med.* 2021 Apr 22;10(9):1817

# **Abstract**

## **Background**

Radiofrequency ablation (RFA) is a minimally invasive alternative in the treatment of bone tumors. Long-term follow-up has not been described in current literature. Detailed analysis of mid- and long-term follow-up after RFA treatment for a cohort of patients with low-grade cartilaginous tumors (atypical cartilaginous tumors and enchondroma) was performed. Results, complications and development of halo dimensions over time are presented.

## **Methods**

Data of all patients with an RFA procedure for a low-grade cartilaginous tumor between 2007-2018 were included. Ablation area is visible on baseline MRI, 3 months post-procedure and is called halo. Volume was measured on MR images and compared between different follow-up moments to determine the effect of time on halo volume. Follow-up was carried out three months, one-, two-, five- and seven years after the procedure. Occurrence of complications and recurrences was assessed.

## **Results**

Of the 137 patients included, 82 were analyzed. Mean follow-up time was 43.6 months. Ablation was complete in 73 cases (89.0%). One late complication occurred, while no recurrences were seen. Halo dimensions of height, width and depth decreased with a similar rate, 21.5% on average in the first year. Subsequently this decrease in halo size continues gradually during follow-up, indicating bone revitalization.

## **Conclusion**

RFA is a safe and effective treatment in low-grade cartilaginous tumors with an initial success rate of 89.0%. Extended follow-up shows no local recurrences and gradual substitution of the halo with normal bone.

## Introduction

Chondrosarcoma are the most common primary bone tumors in adults (1). Atypical cartilaginous tumors (ACT), formerly known as chondrosarcoma grade 1, are the most common type of chondrosarcoma. An ACT is a cartilage-forming tumor with primary location in the long bones (mainly femur) (2). The five-year survival rate reported in literature is 93% (2). An ACT can show aggressive local growth with (very) low tendency to metastasize. Diagnosis is regularly made coincidentally from MR or CT imaging for common skeletal symptoms (2,3). Differentiation between ACT and enchondroma is not always clear on MRI or after biopsy given the continuum between these diagnoses.

First choice of treatment has been topic of discussion in recent literature. Since ACTs show resistance to both radio- and chemotherapy, treatment is often either surgical or conservative with frequent follow-up (4). In surgical treatment most common options are considered intralesional curettage and resection, with a tendency towards intralesional curettage (3,5). Success rates (i.e. no residue or recurrence) are about 90% for curettage and 95% for resection, with complications occurring in 2.8% and 13.3% of cases, respectively (3,6). The use of radiofrequency ablation (RFA) for ACT as a minimally invasive alternative to the above-mentioned options has been developed since 2007. Out of 189 consecutive patients treated with RFA, success rate was 84.4% with a complication in 7.9% of patients (7). Therefore, RFA is considered effective at achieving local tumor control in ACT of long bone. However, long-term follow-up was not described.

In RFA a small tract is drilled towards the tumor under image-guidance (CT, fluoroscopy or computer assisted surgery). Through this tract a needle is brought up and tumor destruction is achieved by application of local heat for several minutes (8,9). Cell death is achieved by desiccation and instantaneous protein coagulation at temperatures over 60 °C. Bone tissue is sensitive to heating at temperatures over 47 °C. At

temperatures between 50-60 °C it takes one to six minutes for necrosis to occur (10-12). The temperature at the tip of the needle, normally between 75-90 °C, is different than the temperature that reaches the edge of the ablation halo because of heat loss during distribution. A special point of interest is the outer layer of the ablation zone. Tissue that does not reach complete necrosis might show remodeling over time. We hypothesize a remodeling process to occur, similar to the remodeling after a fracture. From literature it is known that in the first weeks after a fracture, osteoclasts remove the necrotic tissue. Subsequently osteoblast activity leads to calcification and formation of new trabecular bone (13).

Less invasive treatment leads to better functional outcome, lower hospitalization periods, less complications and in general higher patient satisfaction (14,15). Therefore, RFA might lead to further improvement of outcome and satisfaction. Literature on RFA for ACT has so far been limited (5,7,16). Therefore, the evolution of ablated tissue over time and recurrence rates after ablation are unknown. The present paper aims to evaluate (mid/long-term) follow-up with regular MRI scans and analysis of the ablated tissue over time.

## Materials & Methods

### Procedure

Diagnosis was based on (incidental) conventional radiographic findings and confirmed on additional MRI. Given the possibility of metastatic disease after ACT and majority of symptoms (e.g. pain, uncertainty), the decision was made to also include cases in which differentiation between ACT and enchondroma was unclear.

RFA was generally carried out in the department of interventional radiology under CT-guidance. In case of large tumors, difficult localizations or comorbidities treatment was carried out in the operation room image guided (fluoroscopy or computer assisted surgery) depending on tumor localization, volume and comorbidities. Tumors with diameter over six cm were generally treated in the operation room because of the possibility to place a prophylactic osteosynthesis to prevent fracture. Procedures were carried out under local anesthesia. Ablation was performed with a Cooltip® RFA needle (Medtronic, United States).

All follow-up was performed in the same center. First follow-up was at three months. A baseline MRI (unenhanced T1-weighted, fat-suppressed T2-weighted and gadolinium-enhanced sequences in two perpendicular planes with 4-mm slice thickness) was made to determine the exact ablation area. On MRI, this area is depicted as an ellipse around the tumor tissue. This ablation area is called the ‘halo’. This elliptic halo consists of granulation tissue as a response to ablation (see figure 1). Dierselhuis et al. found the amount of cell death to correlate well with the MRI aspect (14). All measurements of halo volume were first performed by one blinded investigator. Different follow-up moments within the same patients were not measured consecutively to avoid bias. Subsequently, control measurements were performed by another investigator from the same institution, blinded from the initial measurement result.

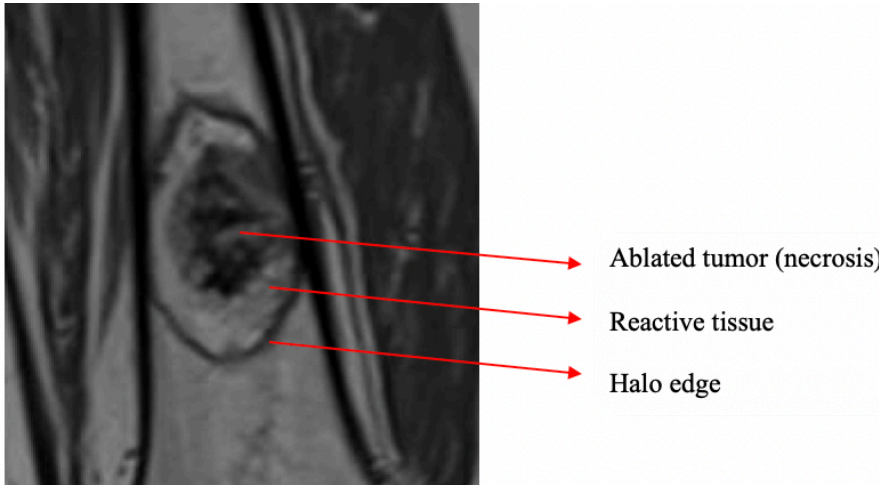


**Figure 1** *Ablation halo around the tumor. The dark outer area of the halo consists of reactive tissue (collateral bone ablation).*

Complete ablation with a margin of  $>2\text{mm}$  all around was considered R0. Complete ablations without this margin were called R1 and incomplete ablations R2. Follow-up was planned for 1-, 2-, 5-, 7- and 10 years after the procedure (17).

### **Data collection**

Data was collected from a prospectively kept tumor database. This study was performed in accordance with the Declaration of Helsinki. According to regulations of the Medical Ethical Review Board of University Medical Center Groningen, patients were informed by means of written information about the fact that anonymous data of the procedure could be used for evaluation of care and scientific research. As the procedure was part of usual care no written or verbal consent was necessary (ethical approval number: METC UMCG 20140028).

All 183 patients with an ACT that were treated with RFA between

2007-2018 were considered for inclusion. Reason for exclusion was intralesional curettage following RFA. For the one-year follow-up moment a difference of four months was accepted. For the later time intervals the maximum accepted difference was 20%. Given the slow growth potential of ACT, tissue outside the ablation halo on the baseline MRI (three months post-operative) has to be the result of incomplete ablation instead of recurrence.

### Data analysis

For all patients tumor volume and halo volume at baseline and after 1-, 2-, 5-, and (if applicable) 7 years was determined. From MR images both tumor- and halo height, width and depth were measured. Since most tumors were elliptical volume was calculated according to the following formula:  $1/6 * \pi * \text{width} * \text{depth} * \text{height}$  (7). To evaluate halo volume, the decrease in volume over time was determined for the periods baseline – one year, baseline – two years, baseline – five years and baseline - seven years follow-up. Figure 2 (A-C) depicts MR images of an ACT in the femur, the ablation halo at baseline and seven years follow-up.

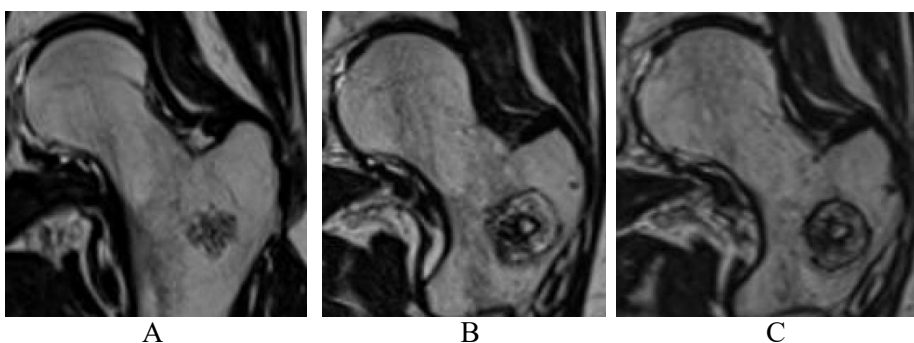


**Figure 2** Low-grade cartilaginous tumor in femur before and after RFA treatment **A.** 3 months pre-operative **B.** 1 year post-operative **C.** 7 years post-operative

Data were analyzed using SPSS Statistics v25 (IBM, Armonk, United States). Data were tested on normality of distribution. To test if volume decrease over time was significant between the different intervals linear regression was used. To examine possible differences between the different time intervals, separate Wilcoxon signed rank tests were performed. For all test an alpha of .05 was chosen.

## Results

In 46 patients intralesional curettage was performed following RFA (in 24 patients as part of a trial with standard curettage four months after RFA) (15). These patients were excluded from analysis. The other 137 patients were eligible for analysis. For 28 patients a re-intervention was carried out within a year (13 times for a complication, 12 times because of incomplete ablation, three times for a different procedure in the same bone). Finally, 27 patients had less than two years follow-up for other reasons (non-adherence, death, other severe disease, follow-up at a different center, other imaging modality than MRI). The halos of the remaining 82 patients were analyzed.

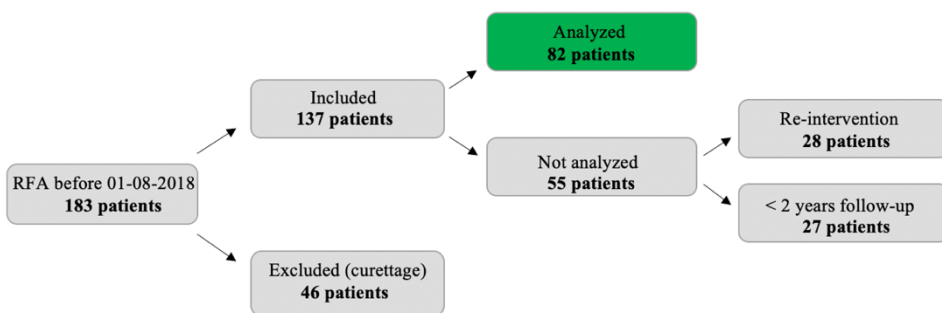


**Figure 3** Flow chart indicating reasons for exclusion



In 73 out of 82 patients (89.0%) complete ablation (R0/R1) was achieved. In these 82 cases one complication (a temporary radial nerve palsy) occurred and no recurrences were found after complete ablation. Halo volume over time was analyzed for all 82 patients. In 45 patients, total follow-up was two years. From the other 37 patients, 30 had five years follow-up, while seven patients had seven years follow-up. Follow-up time was 43.8 months on average (range 19-100 months). Table 1 summarizes the general characteristics of the study population.

**Table 1.** General characteristics of the study population.

| Variable                                | Value              |
|---|--------------------|
| Number of patients                      | 82                 |
| Gender (M/F)                            | 31/51              |
| Age in years                            | 52.0 ( $\pm$ 13.0) |
| Follow-up time in months                | 43.8 (19 – 100)    |
| Treatment result (R0/1/2)               | 63/10/9            |
| Complications                           | 1                  |
| Tumor volume in cm <sup>3</sup>         | 7.67 ( $\pm$ 7.32) |
| Halo volume baseline in cm <sup>3</sup> | 28.6 ( $\pm$ 18.1) |
| Bone (femur/humerus/tibia/fibula)       | 54/20/7/1          |
| Location (diaphysis/DM/metaphysis)*     | 20/11/51           |

\* DM: transition diaphysis to metaphysis

Average halo volume at baseline ( $=28.6 \text{ cm}^3$ ) was 3.7 times larger than the tumor volume ( $7.67 \text{ cm}^3$  on average). Halo volume decreased over time (see figure 4). This was the result of an equal decrease in height, width and depth as depicted in table 2. Volume decrease is expressed relatively to the average volume at baseline (with baseline value separately determined for only the samples with a measurement on that specific time interval). For cases with a measurement both at baseline and after one year, the average halo volume decreased from 28.6 to 22.5 cm<sup>3</sup> ( $= -21.5\%$ ). Between one and two years, average volume decreased from 22.4 to 19.4 cm<sup>3</sup> ( $= -13.5\%$ ). Between two and five years this

decrease was from 14.9 to 12.4 cm<sup>3</sup> (= -5.56% annually) and from five to seven years 7.45 to 6.72 cm<sup>3</sup> (= -4.90% annually). Since not all patients attended all follow-up moments, the absolute volume decrease is mentioned here (not relatively to the average volume at baseline). In none of the patients an increase in halo size was found.

**Table 2** Proportional decrease in halo dimensions between the follow-up moments. Percentages (and range for percentages) are expressed relatively to baseline. Baseline was separately determined for the samples with a measurement at the specific time interval. Since some patients missed one of the appointments, N is not equal for all follow-up moments.

|                    | N  | Height | Width | Depth | Volume            |
|--------------------|----|--------|-------|-------|-------------------|
| Baseline – 1 year  | 73 | 9.00%  | 7.65% | 8.22% | 21.5% (4.55-41.5) |
| Baseline – 2 years | 75 | 13.9%  | 11.9% | 13.3% | 33.6% (9.47-69.2) |
| Baseline – 5 years | 32 | 22.5%  | 18.2% | 19.7% | 47.8% (15.0-83.6) |
| Baseline – 7 years | 7  | 20.7%  | 19.1% | 19.3% | 48.1% (33.4-57.8) |

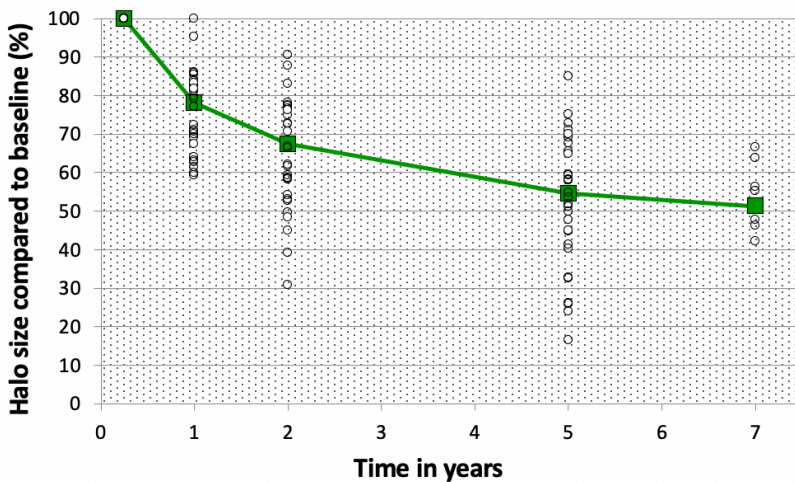


**Figure 4** Halo size compared to baseline value (%) of the ablation halo relatively to the volume at baseline. Percentages are expressed relatively to the volume at baseline. White circles depict the individual cases, the green line depicts the average halo size compared to baseline.

Linear regression showed halo volume decrease over time ( $p < .001$ ). Separate Wilcoxon signed ranks tests demonstrated a significant decrease in volume for every step in follow-up (baseline – 1 year  $p < .001$ , 1 year – 2 years  $p < .001$ , 2 years – 5 years  $p < .001$ , 5 years – 7 years  $p = .043$ ).

## **Discussion**

This is the first study to examine results, complications and halo development during extensive follow-up after RFA for low-grade cartilaginous tumors (ACT, enchondroma). A total of 82 patients with minimum 19 months follow-up was analyzed in the study. Ablation was successful in 73 of 82 cases, complications were rare and halo volume gradually decreased over time. Given the fact additional treatment was carried out for patients with larger residues and for some of the complications, these numbers are slightly lower in clinical practice.

On MRI, the ablation area is depicted as an elliptic halo around the tumor. This halo consists of granulation tissue as a response to ablation. Ablation was considered successful when the complete tumor was within the halo on MRI since the amount of cell death was proven to correlate well with the MRI aspect (14).

Halo volume gradually decreases over time, with about half the volume left after seven years follow-up. Especially in the first two years this decrease is evident, accounting for an average decrease of 32.6%. This is expected to be the result of remodeling around the halo edge. The reactive zone as seen on the edge of the halo on MRI is hypothesized to correspond with inflamed tissue rather than dead/necrotic tissue. Even though the halo volume decreased over time, no tumor tissue was seen outside the halo edge during follow-up. This advocates for a process of bone revitalization around the edge of the halo. Furthermore,

with regard to the fact the average halo volume is already 3.7 times the tumor volume (28.6 vs. 7.67 cm<sup>3</sup>), less aggressive treatment could potentially limit the amount of damaged tissue and therefore lead to a smaller rest defect within less time. However better predictability of the ablation halo is needed to plan for ablations with smaller margin. Future research should be focused on visualizing the ablation area to minimize collateral damage.

Our results are in accordance with literature. Zhao et al. described tissue proliferation and repair to occur between 10 days and 12 weeks after an RFA procedure in six (in vivo) swines, leading to fresh and mature bone trabecula (18). However, they only evaluated the process for 12 weeks. Bucknor et al. found the volume of the ablation zone to decrease with 35.6% for procedures with high energy- and 10.1% for low energy procedures between three and six weeks after ultrasound ablation in eight pigs (19). They reported regeneration of bone with significantly thicker cortices (20). Since in the current data volume was first measured after three months, it cannot be controlled if a similar halo volume decrease can be found for RFA halos in this period.

In the current data there was only one complication and no recurrences were found, meaning that the initial ablation result is a reliable indicator of local tumor control and it is questionable whether long term follow-up is necessary. In contrast, for procedures with incomplete ablation (and subsequently conservative treatment) a profound follow-up still has an important function. Another point of consideration is the fact all volume calculations were done based on measurement of MR images instead of histology. However, in the study of Dierselhuis et al. they found MR images to correspond with histological findings (14). It is expected that new vital tissue develops around the edge of the halo by means of revitalization.

Currently, frequent follow-up (almost annually) is carried out after RFA to control for complications, recurrence or residual tumor activity.

However, the current study indicates such extensive follow-up is not necessary after complete ablation. For instance, a baseline scan at three months followed by a control after one year should be sufficient. Apart from reduced treatment intensity a shorter follow-up might help a patient to finish the experience of being diseased and be able to move on. For incomplete ablations, regular follow-up is still indicated. This hypothesis should be confirmed when our follow-up reaches an average of seven years to include potential late recurrences.

## **Conclusion**

Prolonged follow-up demonstrates halo volume to decrease over time indicating bone regeneration. After seven years, remaining halo volume is only half of its initial value. Ablation result on baseline MRI is a reliable indicator of local tumor control. In 89% of cases RFA is effective at achieving local tumor control in low-grade cartilaginous tumors of long bone, complications are scarce.

## References

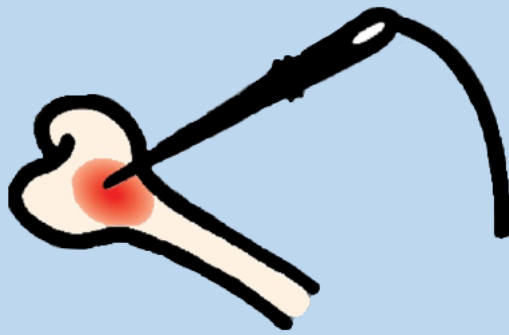
1. Primary bone cancer. (Internet). US National cancer institute; 2021 January 12. Available from: <https://www.cancer.org/cancer/bone-cancer/about/key-statistics.html>
2. Van Praag V, Rueten-Budde AJ, Ho V, Dijkstra PDS, Fiocco M, van de Sande MAJ. Incidence, outcomes and prognostic factors during 25 years of treatment of chondrosarcomas. *Surg Oncol*. 2018 Sep;27(3):402-408
3. Chen X, Yu LJ, Peng HM, Jiang C, Ye CH, Zhu SB et al. Is intralesional resection suitable for central grade 1 chondrosarcoma: A systematic review and updated meta-analysis. *Eur J Surg Oncol*. 2017 Sep;43(9):1718-1726
4. Deckers C, Schreuder BH, Hannink G, de Rooy JW, van der Geest IC. Radiologic follow-up of untreated enchondroma and atypical cartilaginous tumors in the long bones. *J Surg Oncol*. 2016 Dec; 114(8): 987-991.
5. Dierselhuis EF, Gerbers JG, Ploegmakers JJ, Stevens M, Suurmeijer AJ, Jutte PC. Local Treatment with Adjuvant Therapy for Central Atypical Cartilaginous Tumors in the Long Bones: Analysis of Outcome and Complications in One Hundred and Eight Patients with a Minimum Follow-up of Two Years. *J Bone Joint Surg Am*. 2016 Feb 17;98(4):303-13
6. Dierselhuis EF, Goulding KA, Stevens M, Jutte PC. Intralesional treatment versus wide resection for central low-grade chondrosarcoma of the long bones. *Cochrane Database Syst Rev*. 2019 Mar 7;3:CD010778.
7. Nijland H, Overbosch J, Ploegmakers JJW, Kwee TC, Jutte PC. Radiofrequency Ablation for Atypical Cartilaginous Tumors is safe and effective; analysis of 189 consecutive cases. *Open Access Journal of Oncology and Medicine* 3 (5) 2020.
8. Callstrom MR, Charboneau JW: Percutaneous Ablation. Safe, Effective Treatment of Bone Tumors. *Oncology (Williston Park)*. 2005 Oct;19(11 Suppl 4):22-6.
9. Rosenthal DI, Alexander A, Rosenberg AE, Springfield D. Ablation of osteoid osteomas with a percutaneously placed electrode: a new procedure. *Radiology* 1992 Apr;183(1):29-33.
10. Eriksson A, Albrektsson T. Temperature threshold levels for heat-induced bone tissue injury: A vital-microscopic study in the rabbit. *J Prosthet Dent*. 1983 Jul;50(1):101-7.

11. Eriksson A, Albrektsson T, Grane B, McQueen D. Thermal injury to bone. A vital microscopic description of heat effects. *Int J Oral Surg.* 1982 Apr;11(2):115-21.
12. Feldman L, Fuchshuber P, Jones DB. The SAGES Manual on the Fundamental Use of Surgical Energy (FUSE). *Springer* 2012.
13. Schindeler A, Little DG. Bone remodeling during fracture repair: the cellular picture. *Semin Cell Dev Biol.* 2008 Oct;19(5):459-66.
14. Dierselhuis EF, Overbosch J, Kwee TC, Suurmeijer AJH, Ploegmakers JJW, Stevens M et al. Radiofrequency ablation in the treatment of atypical cartilaginous tumours in the long bones: lessons learned from our experience. *Skeletal Radiol.* 2019; 48(6): 881–887
15. Reeves RA, DeWolf MC, Shaughnessy PJ, Ames JB, Henderson ER. Use of minimally invasive spine surgical instruments for the treatment of bone tumors. *Expert Rev Med Devices.* 2017 Nov;14(11).
16. Zou T, Li Q, Zhou X, Yang Z, Wang G, Liu W et al. Remove orthopedic fracture implant with minimal invasive surgery is good for the patient's early rehabilitation. *Int J Clin Exp Med.* 2015 Dec 15;8(12):22377-81.
17. Dierselhuis EF, van den Eerden PJ, Hoekstra HJ, Bulstra SK, Suurmeijer AJ, Jutte PC Radiofrequency ablation in the treatment of cartilaginous lesions in the long bones: results of a pilot study. *Bone Joint J* 2014 96-B(11): 1540-1545.
18. Zhao W, Chen JZ, Hu JH, Huang JQ, Jiang YN, Luo G et al. In vivo effects of radiofrequency ablation on long bones and the repair process in swine models. *Jpn J Radiol.* 2017 Jan;35(1):31-39.
19. Bucknor MD, Rieke V, Seo Y, Horvai AE, Hawkins RA, Majumdar S et al. Bone remodeling after MR imaging-guided high-intensity focused ultrasound ablation: evaluation with MR imaging, CT, Na(18)F-PET, and histopathologic examination in a swine model. *Radiology.* 2015 Feb;274(2):387-94.
20. Bucknor MD, Goel H, Pasco C, Horvai AE, Kazakia GJ. Bone remodeling following MR-guided focused ultrasound: Evaluation with HR-pQCT and FTIR. *Bone.* 2019 Mar;120:347-353.





**Part 2 – looking ahead –  
Towards safe, reliable and  
effective treatment**



# Chapter 5

Experiments on physical ablation of long bone using microwave ablation; defining optimal settings using ex- and in-vivo experiments

H Nijland<sup>1</sup>, J Zhu<sup>2</sup>, TC Kwee<sup>3</sup>, DJ Hao<sup>2</sup>, PC Jutte<sup>1</sup>

1. Department of Orthopaedic Surgery, University Medical Center Groningen, The Netherlands

2. Department of Orthopaedic Surgery, Xi'an Honghui hospital, China

3. Department of Radiology, University Medical Center Groningen, The Netherlands

*PLoS One. 2023 Apr 7;18(4)*

# **Abstract**

## **Background**

Improved survival of cancer patients leads to more skeletal metastatic lesions that need local therapies for tumor control and pain relief. Not all tumors are radiosensitive and alternative therapies are direly needed. Microwave ablation (MWA) is a technique for minimally invasive local tumor control by physical ablation. In soft tissue local temperature ablation is more common, but studies on bone tissue are limited. To ensure safe and effective treatment, studies on local tumor ablation in bone are needed.

## **Method**

Microwave ablation was performed on sheep bone, for both in- and ex-vivo settings. Both a slow-cooking MWA protocol (gradually increasing wattage in the first two minutes of ablation) and a fast-cooking protocol (no warm-up period) were used. Heat distribution through the bone during ablation was determined by measuring temperature at 10- and 15mm from the ablation probe (=needle). Ablation size after procedure was measured using nitro-BT staining.

## **Results**

In-vivo ablations led to up to six times larger halos than ex-vivo with the same settings. Within both ex- and in-vivo experiments, no differences in halo size or temperature were found for different wattage levels (65W vs 80W). Compared to a fast cooking protocol, a two-minute slow cooking protocol led to increased temperatures and larger halos. Temperatures at 10- and 15mm distance from the needle no longer increased after six minutes. Halo sizes kept increasing over time without an evident plateau.

## **Conclusion**

Microwave ablation is technically effective for creating cell death in (sheep) long bone. It is recommended to start ablations with a slow-cooking period, gradually increasing the surrounding tissue temperature in two minutes from 40 to 90°C. Ex-vivo results cannot simply be translated to in-vivo.

## Introduction

Improved survival of cancer patients leads to more skeletal metastatic lesions that are amenable to local therapies for tumor control and pain relief (1). Not all tumors are radiosensitive and alternative therapies are direly needed. Microwave ablation (MWA) is a technique for minimally invasive tumor treatment. It is frequently used for local control in soft tissue malignancies like liver-, kidney- and lung cancer lesions (2,3). Heat distribution depends on power (watts), ablation time (minutes) and bone properties. Higher power and longer time likely lead to larger ablation areas (halo). Literature on relations between time and energy have so far only been published for radiofrequency ablation (4). Therefore, optimal settings for individual lesions are unknown. Safe and effective procedures cannot be done without those studies.

At temperatures over 60 °C instant cell death occurs by coagulative necrosis. Between 50-60 °C it takes 1-6 minutes to reach complete cell death (5-7). Therefore, to ensure complete ablation, temperature at the outer edge of the tumor should reach over 60°C. In the surrounding areas heat-induced stress leads to apoptosis by disturbance in mitochondrial pathways and caspase activation. Furthermore reactive oxygen species (ROS) create oxidative damage and disturb mitochondrial functioning thereby altering the rate of apoptosis (8-10). The cell is protected against heat-induced apoptosis by activation of heat shock proteins (11). They inhibit caspase activation and stabilize proteins, thereby confirming correct folding (chaperone function). In clinical procedures temperature is aimed at 90 °C to ensure temperature over 60°C in the complete tumor. It is expected that temperature decreases during conduction through the tissue as a result of (micro)vascularity. After ablation with temperatures under 60°C tissue has the capability to recover, leading to possible tumor recurrence. At temperatures over 100 °C vaporization of water (leading to desiccation of the cell) and carbonization occur. These factors potentially limit heat

conduction (12-14). In figure 1, a model is shown depicting the tissue reaction to increasing temperatures (15).

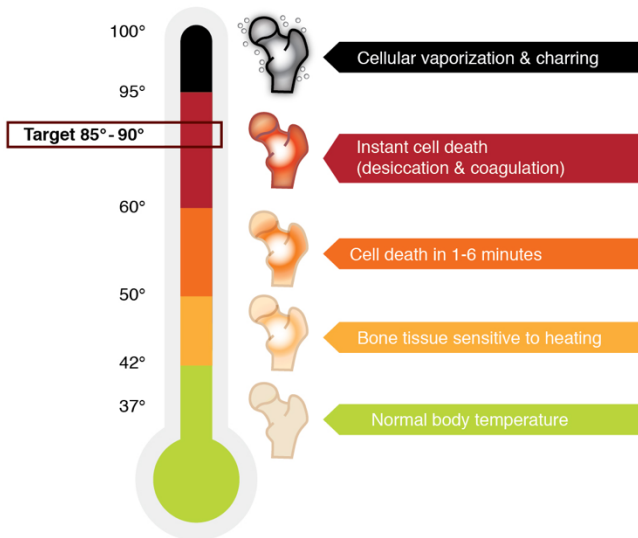


**Figure 1** Tissue reaction to heat (15). Ideal temperature for ablation is 60-95 °C since instant cell death is the aim. Below 60 °C cells may recover. Above 100 °C carbonization occurs, limiting distribution of heat.

Literature on safety and efficacy of local temperature ablation in bone tissue is still limited. A wide range of wattage levels is used for clinical MWA. Given the fact MWA leads to larger ablation zones compared to alternatives like radiofrequency ablation, clinical use might result in excessive margin or incomplete ablation. An excessive margin could lead to damage to surrounding structures, incomplete ablation to lack of local control (16). To ensure safe and effective ablation it is essential to develop a reliable prediction of the ablation area for different settings. In this study we compared different settings to study the effects of wattage level and ablation time on halo size.

## **Method**

### **Ablation procedure**

All ablations were performed with a 2.45GHz Kang-You 2000 microwave ablation generator (Kang-You Medical, Nanjing, China). The needle had an active part of three cm long and a diameter of 17 gauge. Internal cooling of the needle was performed, preventing temperatures over 45 °C in the non-active part. Needles were cleaned with alcohol between procedures and replaced when the protective insulation layer started to show damage. An ex-vivo study was performed to determine heat distribution and halo size for a wide range of settings. Subsequently the most promising settings were transferred into an in-vivo study.

### **Ex-vivo**

Fresh sheep femur (from sheep aged 1 – 1.5 years with an average weight of 50kg) were collected from the slaughterhouse. These bones were chosen given the similarity to human bone anatomy. The lower extremity is the most common location for metastases and tumors in human bone (17). Ablation was performed within 6-12 hours after sacrifice to ensure bone quality was as close to physiological and vital bone as possible. First, the bones were put into a reservoir containing water with an aimed temperature of 37°C (range 37-40°C) for 20-30 minutes to mimic body circumstances. Before starting ablation, inner bone temperature was controlled.

To prevent carbonization as a result of over-rapid temperature increase around the needle tip (which is thought to limit heat distribution), a protocol for slow-cooking was developed. According to this protocol wattage was slowly increased towards the aimed setting: 10W for one minute, followed by one minute at 20W. These two minutes were included in the time intervals as mentioned for the slow-cooking ablations (see next paragraph). Furthermore, a fast-cooking protocol was developed. In this protocol ablation was directly started at the

aimed maximum wattage. Results of both protocols were compared.

### *Heat distribution*

The tract for the ablation needle was drilled in the proximal metaphysis of sheep femur at a depth of 30mm. Through this tract the ablation needle was brought up. Temperature was measured by a Kang-You temperature probe (21 gauge). Tracts for the temperature probe were drilled 5, 10 or 15mm lower in the same direction as the ablation needle (see figure 2a). Only one distance was measured per ablation session to prevent heat leakage. During ablation, temperature was live recorded. A 3D-printed navigation tool (see figure 2B) was designed to standardize distance and needle direction, thereby minimizing variation between measurements. The tool was made from PA12 nylon and had holes with a diameter of two mm at 5-, 10- and 15mm from a central tunnel.

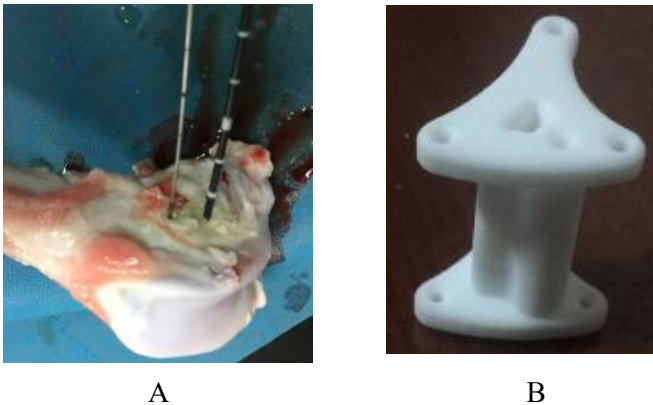


**Figure 2:** *A. Ablation in a sheep femur metaphysis with temperature probe at 10mm. B. The 3D-printed navigation tool.*

A total of ten settings was used, with wattages of 65W (6 and 12 minutes fast-cooking and 6, 8, 10, 12 minutes slow cooking) and 80W (6, 8, 10, 12 minutes slow-cooking). The aim of this was to determine the contribution of each parameter or setting on halo size. For each setting 10 measurements were performed.



Between two and eight hours after ablation the bones were cut in the coronal plane at the insertion point of the needle using an automatic saw with a 1-mm thick blade. Subsequently the coupes were stained in a Nitro-BT solution (nitro blue tetrazolium chloride) and incubated in a 37 °C incubator for three hours (see figure 3b). This solution was made according to Nachlas et al. using eight parts of H<sub>2</sub>O, one part phosphate buffer solution and one part Nitro-BT (18). As a result of staining, healthy tissue turns purple (see figure 3c). Dimensions before and after staining were measured and compared. Measurements were corrected with 1mm to correct for the bone loss by the saw blade (1mm loss was objectivated in our trials).

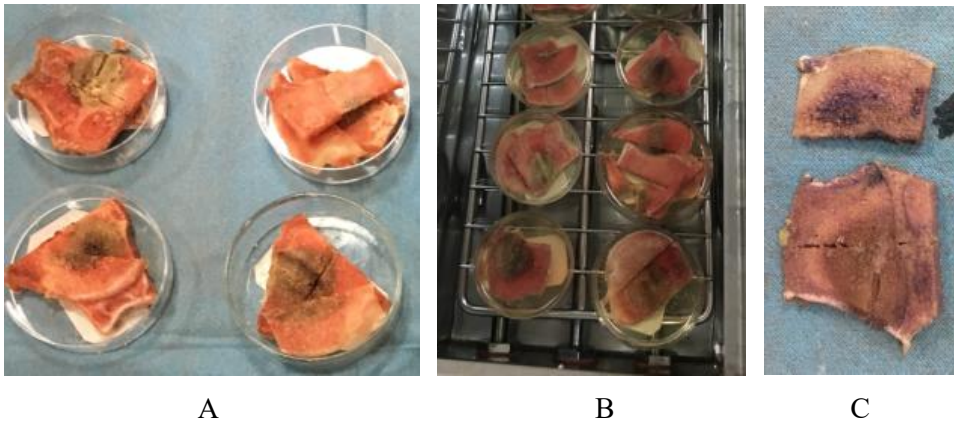


**Figure 3** Staining of sheep proximal femur metaphysis samples after ablation. *A.* Samples before staining. *B.* Samples in the incubator. *C.* Sample after staining in Nitro-BT solution.

### **In-vivo**

In-vivo MWA was performed in 12 sheep femurs, using the same protocol as the ex-vivo experiments. For four sheep ablation was performed with 65W for six minutes, for four sheep 65W for 12 minutes and for four sheep 80W for six minutes. Heat distribution was measured at 10- and 15mm for 65W ablations (one distance per ablation) and at

10mm for 80W ablations (not at 15mm based on ex-vivo results and to limit the number of sheep needed). Before starting the procedure, the sheep were sedated by a veterinarian with an intramuscular injection of 5 ml Shutai (1 : 1 combination of Tiletamine 50mg/ml & Zolazepam hydrochloride 50mg/ml) (Virbac, France) and subsequently intubated. During the procedure inhaled isoflurane (1-5%) was used for general anesthesia and a maintenance dose up to 2.5ml Shutai was given in case deemed necessary by the veterinarian. Sheep were sacrificed one week after the procedure, bones were cut and halo size was determined after staining (with the same procedure as ex-vivo). The in-vivo study was approved by the medical ethical committee of the Xi'an HongHui hospital.

### **Data analysis**

Technical issues like sudden temperature drops, temperature differences more than two standard deviations (SDs) from the average value (for at least three time intervals) and high impedance (desiccated tissue in a few ex-vivo bones) warranted exclusion from the analysis.

Data were analyzed using SPSS v25 (IBM, Armonk, United States). Values for temperature and halo dimensions were noted as mean ( $\pm$ SD). Halo volume was calculated according to the formula:

$$\frac{4}{3} * \pi * (\frac{1}{2} * \text{height}) * (\frac{1}{2} * \text{width}) * (\frac{1}{2} * \text{depth}) = \frac{1}{6} * \pi * \text{height} * \text{width} * \text{depth}.$$

Data were examined using non-parametric tests due to the relatively small group size. Differences between fast- and slow-cooking, 65W and 80W, and in- and ex-vivo were tested using a mixed repeated measures ANOVA design. Sphericity and equality of differences were controlled. Data were tested for time up to six minutes (after six minutes temperature remained stable and variance at these intervals is very limited). For all tests a p-value of  $< .05$  was considered significant.

# Results

## Ex-vivo heat distribution

For the slow-cooking samples, temperature remained below 60 °C during the two-minute slow-cooking period. For both 65W and 80W temperature exceeded 60 °C within three minutes at 10mm and within five minutes at 15mm. There was no significant difference in temperature over time between 65W and 80W (at 10mm  $F(5,55) = 1.43$ ,  $p = .228$ , at 15mm  $F(5,60) = 1.68$ ,  $p = .152$ ). For the fast-cooking samples, initial temperature increase was fast with temperature reaching up to 60 °C within two minutes at 10mm from the needle. At 15mm temperature increase was similar to the slow-cooking samples. After the initial fast increase, temperatures increased more gradually compared to the slow-cooking samples. From five minutes onwards temperature was significantly lower at both 10mm ( $F(5,55) = 35.19$ ,  $p < .01$ ) and 15mm ( $F(5,65) = 7.23$ ,  $p < .01$ ). The values are depicted in table 1 and figure 4 (A-B).

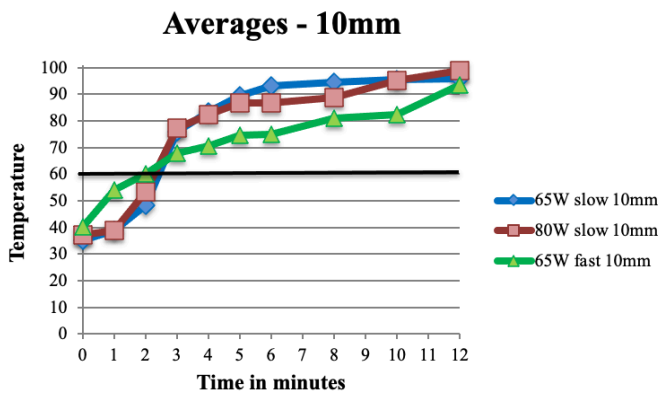


**Figure 4 A.** Averages at 10mm for 65W slow- and fast cooking and 80W slow-cooking. Black line depicts the aimed temperature of 60°C.

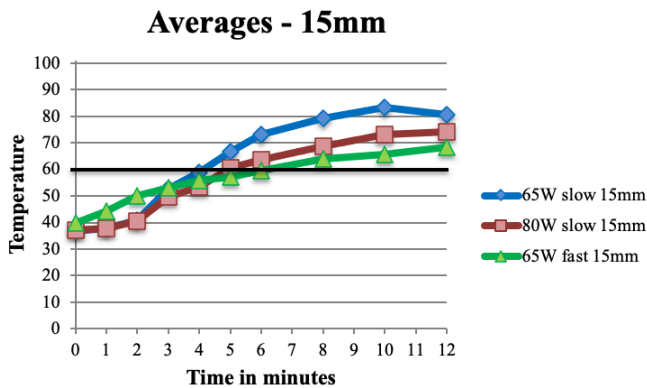


**Figure 4 B.** Averages at 15mm for 65W slow- and fast cooking and 80W slow-cooking. Black line depicts the aimed temperature of 60°C.

### Ex-vivo halo size

Halo volume gradually increased over time. The major part of the halo was formed within the first six minutes. Halo size continued to increase up to the 12-minute measurement but was not significantly larger at twelve minutes compared to six minutes for the slow cooking samples (65W  $p = .067$ , 80W  $p = .421$ ). For the fast cooking samples halo size after 12 minutes was significantly larger ( $p = .024$ ). This is contrary to the heat distribution data where almost no further increase was seen in the period after six minutes. There was no difference in halo size between 65W and 80W ( $p = .890$ ) or between fast- and slow-cooking ( $p = .861$ ). Values for volume are depicted in table 1.

**Table 1.** Halo volume vs time for different settings for microwave ablation. Blue = 65W slow-cooking, red = 80W slow-cooking, green = 65W fast-cooking.

| Setting           | Height (mm)  | Width (mm)   | Depth (mm)   | Volume (cm <sup>3</sup> ) |
|-------------------|--------------|--------------|--------------|---------------------------|
| 65W, 6 min, fast  | 14.7 (±0.58) | 20.3 (±1.15) | 14.3 (±1.53) | 2.23 (±0.36)              |
| 65W, 12 min, fast | 19.8 (±3.13) | 19.0 (±1.10) | 18.7 (±2.42) | 3.68 (±1.10)              |
| 65W, 6 min, slow  | 14.7 (±2.08) | 20.3 (±3.06) | 16.0 (±1.00) | 2.50 (±0.36)              |
| 65W, 8 min, slow  | 16.0 (±1.84) | 20.8 (±1.83) | 17.8 (±2.68) | 3.10 (±0.83)              |
| 65W, 10 min, slow | 16.5 (±3.33) | 21.4 (±1.80) | 19.5 (±2.38) | 3.61 (±0.95)              |
| 65W, 12 min, slow | 17.6 (±3.57) | 21.4 (±1.77) | 20.2 (±2.07) | 3.98 (±1.23)              |
| 80W, 6 min, slow  | 13.0 (±1.87) | 20.2 (±1.92) | 19.6 (±1.14) | 2.69 (±0.66)              |
| 80W, 8 min, slow  | 14.6 (±2.64) | 20.8 (±2.31) | 18.5 (±4.41) | 2.94 (±0.70)              |
| 80W, 10 min, slow | 14.9 (±2.97) | 20.3 (±1.04) | 18.3 (±3.01) | 2.90 (±0.90)              |
| 80W, 12 min, slow | 16.7 (±2.26) | 21.6 (±1.75) | 19.5 (±2.45) | 3.68 (±0.75)              |

### In-vivo heat distribution

For in-vivo ablations, heat distribution was significantly smaller compared to ex-vivo (at 10mm  $F(5,65) = 17.69$ ,  $p < .01$ , at 15mm  $F(5,65) = 6.58$ ,  $p < .01$ ). At 10mm temperature reached over 60 °C after four to five minutes (for 80W and 65W respectively), at 15mm (with 65W) this occurred after nine minutes. Temperature remained below the ‘safe’ 60 °C for a longer time than in ex-vivo. Values are depicted in figure 5.

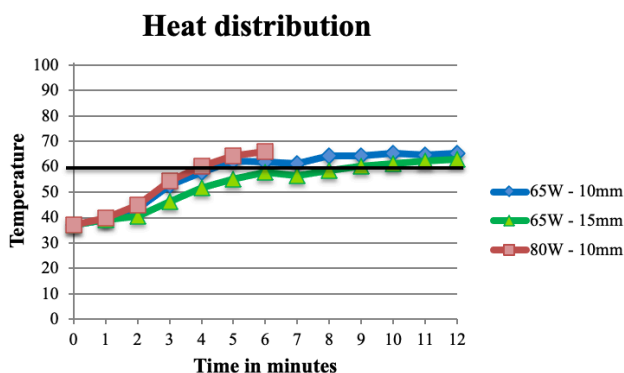


**Figure 5** Heat distribution for in-vivo MWA in sheep femur. Blue = 65W – 10mm, green 65W – 15mm, red = 80W – 10mm. Black line depicts the aimed temperature of 60°C.

### In-vivo halo size

Halo size in-vivo was significantly larger than ex-vivo ( $p < .01$ ). Halo size did not significantly increase between six and twelve minutes ablation ( $p = .857$ ). There was no significant difference in halo size between 65W and 80W either ( $p = .057$ ). Table 2 depicts the mean dimensions for in-vivo ablation. In figure 6 the heat distribution ex-vivo is compared to in-vivo.

**Table 2** Halo size in vivo.

| Setting     | Height (mm)         | Width (mm)          | Depth (mm)          | Volume (cm <sup>3</sup> ) |
|-------------|---------------------|---------------------|---------------------|---------------------------|
| 65W, 6 min  | 35.3 ( $\pm 6,11$ ) | 33 ( $\pm 8,37$ )   | 30 ( $\pm 9,20$ )   | 23.0 ( $\pm 5,42$ )       |
| 65W, 12 min | 34.8 ( $\pm 11,8$ ) | 39.0 ( $\pm 2,16$ ) | 40.8 ( $\pm 6,55$ ) | 28.9 ( $\pm 11,0$ )       |
| 80W, 6 min  | 29.3 ( $\pm 0,96$ ) | 30.0 ( $\pm 4,08$ ) | 31.0 ( $\pm 5,89$ ) | 14.4 ( $\pm 4,10$ )       |

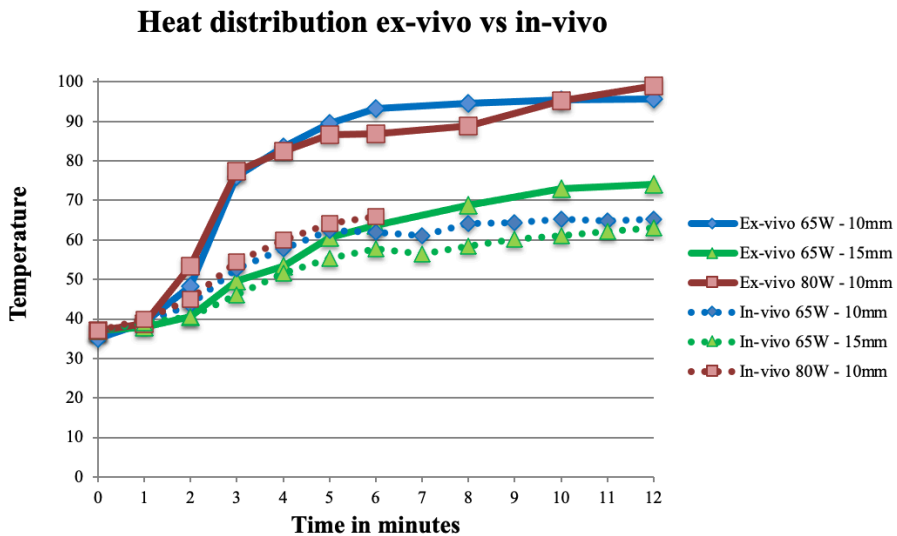


**Figure 6** Heat distribution ex-vivo vs in-vivo. In-vivo temperatures are significantly lower.

## Discussion

This study is the first to examine the effect of different settings for microwave ablation in long bone in an experimental setting. Since both ex-vivo and in-vivo experiments were performed, results are likely transferrable to the clinical setting. Results prove microwave ablation is technically effective for creating cell death in (sheep) long bone in a minimally invasive manner. Ablation with 65W is sufficient, the major portion of cell death is formed in the first six minutes of ablation, slow-cooking is better than fast-cooking and ex-vivo halo size is smaller than in-vivo halo size. This data indicates ‘aggressive’ ablation with high wattages and longer time intervals does not lead to better results. To reduce risk of complications ablation settings must be determined with caution.

Assumptions regarding the relationship between cell death and temperature as postulated in literature (see figure 1) do not match with the current (ex-vivo) data. According to literature, cell death occurs instantly at temperatures over 60 °C or after 1-6 minutes at 50-60 °C (5-7, 18). In the present study, temperatures measured at 10mm from the needle exceeded 60° C within three minutes for ex-vivo ablations. This indicates a 20mm diameter halo with temperature over 60 °C, when assuming equal distribution of heat through the bone. The ablation halo only reached a diameter of 20mm after 10-12 minutes in the ex-vivo experiments. Therefore, there seems to be a delay between temperature over 60 °C and corresponding cell death. This is in line with the fact that temperature at 10- and 15mm from the needle does not further increase after six minutes, whereas halo size gradually does. A probable explanation for this is slow growing heat flow due to conduction of the tissue. This becomes slower as tissue loses its water content. However, halo size after 12 minutes was not significantly larger than after six minutes ( $p = .857$ ). In-vivo halo size corresponded better with the expected halo size based on assumptions of cell death as described in figure 1 than ex-vivo (cell death at temperatures over

60°C). Temperatures at 15mm were close to 60 °C after six minutes. Halo dimensions around 30mm for height, width and depth correspond to this (when assuming equal distribution of heat through the bone).

### **Heat distribution**

Temperatures at 10- and 15mm from the needle were higher ex-vivo than in vivo. This is most likely due to in-vivo heat sink, for instance by (micro)vascularity in and around the bone. In the study of Ji et al. they measured temperature at 5, 10, 15 and 20mm (parallel array of probes) from the needle tip during a 36-minute microwave ablation in dog femur (amount of Watt not described) (19). They found temperature to increase rapidly in the first six minutes leading to temperatures of 86.4 °C at 5mm, 74.0 °C at 10mm and 54.1 °C at 15mm after six minutes. At 20mm, temperature only reached 42.0 °C. In the next 30 minutes temperature only increased with another 5-10% at all distances. A limitation of their study is that they used a parallel array of probes. This potentially creates a large artificial heat sink (dependent of thermal couple properties) because the metal of the antenna will conduct heat more easily than the surrounding bone, leading to a significant amount of heat loss. Furthermore, they only used one ablation setting and a small number of cases.

### **Halo size**

Interestingly, halo size was larger in the in-vivo samples than ex-vivo, regardless of the lower temperatures at 10- and 15mm from the needle. A possible explanation for the difference between in- and ex-vivo halo size is the time between ablation and halo measurement. In the in-vivo experiment the animals were sacrificed after one week and subsequently halo size was measured whereas ex-vivo measurement was done within hours after the ablation. The cells that were identified dead in the in-vivo experiment could be the effect of both necrosis as well as apoptosis, whereas in the ex-vivo experiment only the effect of necrosis can be seen (since analysis was done shortly after ablation). There might also be an effect of late-apoptosis in the in-vivo



experiments, for instance because of ROS activity. However, it is not likely that differences as large as found in our data only originate from follow-up time after ablation (20-21).

### **Settings**

An increase in wattage level from 65W to 80W did not lead to larger halos or higher temperatures at 10- and 15mm from the needle. Therefore, a wattage of 65W is considered sufficient. Further increase of the wattage only increases risk of complications. Potentially a similar outcome could be found for even lower wattage levels. This could be examined in further research. Between fast- and slow cooking significant differences in heat distribution were seen. In the fast-cooking group temperature at 10- and 15mm is higher during the first two minutes of ablation compared to slow-cooking. However, from five minutes onwards the temperature of the slow-cooking group is significantly higher. This effect is hypothesized to be the result of carbonization around the needle as a result of over-rapid heating in the fast-cooking samples. This carbonized tissue can (partially) block the distribution of heat through the bone. Therefore, we recommend to use a two-minute slow-cooking period at every ablation to ensure gradual heating of the tissue. Since halo size mainly increased in the first six minutes, longer ablations than six minutes are not encouraged.

This study had some limitations. First, positioning of the drill was done by hand and without image-guidance. Therefore, small differences between the measurements cannot be ruled out. For all ex-vivo experiments at least seven samples were included to ensure a reliable outcome. Distance between needle and temperature probe was standardized using a navigation tool, thereby also ensuring same direction and limiting variation between samples as a result of human error. This tool was also used for the in-vivo experiments. Second, for the in vivo experiments only four animals were used per setting and there was substantial variance in halo size between the animals. For the in-vivo study animals were sacrificed after one week and subsequently

analyzed whereas ex-vivo analysis was performed on the day of ablation. Finally, experiments were performed in healthy bone without tumor tissue.

## **Conclusion**

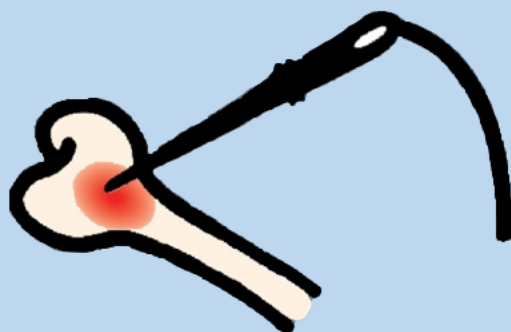
Microwave ablation is technically effective for creating cell death in (sheep) long bone. It is recommended to start ablations with a slow-cooking period, gradually increasing the surrounding tissue temperature in two minutes from 40 to 90°C. Ex-vivo results cannot simply be translated to in-vivo, given in-vivo halo volume was up to six times larger than ex-vivo. The technique still faces issues like high variability and therefore limited predictability, before it can become mainstream treatment. Future experiments and development should focus on ways to reduce this.

## References

1. Coleman RE. Clinical features of metastatic bone disease and risk of skeletal morbidity. *Clin Cancer Res.* 2006;12(20 Pt 2):6243s-6249s.
2. Facciorusso A, Di Maso M, Muscatiello N. Microwave ablation versus radiofrequency ablation for the treatment of hepatocellular carcinoma: A systematic review and meta-analysis. *Int J Hyperthermia.* 2016;32(3):339-344.
3. Caroline F. Simon, Damian E. Dupuy, William W. Mayo-Smith, Microwave ablation: Principles and applications, *Radio Graphics*, 25, S69-S83, 2005.
4. Goldberg SN, Gazelle GS, Halpern EF, Rittman WJ, Mueller PR, Rosenthal DI. Radiofrequency tissue ablation: importance of local temperature along the electrode tip exposure in determining lesion shape and size. *Acad. Radiol.* 1996 Mar;3(3):212-8.
5. Eriksson AR, Albrektsson T: Temperature threshold levels for heat-induced bone tissue injury: A vital-microscopic study in the rabbit. *J Prosthet Dent.* 1983 Jul;50(1):101-7.
6. Eriksson A, Albrektsson T, Grane B, McQueen D. Thermal injury to bone. A vital microscopic description of heat effects. *Int J Oral Surg.* 1982 Apr;11(2):115-21.
7. Feldman L, Fuchshuber P, Jones DB. The SAGES Manual on the Fundamental Use of Surgical Energy (FUSE). *Springer* 2012.
8. Nijhuis EHA, Poot AA, Feijen J, Vermes I. Induction of apoptosis by heat and  $\gamma$ -radiation in a human lymphoid cell line; role of mitochondrial changes and caspase activation. *International Journal of Hyperthermia*, 22:8, 687-698,
9. Gu ZT, Wang H, Li L, et al. Heat stress induces apoptosis through transcription-independent p53-mediated mitochondrial pathways in human umbilical vein endothelial cell. *Sci Rep.* 2014;4:4469. Published 2014 Mar 26.
10. Thompson SM, Callstrom MR, Butters KA, et al. Heat stress induced cell death mechanisms in hepatocytes and hepatocellular carcinoma: in vitro and in vivo study. *Lasers Surg Med.* 2014;46(4).
11. Beere HM. 'The stress of dying': the role of heat shock proteins in the regulation of apoptosis. *J. Cell Sci.* 2004 Jun 1;117(Pt 13)
12. Brace CL. Thermal Tumor Ablation in Clinical Use. *IEEE Pulse* 2011;2(5):28-38.

13. Lavergne T, Sebag C, Ollitrault J, Chouari S, Copie X, Le Heuzey JY et al. Radiofrequency ablation: physical bases and principles. *Arch Mal Coeur Vaiss* 1996 Feb;89 Spec No 1: 57-63.
14. Issa ZF, Miller JM, Zipes DP. Clinical Arrhythmology and Electrophysiology. Chapter 7: Ablation energy sources. 2nd ed. Elsevier 1983.
15. Nijland H, Overbosch J, Ploegmakers JJW, Kwee TC, Jutte PC. Radiofrequency Ablation for Atypical Cartilaginous Tumors is safe and effective; analysis of 189 consecutive cases. *J Clin Med*. 2021 Apr 22;10(9):1817.
16. Vietti Violi N, Duran R, Guiu B, Cercueil JP, Aubé C, Digkila A et al. Efficacy of microwave ablation versus radiofrequency ablation for the treatment of hepatocellular carcinoma in patients with chronic liver disease: a randomised controlled phase 2 trial. *Lancet Gastroenterol Hepatol*. 2018 May;3(5):317-325.
17. Website: [www.cancer.org/treatment/understanding-your-diagnosis/advanced-cancer/bone-metastases.html](http://www.cancer.org/treatment/understanding-your-diagnosis/advanced-cancer/bone-metastases.html) - accessed on August 8, 2021
18. Nachlas MM, Shnitka TK. Macroscopic identification of early myocardial infarcts by alterations in dehydrogenase activity. *Am J Pathol*. 1963 Apr;43:379-405
19. Ji Z, Ma Y, Li W, Li X, Zhao G, Yun Z et al. The Healing Process of Intracorporeally and In Situ Devitalized Distal Femur by Microwave in a Dog Model and Its Mechanical Properties In Vitro. *PLoS One* (2012);7(1).
20. Gu ZT, Wang H, Li L, et al. Heat stress induces apoptosis through transcription-independent p53-mediated mitochondrial pathways in human umbilical vein endothelial cell. *Sci Rep*. 2014;4:4469.
21. Vanagas T, Gulbinas A, Sadauskiene I, Dambrauskas Z, Pundzius J, Barauskas G. Apoptosis is activated in an early period after radio-frequency ablation of liver tissue. *Hepatogastroenterology* 56 (93).





# Chapter 6

Animal experiments show that minimally  
invasive microwave ablation of bone is not  
safe enough for clinical application

H Nijland<sup>1</sup>, J Zhu<sup>2</sup>, DJ Hao<sup>2</sup>, TC Kwee<sup>4</sup>, PC Jutte<sup>1</sup>

1. Department of Orthopaedic Surgery, University Medical Center  
Groningen, The Netherlands

2. Department of Orthopaedic Surgery, Xi'an Honghui hospital, China

3. Department of Radiology, University Medical Center Groningen,  
The Netherlands

*Submitted to International Journal of hyperthermia*

# Abstract

## Background

Microwave ablation (MWA) is a technique for minimally invasive local tumor treatment. Studies on local tumor ablation in bone tissue are limited. To ensure safe and effective treatment, more knowledge on the direct effects and the processes taking place in the first weeks after ablation is needed.

## Method

In-vivo bone MWA was applied on 24 sheep femurs with different settings for power and time. Sheep were sacrificed one or six weeks after treatment. Before sacrifice, halo size (ablation area) was measured on MRI. After sacrifice, lactate dehydrogenase (LDH) staining of specimen was performed to assess vitality of cells. Both measurements were compared to validate the accuracy and safety of MWA as well as the accuracy of MRI in predicting actual tissue death.

## Results

There was a large variability in halo size within the same and between different settings. No significant decrease in halo size was seen between one and six weeks follow-up. No differences in halo size were found for different time- or wattage settings after one week follow-up. After six weeks halo size was larger for increased ablation time ( $p = .029$ ). At six weeks follow-up, halo size on MRI was 43% larger than on histology ( $p = .002$ ). In 10 out of 24 sheep a complication occurred.

## Conclusion

MWA is effective in bone tissue. However, given the high variability in halo size and high complication rates, the current data advocate against MWA to replace current treatment options for bone tumors like curettage surgery and radiofrequency ablation.



## Introduction

With increased cancer survival there is a rise of (secondary) bone malignancies that require treatment (1). One of the main aims of treatment is local tumor control and relief of pain. Microwave ablation (MWA) is a technique for minimally invasive local tumor treatment (2-4). So far, it has mainly been used in liver and lung tissue (5-6). The effect of MWA in bone has only recently been described in the literature (7). To ensure safe and effective treatment in bone, more knowledge is needed on the direct effects of MWA and the processes taking place (during follow-up) after treatment. Furthermore, the effect of different factors of treatment (for instance ablation time, wattage level) on the size of the treated area (halo size) is unknown.

In MWA, heat is produced by continuous realignment of H<sub>2</sub>O molecules (i.e. spinning) (4). According to an earlier model developed by our group, instant cell death occurs at temperatures over 60°C (8). Between 50-60°C it takes 1-6 minutes to reach complete cell death (9-10). To ensure complete ablation, a target temperature of >60°C should be reached up to the edge of the tumor. The result of ablation is a halo of necrotic tissue around the tumor. Around the edge of this halo an area with thermally damaged, but not necrotic tissue exists. We hypothesize regeneration of this tissue to occur in the period after ablation.

For clinical follow-up of the halo, MRI is the most commonly used modality. On MRI the halo appears as an isointense center with hyperintense rim on T1-weighted MRI and as a slightly hypointense center with hyperintense rim on T2-weighted MRI (11). The hyperintense rim on both T1-weighted MRI and T2-weighted MRI is thought to represent the edge of the halo. However, no literature has been published comparing halo size on MRI with histology. If MRI is validated for estimating halo size, it could be used to follow-up lesions over time.

The purposes of this study were to determine whether MWA is effective in bone tissue, what the effect of time and wattage on ablation result are and whether minimally invasive MWA could safely be applied in an in-vivo setting.

## **Method**

### **Microwave ablation**

All ablations were performed with a 2.45GHz Kang-You 2000 microwave ablation generator (Kang-You Medical, Nanjing, China). Needles were internally cooled to prevent temperatures over 45°C in the non-active part. The active part of the needle was three cm long and needle diameter was 17 gauge. From clinical experience with radiofrequency ablation (RFA) and pilot studies with MWA we developed a model for slow-cooking, in which temperature is slowly increased towards the aimed temperature. Maximum temperature should always remain below 100 °C, to prevent local carbonization. Every ablation started with 10W for one minute, followed by one minute at 20W.

### **Procedure**

For the experiments, permission was obtained from the medical ethical committee of the HongHui hospital, Xi'an. All sheep were aged 1 – 1.5 years and had an average weight of 50kg, to mimic human bone specifics. Before starting the procedure, the sheep were sedated by a veterinarian with an intramuscular injection of 5 ml Shutai (1 : 1 combination of Tiletamine 50mg/ml & Zolazepam hydrochloride 50mg/ml) (Virbac, France) and subsequently intubated. During the complete procedure inhaled isoflurane (1-5%) was used for general anesthesia and a maintenance dose up to 2.5ml Shutai was given in case deemed necessary by the veterinarian. Ablation was carried out in the

distal metaphysis of the femur, at a depth of 30mm. Both a one-week follow-up group and a six-week follow-up group were used to examine differences in halo size as a result of early regeneration of damaged (but not necrotic) tissue around the halo edge. Sheep were randomly divided into the one- or six week group. For both follow-up periods, three settings were examined; 65W – 6 min, 65W – 12 min and 80W – 6 min. Each setting was performed in four different sheep, leading to a total of 24 sheep. The sheep in the one-week group went for MRI seven days after surgery and were sacrificed the day after. The other sheep had an MRI after six weeks and were sacrificed afterwards. Sheep were controlled for possible complications of treatment before sacrifice. Complications were registered for analysis.

MRI examinations were performed on a 3T system. Unenhanced T1-weighted, and fat-suppressed T2-weighted sequences in two perpendicular planes (coronal and axial) to the bone with 4-mm slice thickness were acquired in each sheep.

After the MRI the sheep were sacrificed. The bones were harvested and cut in the coronal plane at the insertion point of the needle using a 1mm automatic saw. Subsequently, samples were cut in the sagittal plane. Samples were stained in a Nitro-BT solution (nitro blue tetrazolium chloride) and incubated in a 37°C incubator for three hours. This solution was made according to Nachlas et al. using eight parts of H<sub>2</sub>O, one part phosphate buffer solution and one part Nitro-BT (12). In this staining, healthy tissue turns from pink/orange into purple. Measurements were corrected with 1mm since the samples were split by the saw. To ensure the halo edge as observed by bare eye and on MRI corresponds with cell death on a microscopic level, the halo edge of all samples in the six-weeks group was microscopically analyzed. A sample of 10×10mm was cut from the edge of the halo and subsequently decalcified (96 hours) and embedded into paraffin wax. The samples were stained in hematoxylin-eosin (H&E) and cut by a microtome. Analysis was done by a pathologist.

**Data analysis**

Data were analyzed using SPSS v25 (IBM, Armonk, United States). Halo dimensions were noted as mean ( $\pm$ SD). Data was examined using Mann-Whitney-U tests due to the relatively small group size and low amount of variance within the groups. P-values of  $< .05$  were considered significant. Effect of wattage level (65W vs 80W) and ablation time (6 vs 12 minutes for ablations with 65W) on halo size were assessed. Furthermore, halo size after histology was compared to MRI within samples.

## Results

At both one week and six weeks follow-up, halos were round/elliptically shaped and filled the major part of the metaphysis. The central part of the halo was darker though not carbonized. Around this dark core there was a lighter zone, surrounded by another dark rim (see figure 1a). This rim turned purple after staining at both time intervals (see figure 1b). The lighter zone around the core did not turn purple after one week, but did after six weeks for the majority of samples (see figure 1c). Therefore, this zone was interpreted as reactive tissue instead of necrosis. However, there was a lot of variance in halo size within and between settings.

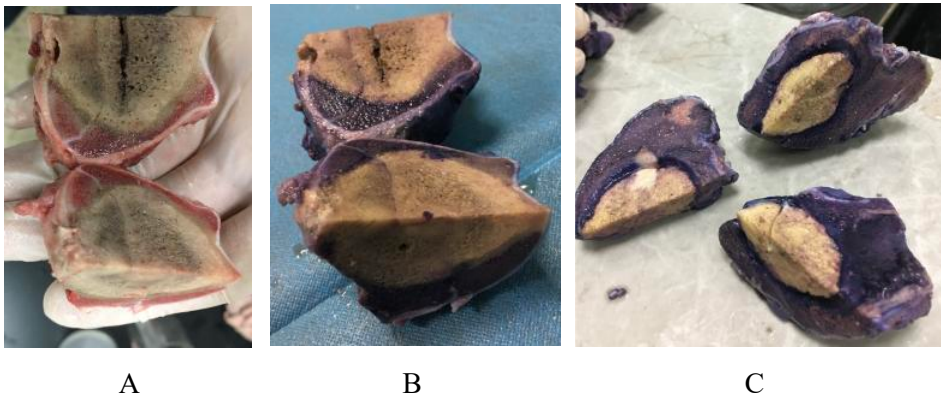


**Figure 1** *Samples after ablation, cut in the coronal and sagittal plane. Red/purple parts are considered healthy tissue, brown parts are ablation zone. A. Sample from the one week group before staining (65W, 12min). B. Same sample after H&E staining. C. Samples from the six-week follow-up group, 65W, 6 min. The 'reactive' zone around the dark core turns purple after staining.*

## Edge histology

At the edge of the halo different zones can be recognized (figure 2).

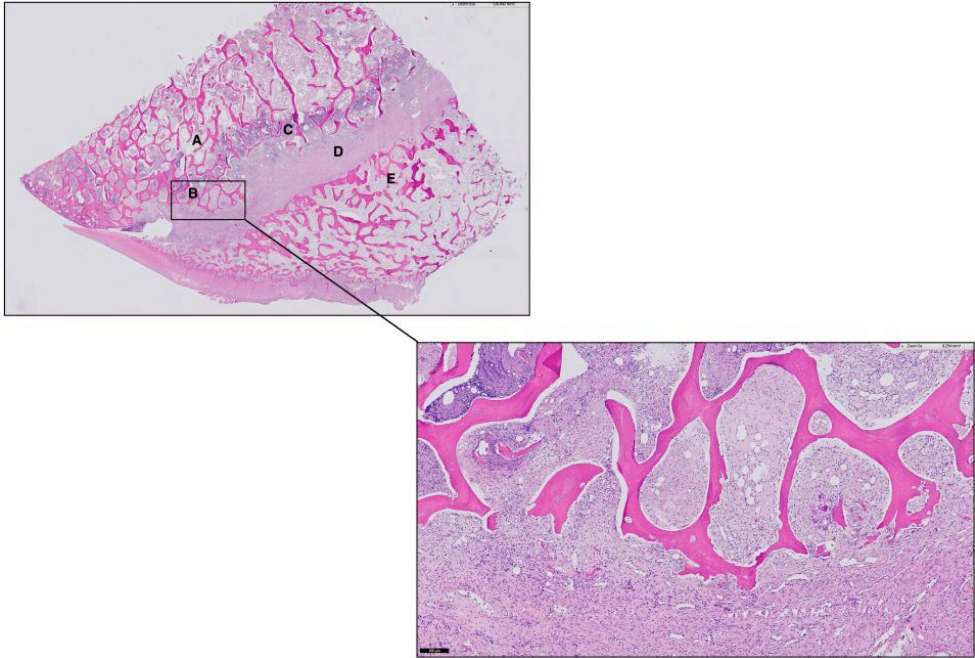


**Figure 2** *Histologic sample of the halo edge, six weeks after a 65W – 12 min ablation.*

The central part of the halo consists of necrotic tissue, which is characterized by empty trabeculae (A). Around this necrosis an area of inflammation can be seen (B). This is surrounded by fibrosis (C) and reactive bone (D). On the outer layer healthy bone tissue (filled trabeculae) can be seen (E).

## Ablation result

Figure 3 depicts a Bland-Altman plot representing differences in halo size within samples for histology vs MRI.

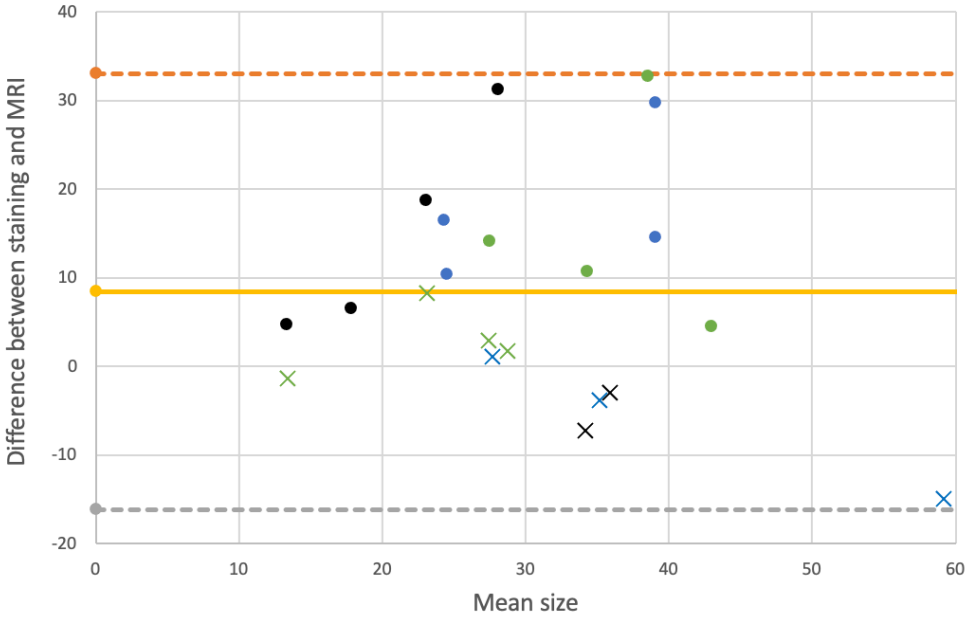


**Figure 3:** Bland-Altman plot representing differences in halo size within samples measured in histology vs on MRI (for different settings and follow-up intervals). Black = 65W – 6 minutes, green = 80W – 6 minutes, blue = 65W – 12 minutes, × = 1 week follow-up, • = 6 weeks follow-up. For the 65W ablation with 1 week follow-up not all samples had an MRI. Orange line = upper limit of agreement, yellow = bias, grey = lower limit of agreement.

#### *Effect of ablation time on halo dimensions*

On one week follow-up MRI, halo size for the 12-minute ablations was 33.1% larger than for six minutes. After six weeks follow-up halos for the 12 minute ablations were 43.5% larger ( $p = .200$ ). On histology halo size was 25.8% larger for the 12-minute ablations ( $p = .857$ ) after one week follow-up and 75.4% ( $p = .029$ ) after six weeks follow-up.

#### *Effect of wattage on halo dimensions*

No significant differences in halo size were found for any of the follow-up intervals when comparing 65W to 80W (one week: MRI - not

enough samples for testing, histology–  $p = .057$ , six weeks: MRI –  $p = .114$ , histology –  $p = .057$ ).

### *MRI vs staining*

At one week follow-up, halo size between MRI and histology was similar ( $p = .930$ ). At six weeks, halo size was 43% larger on MRI compared to histology ( $p = .002$ ).

### **Safety**

Halo shape did not differ as a result of a location close to the growth plate or cortex. In the 24 ablations in the in-vivo study ten complications occurred (see also figures 4A/B and 5A/B). In three samples there was (thermally induced) cartilage damage, in two samples there was a skin burn, two faced a fracture, two a bone infection and one had an abscess. In one of the cases of cartilage damage this was the result of incorrect probe placement (too distally, see figure 4b).

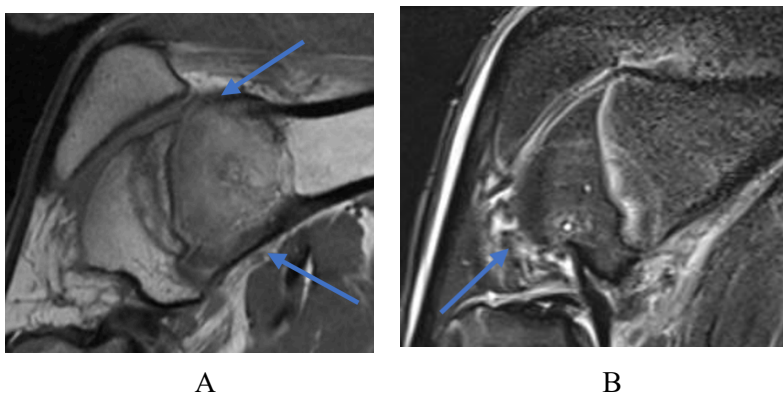


**Figure 4 A.** T1-weighted MRI six weeks after a 65W, 12 minute ablation. The halo reaches over the anterior and posterior cortex (indicated with blue arrows), thereby leading to damage to the cartilage and soft tissue. Halo shape is not dependent of the cortex or growth plate. **B.** T2-weighted MRI one week after 80W, 6 min ablation. There is damage to the cartilage (as a result of incorrect probe placement) (blue arrow).



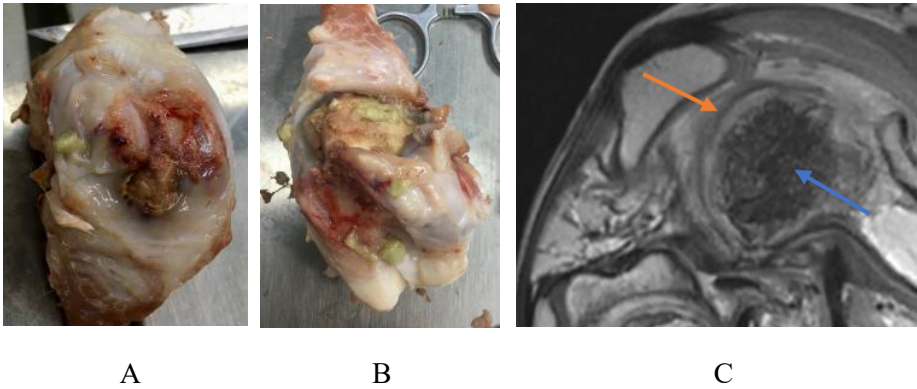


**Figure 5** *Complications after MWA. A. Damaged cartilage distal femur. B. Damage to the cartilage as a result of a bone infection. C. Abscess (blue arrow) six weeks after MWA. The orange arrow indicates the edge of the ablation zone.*

## Discussion

This study is the first to examine effectiveness and safety of MWA in long bone for multiple settings in an in-vivo animal experiment. Furthermore, it is the first to compare histologic changes to MRI findings after MWA in bone. MWA was proven to cause cell death in bone tissue. However, given the high rate of complications, safety is doubtful when the procedure is performed minimally invasive. The ablation result was not consistent, there was a high degree of variation in halo size between the samples, even though sheep with similar size and weight were selected.

A number of other strategies for using heat as local treatment have been described in literature. For high-intensity focused ultrasound ablation (HIFU) in swine femur a clear focus of ossification (i.e. new bone formation) was reported within the ablation area six weeks after treatment (13). In another study by that same group histopathologic analysis depicted areas of endosteal inflammation, scarring, fat

necrosis, and new extra-cortical bone formation at the halo edge six weeks after HIFU (14). For RFA a 22.4% halo decrease was reported in the first year after treatment (15). These studies indicate there is a zone of reactive tissue on the edge of the halo with potential regeneration. Such an effect has not been described for MWA in bone yet. However, halo volume after MWA in breast tissue was found to decrease rapidly. In 21.5% of patients no lesion could be identified any more one year after treatment (16).

Our data support the hypothesis of regenerative potential. For the 65W samples there was a decrease in halo size ( $p = .001$ ) on histology between one and six weeks follow-up, which was not seen in the 80W samples. It is expected that the halo of 65W samples after 1 week consists of a necrotic central area surrounded by a large zone of reactive tissue with the ability to regenerate/recover. Possibly this zone turns into necrosis at 80W. However, on MRI halo size of the 65W samples did not change between one and six weeks after treatment. An explanation could be that a six week interval is too short to notify decrease in halo size.

An increase in ablation time from six to twelve minutes leads to larger halo size at six weeks follow-up. In the histology measurements this was significant ( $p = .029$ ). This corresponds to the findings in our previous ex-vivo study in which halo size gradually increased over time (however, without a significant difference between six and twelve minutes ablation) (7). At one week follow-up no difference was seen. Possibly the tissue at the halo edge is reactive (and has the ability to recover) for the six-minute ablations, whereas after twelve minutes this tissue turns into necrosis. The process of regeneration between one and six weeks as described above does not apply to necrotic tissue.

No difference in halo size was observed between MRI and at one week follow-up. This finding supports MRI as a reliable instrument for

clinical follow-up of halo size after MWA. However, at six weeks follow-up, halos were 43% larger on MRI compared to histology. Possibly the reactive tissue at the edge of the halo is still visible on MRI whereas it does not change color on histology because (partial) regeneration already occurred.

Since the shape of the halo is not influenced by the proximity of cortical bone, it can be inferred that cortex does not block heat in MWA. Therefore there is a risk of damage to sensitive structures surrounding the bone, for instance the cartilage in long bones. This is reflected by the amount of thermally induced complications (skin burn, infection, cartilage damage), especially given the fact ample cooling and rinsing was performed during the procedure. During ablation, temperature on the outside of the bone was constantly monitored to keep it under 45 °C. Probably the temperature on the inside of the bone remained high for prolonged time after the procedure, thereby causing damage to the surrounding tissue. This corresponds with the halos reaching over the cortex (for instance the halos in figure 4). This finding advocates against MWA as a minimally treatment alternative for bone tumors. In minimally invasive procedures cooling ability is insufficient and thermally induced complications are to be expected. MWA in an open setting could be an option. However, when the procedure is carried out in an open manner, the advantages compared to curettage surgery (which has proven to be safe and effective) no longer exist (17).

## **Conclusion**

MWA is effective in bone tissue. However, given the high variability in ablation size and high complication rates, the current data advocate against MWA to replace current treatment options for bone tumors like curettage surgery and (minimally invasive) RFA and indicate the urge for further fundamental understanding of ablation guidance.

## References

1. Coleman RE. Clinical features of metastatic bone disease and risk of skeletal morbidity. *Clin Cancer Res.* 2006;12(20 Pt 2):6243s-6249s.
2. Kastler A, Alnassan H, Aubry S, Kastler B. Microwave thermal ablations of spinal metastatic bone tumors. *J vasc interv Radiol* 2014; 25:1470-1475
3. Khan MA, Deib G, Delbar B, Patel AM, Barr JS. Efficacy and Safety of Percutaneous Microwave Ablation and Cementoplasty in the Treatment of Painful Spinal Metastases and Myeloma. *AJNR Am J Neuroradiol.* 2018 Jul;39(7):1376-1383.
4. Brace CL: Microwave Tissue Ablation: Biophysics, Technology and Applications. *Crit Rev Biomed Eng.* 2010; 38(1): 65–78.
5. Facciorusso A, Di Maso M, Muscatiello N. Microwave ablation versus radiofrequency ablation for the treatment of hepatocellular carcinoma: A systematic review and meta-analysis. *Int J Hyperthermia.* 2016;32(3):339–344.
6. Simon Caroline F., Dupuy Damian E., William W. *Mayo-Smith, Microwave ablation: Principles and applications, Radio Graphics*, 25, S69–S83, 2005.
7. Nijland H, Zhu J, Kwee T, Hao D, Jutte P. Experiments on physical ablation of long bone using microwave ablation; defining optimal settings using ex- and in-vivo experiments. *PLoS One.* 2023 Apr 7;18(4).
8. Nijland H, Overbosch J, Ploegmakers JJW, Kwee TC, Jutte PC. Radiofrequency Ablation for Atypical Cartilaginous Tumors is safe and effective; analysis of 189 consecutive cases. *Open Access Journal of Oncology and Medicine.* June 2020.
9. Dewhirst MW, Viglianti BL, Lora-Michiels M, Hanson M, Hoopes PJ. Basic principles of thermal dosimetry and thermal thresholds for tissue damage from hyperthermia. *Int. J. Hyperth., vol. 19, no. 3, pp. 267–294, 2003.*
10. Eriksson AR, Albrektsson T: Temperature threshold levels for heat-induced bone tissue injury: A vital-microscopic study in the rabbit. *J Prosthet Dent.* 1983 Jul;50(1):101-7.
11. Wallace AN, Hillen TJ, Friedman MV, et al. Percutaneous Spinal Ablation in a Sheep Model: Protective Capacity of an Intact Cortex, Correlation of Ablation Parameters with Ablation Zone Size, and Correlation of Postablation MRI and Pathologic Findings. *AJNR Am J Neuroradiol.* 2017;38(8):1653-1659.

12. Nachlas MM, Shnitka TK. Macroscopic identification of early myocardial infarcts by alterations in dehydrogenase activity. *Am J Pathol.* 1963 Apr;43:379-405.
13. Bucknor MD, Rieke V, Seo Y, Horvai AE, Hawkins RA, Majumdar S et al. Bone remodeling after MR imaging-guided high-intensity focused ultrasound ablation: evaluation with MR imaging, CT, Na(18)F-PET, and histopathologic examination in a swine model. *Radiology.* 2015;274(2):387-394.
14. Bucknor MD, Goel H, Pasco C, Horvai AE, Kazakia GJ. Bone remodeling following MR-guided focused ultrasound: Evaluation with HR-pQCT and FTIR. *Bone.* 2019;120:347-353.
15. Nijland H, Overbosch J, Ploegmakers JJW, Kwee TC, Jutte PC. Nijland H, Overbosch J, Ploegmakers JJW, Kwee TC, Jutte PC. Long-Term Halo Follow-Up Confirms Less Invasive Treatment of Low-Grade Cartilaginous Tumors with Radiofrequency Ablation to Be Safe and Effective. *J Clin Med.* 2021 Apr 22;10(9):1817.
16. Zhang W, Li JM, He W, et al. Ultrasound-guided percutaneous microwave ablation for benign breast lesions: evaluated by contrast-enhanced ultrasound combined with magnetic resonance imaging. *J Thorac Dis.* 2017;9(11):4767-4773.
17. Dierselhuis EF, Goulding KA, Stevens M, Jutte PC. Intralesional treatment versus wide resection for central low-grade chondrosarcoma of the long bones. *Cochrane Database Syst Rev.* 2019 Mar 7;3:CD010778.



# Chapter 7

Mechanical bone strength decreases considerably after microwave ablation – ex-vivo and in-vivo analysis in sheep long bones

H Nijland<sup>1</sup>, J Zhu<sup>2</sup>, TC Kwee<sup>3</sup>, DJ Hao<sup>2</sup>, PC Jutte<sup>1</sup>

1. Department of Orthopaedic Surgery, University Medical Center Groningen, The Netherlands

2. Department of Orthopaedic Surgery, HongHui Medical Center Xi'an, China

3. Department of Radiology, University Medical Center Groningen, The Netherlands

*PLoS One. 2023 Oct 12;18(10)*

# **Abstract**

## **Background**

Bone metastases are on the rise due to longer survival of cancer patients. Local tumor control is required for pain relief. Microwave ablation (MWA) is a technique for minimally invasive local tumor treatment. Tumor tissue is destroyed by application of local hyperthermia to induce necrosis. Given the most common setting of palliative care, it is generally considered beneficial for patients to start mobilizing directly following treatment. No data on mechanical strength in long bones after MWA have been published so far.

## **Materials and methods**

In- and ex-vivo experiments on sheep tibias were performed with MWA in various combinations of settings for time and power. During the in-vivo part sheep were sacrificed one or six weeks after ablation. Mechanical strength was examined with a three-point bending test for ablations in the diaphysis and with an indentation test for ablations in the metaphysis.

## **Results**

MWA does not decrease mechanical strength in the diaphysis. In the metaphysis strength decreased up to 50% six weeks after ablation, which was not seen directly after ablation.

## **Conclusion**

MWA appears to decrease mechanical strength in long bone metaphysis up to 50% after six weeks, however strength remains sufficient for direct mobilization. The time before normal strength is regained after the remodeling phase is not known.



## Introduction

The incidence of bone metastases is on the rise due to improved survival of cancer patients (1). Local tumor control is required for pain relief. Current practice includes radiation, intralesional curettage and wide resection as potential treatment approaches. Microwave ablation (MWA) is a technique for minimally invasive tumor treatment and is therefore an alternative to current, more invasive forms of treatment. In MWA tumor tissue is destructed by application of local hyperthermia. MWA is frequently used for local control of metastases in organs like liver, kidney and lung (2). However, the use of MWA in bone is still limited and therefore literature on its working mechanism is scarce. No literature exists on the effect of MWA on bone strength. In bone tumor ablation with Radiofrequency Ablation (RFA) fractures occur in 2.6-4.8% of cases (3,4). This is comparable to intralesional curettage (4.0%) and lower than for wide resection (23.1%) (5,6).

When standing, a load of 'body mass \* 9,81 m/s<sup>2</sup> (gravity acceleration)' is put on the legs. For an average patient of 80 kg this comes down to almost 400N load per leg. When walking, this load is only slightly higher. However, this load doubles when running at low speed, is threefold for running at higher speed and even sevenfold for jumping and landing (7-9). Since there is no literature on the mechanical effects of MWA in long bone it is uncertain whether direct mobilization is safe and what the risk is of early return to full activity.

To ensure safe treatment and more evidence-based practice after MWA treatment the present study was performed to assess the biomechanical effect of local tumor ablation in long bone using MWA in an experimental model. Initial strength directly after ablation was hypothesized to be unchanged as local bone architecture is unchanged. As a result of osteoclast activity and remodeling, weakening of bone strength is hypothesized in the weeks after ablation.

## Method

### Microwave ablation

All ablations were performed with a 2.45GHz Kang-You 2000 microwave ablation generator (Kang-You Medical, Nanjing, China). For mechanical testing three-point bending test and indentation test were used, as described in a later section. For the three-point bending test ablation was carried out in the center of the diaphysis. For the indentation test ablation was performed in the proximal metaphysis, at a depth of 30mm, 25mm distal from the cortex. Both an ex-vivo and an in-vivo study were performed.

### *Ex-vivo*

Fresh sheep bones were collected from the slaughterhouse on the day of experiments. Bones were from similar size and mass. MWA procedures were performed 6-12 hours after the sheep were sacrificed to ensure good fresh bone quality. First, bones were put into 37°C water (range 37-40°C) for 20-30 minutes to mimic body temperature. Holes for the ablation needle and temperature probe were drilled directly before ablation to prevent water getting inside the bone. Ablation was carried out with four different settings: 60W – 10 min, 60W – 20 min, 80W – 20 min and 80W – 10 min. With these settings the effects of time and wattage could be evaluated separately. Wattage levels were chosen based on pilots and earlier reported results by our group (10). For every setting six bones were used for both mechanical tests. A slow-cooking algorithm for temperature was used (10). This consists of slowly increasing temperature towards the aimed temperature to lower the risk of carbonization around the needle to occur. Every ablation started with 10W for one minute, followed by one minute at 20W. These two minutes are included in the time settings as mentioned. After ablation, bones were prepared for mechanical testing.

### *In-vivo*

For the experiment permission was obtained from the medical ethical committee of the HongHui hospital, Xi'an, China. Ablations were performed in tibia of male sheep (Small-tail Han) aged 1 – 1.5 years with aimed mass of 50 kg (in vivo experiment: range 45-50 kg). Three settings were examined for both a one week- and a six weeks follow-up group: 60W 10min, 60W – 20 min and 80W – 10 min. For each group four sheep were included, leading to a total of 24 sheep. As controls the contralateral tibias were used. Sheep were randomly divided in the one- or six week group. Before starting the procedure (figure 1A), the sheep were sedated with an intramuscular injection of 5 ml Shutai (1 : 1 combination of Tiletamine 50mg/ml & Zolazepam hydrochloride 50mg/ml) (Virbac, France) and subsequently intubated (figure 1B. During the complete procedure inhaled isoflurane (1-5%) was used for general anesthesia and a maintenance dose up to 2.5ml Shutai was given in case deemed necessary. For post-procedural analgesia meloxicam injections were used. After the follow-up period sheep were euthanized by an experienced veterinarian (bleed out under intramuscular sedation). Sheep with a (deep) infection or fracture were excluded from mechanical analysis to prevent finding differences in strength based on other factors than the mechanical effect of MWA on bone.

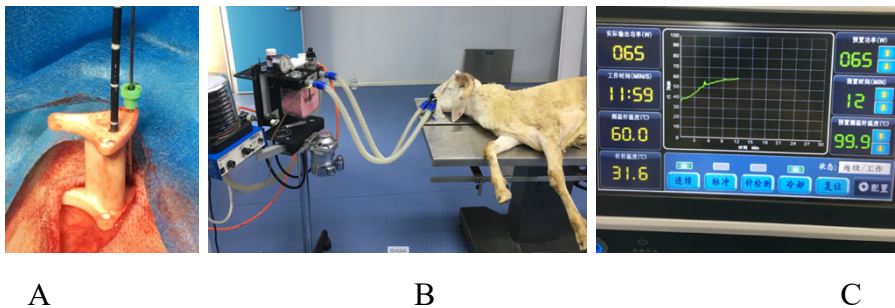


**Figure 1** *in-vivo* procedure. **A.** Ablation probe (black) and temperature probe inserted in the bone through a positioning device. **B.** Intubated sheep before procedure. **C.** the MWA generator.

## **Mechanical testing**

For the ex-vivo experiments both indentation test and three-point bending test were performed. These are both generally used tests (11,12). To limit the number of animals needed, only indentation test was performed in the in-vivo experiments after analyzing the ex-vivo results.

### *Three-point bending test*

For the three-point bending test bones were cut both proximal and distal from the ablation site, leaving six cm on both sides (thereby guaranteeing equal length for all samples). Width and height of the sample were measured. The maximum differences for width and height from the average were only 1mm. Samples were placed on a hydraulic test machine (Model 64, MTS Systems, Eden Prairie, United States) with on both ends two cm supported by the machine. Subsequently force was gradually increased on the entry point from the needle with a blunt-shaped edge (see figure 2A). Load deflection curve, maximal load (N) and displacement (mm) were measured. Testing was ended when the sample fractured. From these data stress and stiffness were determined. Stress is defined as the amount of force per mm<sup>2</sup> (N/mm<sup>2</sup>) that the sample can bear before breaking. For calculating stress the following formula was used:

$$\text{Stress} = (3 * F_{\text{max}} * \text{length}) / (2 * \text{width} * \text{height}^2)$$

The shape of sheep tibia was in between spherical and rectangular. For our calculations we decided to consider the bones as rectangular. Stiffness was defined as the amount of force needed for one mm displacement (N/mm). Force was not reported since stress is a better predictor of strength in this test, accounting for the dimensions of the sample as well, where force does not hold this into account.

### *Indentation test*

For the indentation test the bones were cut through the diaphysis making samples 13 cm high. The distal end was fixated in cement in a paper cup. Samples were kept in a fridge overnight, to prevent decrease in bone quality during the time the cement hardened. The next day indentation test was performed in the mechanical lab on a hydraulic test machine (Model 64, MTS Systems, Eden Prairie, United States). A bar with a 13mm diameter was used as indenter and fixed in the machine (see figure 2B). Subsequently pressure was gradually built up. The machine measured the force needed per mm indentation into the bone (= displacement). Stress was calculated by applying the formula 'test force (in N) / area of indentation (A)'. The area of indentation was a constant 132.73 mm<sup>2</sup> (given the radius of the indenter was 6.5mm). Testing was ended when a sudden drop in force occurred, indicating fracture of the internal structure of the bone.

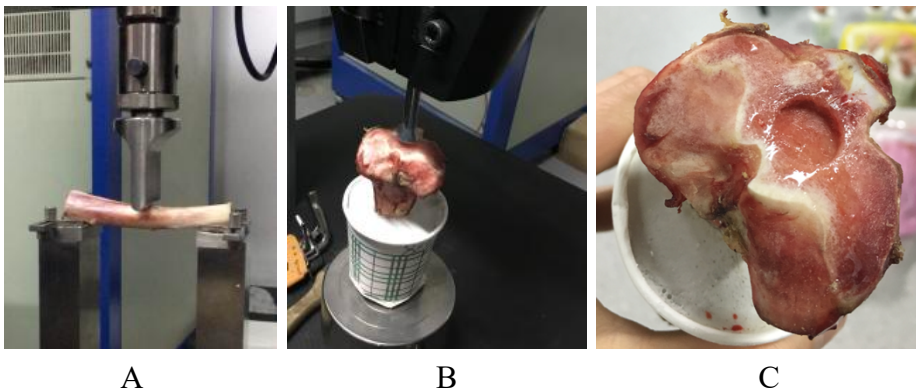


**Figure 2** Mechanical testing. *A. Three-point bending test. B. Indentation test. C. Proximal tibia after indentation test.*

### **Data analysis**

Data was reported as mean value  $\pm$  standard deviation (SD). Data were analyzed using SPSS statistics v25 (IBM, Armonk, United States).

Given the relatively small sample size non-parametric testing was performed. Differences between ablation settings and controls were examined using a Mann-Whitney-U test. For all tests an alpha of .05 was chosen. For the in-vivo experiment no statistical testing was performed given the small group sizes.

## Results

### Ex-vivo

Values for maximum stress and stiffness in the three-point bending test are depicted in table 1. The amount of stress needed to break the sample was significantly higher in the ablated samples compared to controls for the 60W - 10 min ( $p < .01$ ) and 80W - 20 min ( $p = .015$ ). The amount of stress needed to break the sample did not significantly differ between controls and 60W - 20 min ( $p = .093$ ) and 80W - 10 min ( $p = .485$ ). There was no difference in maximum stress between the four different settings. For stiffness no differences were found between the different settings ( $p > .05$ ).

**Table 1** Stress and stiffness (mean  $\pm$  SD) in ex-vivo three-point bending test

| Setting     | Max stress (N/mm <sup>2</sup> ) | Stiffness (N/mm)       |
|-------------|---------------------------------|------------------------|
| 60W, 10 min | 118.51 ( $\pm$ 4.8)*            | 1618.07 ( $\pm$ 148.9) |
| 60W, 20 min | 108.94 ( $\pm$ 12.7)            | 1288.17 ( $\pm$ 169.3) |
| 80W, 10 min | 97.07 ( $\pm$ 23.5)             | 1433.05 ( $\pm$ 83.1)  |
| 80W, 20 min | 112.40 ( $\pm$ 12.5)*           | 1397.29 ( $\pm$ 335.2) |
| Control     | 93.05 ( $\pm$ 12.9)             | 1361.10 ( $\pm$ 435.4) |

\* = significant

Maximum force/maximum stress and stiffness as measured during the indentation test are depicted in table 2. The force needed to break the control samples was significantly higher compared to the 60W - 10 min

setting ( $p = .026$ ). For 60W - 20 min ( $p = .132$ ), 80W - 10 min ( $p = .065$ ) and 80W - 20 min ( $p = .180$ ) no significant difference was found despite the large difference in average values. Between the different settings no differences were found. For stiffness no differences were found between the different settings or between settings and controls ( $p > .05$ ). Figure 3 depicts load displacement curves of both mechanical tests.

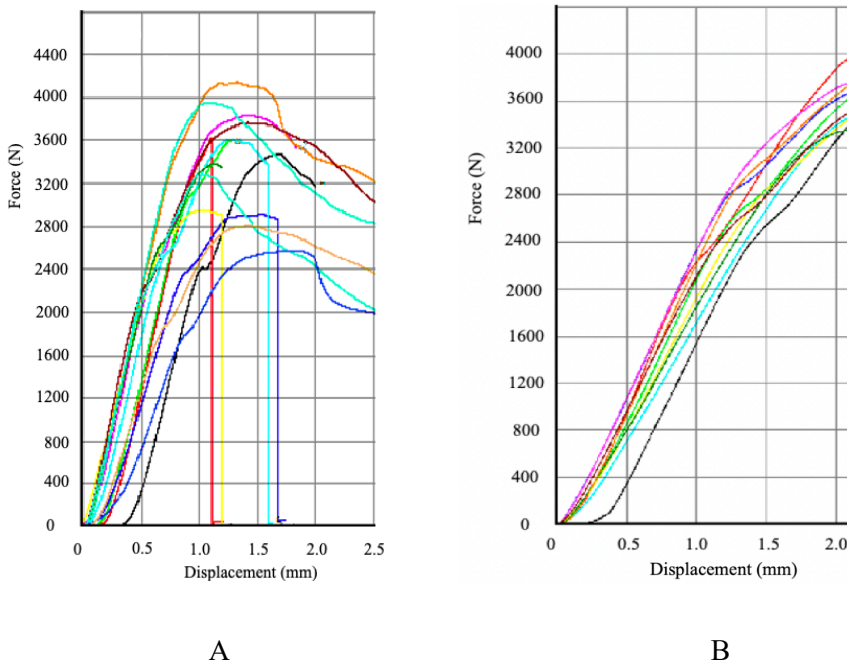


**Figure 3** Load displacement curves of indentation test (A) and three-point bending test. Different lines represent individual samples. Figures only represent a limited number of samples.

**Table 2** Stress and stiffness (mean  $\pm$  SD) in ex-vivo indentation test. \* = significant.

| Setting     | Force (N)              | Max stress (N/mm <sup>2</sup> ) | Stiffness (N/mm)      |
|-------------|------------------------|---------------------------------|-----------------------|
| 60W, 10 min | 981.79 ( $\pm$ 285.2)* | 7.40 ( $\pm$ 2.1)               | 548.29 ( $\pm$ 155.5) |
| 60W, 20 min | 1266.31 ( $\pm$ 403.4) | 9.54 ( $\pm$ 3.0)               | 474.50 ( $\pm$ 114.5) |
| 80W, 10 min | 1128.20 ( $\pm$ 381.8) | 8.50 ( $\pm$ 2.9)               | 500.53 ( $\pm$ 190.4) |
| 80W, 20 min | 1232.43 ( $\pm$ 776.5) | 9.29 ( $\pm$ 5.8)               | 569.81 ( $\pm$ 274.8) |
| Control     | 1809.59 ( $\pm$ 737.9) | 13.63 ( $\pm$ 5.6)              | 470.69 ( $\pm$ 244.1) |

### In vivo

In two sheep in the in-vivo experiment a complication occurred. One (80W - 10 min, one week) had a fracture of the tibia (already before mechanical testing), the other one (60W - 10 min, six weeks) a deep infection. Both sheep were excluded from the analysis. In table 3 the maximum stress and stiffness of the in vivo samples after one- and six weeks follow-up are depicted, as well as the average individual differences compared to the controls (contralateral tibia). Values for maximum stress and stiffness in the one week follow-up group were similar to the control tibias. Furthermore, no differences were found between a complete setting and the average control values after one week follow-up. However, after six weeks follow-up both maximum tolerable stress and stiffness for 60W – 20 min and stiffness for 80W – 10 min appear smaller than the control values. Stress for the 80W – 10 minute group did not differ from controls.



**Table 3** Force, stress and stiffness of in-vivo indentation test (mean  $\pm$  SD). Controls were measured in the contralateral tibia of the same animal.

| Setting        | Force (N)                 | Max stress (N/mm <sup>2</sup> ) | Difference to control  | Stiffness (N/mm)         | Difference to control      |
|----------------|---------------------------|---------------------------------|------------------------|--------------------------|----------------------------|
| <b>1 Week</b>  |                           |                                 |                        |                          |                            |
| 60W, 10 min    | 818.89<br>( $\pm$ 199.0)  | 6.06<br>( $\pm$ 1.6)            | - 0.12<br>( $\pm$ 3.6) | 505.44<br>( $\pm$ 92.5)  | + 95.20<br>( $\pm$ 210.4)  |
| 60W, 20 min    | 1043.29<br>( $\pm$ 394.9) | 7.86<br>( $\pm$ 3.0)            | + 0.08<br>( $\pm$ 0.6) | 516.71<br>( $\pm$ 137.7) | - 162.99<br>( $\pm$ 293.3) |
| 80W, 10 min    | 980.03<br>( $\pm$ 225.1)  | 7.38<br>( $\pm$ 1.7)            | - 0.13<br>( $\pm$ 0.8) | 691.37<br>( $\pm$ 225.6) | + 170.42<br>( $\pm$ 213.0) |
| Control        | 945.78<br>( $\pm$ 285.9)  | 7.12<br>( $\pm$ 2.2)            |                        | 538.43<br>( $\pm$ 235.5) |                            |
| <b>6 Weeks</b> |                           |                                 |                        |                          |                            |
| 60W, 10 min    | 1437.37<br>( $\pm$ 229.9) | 10.8<br>( $\pm$ 1.7)            | + 1.57<br>( $\pm$ 4.0) | 635.73<br>( $\pm$ 52.6)  | + 71.28<br>(213.5)         |
| 60W, 20 min    | 666.73<br>( $\pm$ 195.0)  | 5.02<br>( $\pm$ 1.5)            | - 5.30<br>( $\pm$ 3.2) | 279.52<br>( $\pm$ 127.2) | - 378.86<br>( $\pm$ 287.4) |
| 80W, 10 min    | 891.29<br>( $\pm$ 384.7)  | 6.72<br>( $\pm$ 2.9)            | - 3.42<br>( $\pm$ 2.8) | 341.92<br>( $\pm$ 248.7) | - 449.70<br>( $\pm$ 307.7) |
| Control        | 1322.47<br>( $\pm$ 413.2) | 9.96<br>( $\pm$ 3.1)            |                        | 681.21<br>( $\pm$ 197.3) |                            |

## Discussion

This is the first study to report both in- and ex-vivo mechanical effects of microwave ablation in long bone. Our results indicate no differences in mechanical properties ex-vivo and after one week follow-up for in-vivo ablations. After six weeks follow-up, a decrease in both stress and stiffness for the more aggressive settings was assumed.

Our results are in line with the findings of Herman et al (13), who found a 30% decrease in mechanical strength six weeks after MR-guided focused ultrasound ablation in pig ribs (13). Yamamoto et al. (14) found no change in bone strength two months after RFA in rabbit femurs. Bucknor et al. (15) found subperiosteal new bone formation six weeks after MR-guided high-intensity focused ultrasound ablation. For MWA only ex-vivo data exists in literature. Ji et al. (16) found no change in mechanical strength in dog bone after microwave ablation (sacrifice intervals ranging from two weeks – one year). However, after sacrifice they kept the bones in a -80 °C freezer for a non-documented time before examining mechanical strength (16). This may have affected bone strength.

There was no decrease in stress and stiffness as a result of ablation in the three-point bending test. Therefore it was concluded that in an ex-vivo setting MWA did not influence immediate mechanical strength in the diaphysis. For 60W – 10 min and 80W – 20 min the stress (N/mm<sup>2</sup>) required to break the bone was even higher compared to controls. Due to limitations in the number of animals no testing was performed in-vivo and conclusions on three-point bending strength cannot be drawn from the present study for in-vivo applications. It seems likely that immediate strength is unaffected, but effects on mechanical strength after six weeks are not known and may very well be in line with the weakening seen in the metaphysis as a result of bone remodeling.

In the ex-vivo samples, the maximum force/stress needed to break the bone in the indentation test was only significantly lower for the 60W – 10 min ablations compared to controls. Average values were lower for all settings, though not significant. This is most likely due to the small number of samples and the relatively large standard deviation. After six weeks, stiffness appeared lower for the more aggressive settings (60W – 20 min, 80W – 10 min). Force/stress appears lower for these settings too. From these observations it can be concluded that there is no effect on mechanical strength one week after ablation. The decrease in strength found in the six week samples is probably the result of osteoblast/clast activity during remodeling. We hypothesize mechanical strength to increase again in the subsequent weeks as a result of increased osteoblast activity. It would be interesting to repeat the experiment with a 12-week follow-up group and larger group size to be able to perform statistical analysis on the in-vivo experiments.

Ji et al. (16) reported newly formed bone eight weeks after MWA. Bucknor et al. (15) reported new bone formation six weeks after high-intensity focused ultrasound ablation. This kind of biological rebuild can be expected from MWA as well, but cannot be confirmed in the present study. In the study of Ghomashchi et al. (17) histological effects of RFA were analyzed. They found no evidence of cortical thinning. Furthermore they demonstrated formation of newly formed trabeculae in the RFA zone with similar architecture, connectivity and mineral content compared to normal bone.

From the in-vivo indentation test data it was found that an average force of 1000N is needed to break the sample (for both one week and six weeks). This comes down to a mass of 100 kg on one leg (200 kg total body mass). Given an average human body mass of 80 kg, an average load up to 2.5 times the body mass is considered safe. Given the large variation in the data (for instance a force of 666.7N needed to break the sample six weeks after 60W – 20 min, corresponding to only an average load of 1.7 times the average mass) some caution in mobilization is

recommended. However, these data support immediate mobilization after treatment. Since we removed the proximal cortical bone in the samples to create a flat surface for the indentation test, clinical mechanical strength will be even higher. In the in-vivo experiment sheep were allowed to freely mobilize after treatment. Only in one out of 24 sheep a fracture occurred (= 4.2%). This corresponds to literature on minimally invasive treatment (fracture in 2.6-4.8% of cases) and curettage surgery (4.0%) and is lower than for wide resection (10.5%) (2,5,6).

The low number of fractures in minimally invasive treatment is potentially due to the fact that the integrity of the cortex is hardly affected by the technique. One major study limitation is the small number of samples per group, especially in-vivo.

## **Conclusion**

Based on our initial results it appears that MWA decreases mechanical strength in bone to a small extent. However mechanical strength as measured in our study remains on a level sufficient to carry a patient's mass. Therefore we think it is safe for patients to quickly start mobilizing again on the treated leg without significant risk of complications. However, since bone quality appears weaker after six weeks than after one week, caution is advised with the more aggressive settings. Further studies with larger sample sizes are required to confirm our findings.

## References

1. Coleman RE. Clinical features of metastatic bone disease and risk of skeletal morbidity. *Clin Cancer Res.* 2006;12(20 Pt 2):6243s-6249s.
2. Facciorusso A, Di Maso M, Muscatiello N. Microwave ablation versus radiofrequency ablation for the treatment of hepatocellular carcinoma: A systematic review and meta-analysis. *Int J Hyperthermia.* 2016;32(3):339-344.
3. Nijland H, Overbosch J, Ploegmakers JJW, Kwee TC, Jutte PC. Radiofrequency Ablation for Atypical Cartilaginous Tumors is safe and effective; analysis of 189 consecutive cases. *OAJOM aug 2020.*
4. Fan QY, Zhou Y, Zhang M, et al. Microwave ablation of malignant extremity bone tumors. *Springerplus.* 2016;5(1):1373
5. Chen X, Yu LJ, Peng HM, et al. Is intralesional resection suitable for central grade I chondrosarcoma: A systematic review and updated meta-analysis. *Eur J Surg Oncol.* 2017;43(9):1718-1726.
6. Dierselhuis EF, Goulding KA, Stevens M, Jutte PC. Intralesional treatment versus wide resection for central low-grade chondrosarcoma of the long bones. *Cochrane Database Syst Rev.* 2019 Mar 7;3:CD010778.
7. Nandikolla VK, Bochen R, Meza S, Garcia A. Experimental Gait Analysis to Study Stress Distribution of the Human Foot. *J Med Eng.* 2017;2017:3432074.
8. Cross R. Standing, walking, running, and jumping on a force plate. *American Journal of Physics April 1999,* 67(4):304-309.
9. Prajapati, K, Barez F, Kao J, Wagner D. Dynamic Force Response of Human Legs due to Vertical Jumps. *Proceedings of the ASME 2011 International Mechanical Engineering Congress and Exposition Volume 2: Biomedical and Biotechnology Engineering; Nano-engineering for Medicine and Biology.* November 11–17, 2011 pp. 1-8.
10. Nijland H, Zhu J, Kwee TC, Hao D, Jutte PC: Experiments on physical ablation of long bone using microwave ablation; defining optimal settings using in- and ex-vivo experiments. *PLoS One.* 2023 Apr 7;18(4)
11. Boughton OR, Ma S, Zhao S, Arnold M, Lewis A, Hansen U, Cobb JP, Giuliani F, Abel RL. Measuring bone stiffness using spherical indentation. *PLoS One.* 2018 Jul 12;13(7):e0200475.
12. Leppänen O, Sievänen H, Jokihaara J, Pajamäki I, Järvinen TL. Three-

point bending of rat femur in the mediolateral direction: introduction and validation of a novel biomechanical testing protocol. *J Bone Miner Res.* 2006 Aug;21(8):1231-7.

13. Herman A, Avivi E, Brosh T, Schwartz I, Liberman B. Biomechanical properties of bone treated by magnetic resonance-guided focused ultrasound - an in vivo porcine model study. *Bone.* 2013;57(1):92-97.

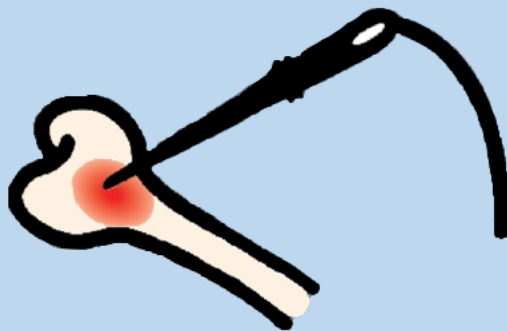
14. Yamamoto S, Kaminou T, Ono Y, et al. Thermal influence of radiofrequency ablation for bone: an experimental study in normal rabbit bone. *Skeletal Radiol.* 2014;43(4):459-465.

15. Bucknor MD, Rieke V, Seo Y, Horvai AE, Hawkins RA, Majumdar S et al. Bone remodeling after MR imaging-guided high-intensity focused ultrasound ablation: evaluation with MR imaging, CT, Na(18)F-PET, and histopathologic examination in a swine model. *Radiology.* 2015 Feb;274(2):387-94.

16. Ji Z, Ma Y, Li W, et al. The healing process of intracorporeally and in situ devitalized distal femur by microwave in a dog model and its mechanical properties in vitro. *PLoS One.* 2012;7(1):e30505.

17. Ghomashchi S, Whyne CM, Chinnery T, Habach F, Akens MK. Impact of radiofrequency ablation (RFA) on bone quality in a murine model of bone metastases. *PLoS One.* 2021 Sep 8;16(9):e0256076.







# Chapter 8

## Microwave ablation in vertebral bodies in sheep – assessment of safety at sensitive structures

H Nijland<sup>1</sup>, J Zhu<sup>2</sup>, TC Kwee<sup>3</sup>, DJ Hao<sup>2</sup>, PC Jutte<sup>1</sup>

1. Department of Orthopaedic Surgery, University Medical Center Groningen, The Netherlands

2. Department of Orthopaedic Surgery, HongHui Medical Center Xi'an, China

3. Department of Radiology, University Medical Center Groningen, The Netherlands

*Int J Hyperthermia. 2024;41(1):2434607*

# **Abstract**

## **Background**

Bone metastases are on the rise due to improved survival of cancer patients. Local tumor control is required for pain relief. Spine is the most common location for bone metastases. Microwave ablation (MWA) is a technique for minimally invasive tumor treatment. The aim of the current study was to determine whether MWA is a safe option for treatment in vertebral bodies and to gain data on the amount of cortical insulation in spine.

## **Method**

MWA was applied with different settings for power and time in both in- and ex-vivo sheep vertebral bodies. Safety was evaluated by temperature measurements at critical surrounding structures (e.g. spinal cord, nerve root). Furthermore, distribution of heat through the bone at 5mm from the ablation needle was measured and compared to temperature at the posterior wall.

## **Results**

Our results indicate a partial effect of cortical insulation in spine. However, for higher wattages this no longer accounts. Ablations with wattage levels over 30W lead to instant damage to the spinal cord (local temperature over 60 °C). For ablations with 20- or 30W a maximum time of three to four minutes appears safe ex-vivo. However, in the in-vivo experiment paraplegia was frequently seen and the experiment was therefore terminated.

## **Conclusion**

MWA is an effective minimally invasive approach for local bone metastasis control. It has an aggressive nature, which is beneficial for treatment of larger tumors. However, given the high risk of complications, treatment in vertebral bodies is not recommended. When used, recommended maximum ablation settings are 10-20W for three minutes. Cortical insulation in vertebral bodies is insufficient to protect the spinal canal from excess heat, paraplegia occurs frequently.

## Introduction

Bone metastases are on the rise due to improved survival of cancer patients (1). Local tumor control is required for pain relief. Spine is the most common location for bone metastases (2). These metastases commonly originate from primary tumors in lung (24%), breast (24%), liver (12%), prostate (11%) and kidney (11%) (3). Multiple studies have been performed comparing minimally invasive treatment to open surgery in patients with spinal metastases (4-6). Advantages of minimally invasive options are less blood loss, lower infection risk and shorter hospitalization periods, whereas treatment results are comparable (4). A common type of minimally invasive treatment is a laminectomy followed by posterior stabilization with pedicle screws and rods (4, 5). An alternative option is radiofrequency ablation (RFA) followed by stabilization (2). In RFA tumor tissue is destroyed by hyperthermia. Complication rate is low, however lower extremity paralysis after RFA has been reported in literature (7).

Microwave ablation (MWA) is another minimally invasive technique using hyperthermia. It is already widely used in treatment of liver, kidney, and lung tumors, but experience in bone tissue is still limited (8-9). In current literature there is only one large study describing MWA in spine. Khan et al. used MWA (3.0-10.5 minutes with 13.3W ( $\pm 3.25$ )) on 102 spinal metastases in 69 patients (9). From the 61 patients with over six months survival a total of 59 remained free of locoregional progression and an average five-point reduction in VAS-score was achieved. Only two complications were reported (thermal nerve injury, skin burn). They did not face paraplegia. This study suggests that MWA is safe and effective in spine. However, from earlier experiments by our group in long bone we found large variability in halo size, making the ablation result hard to predict.

### **Cortical insulation**

The cortical bone potentially serves as a barrier for heat distribution. In literature this is described to a limited extent and mainly focused on RFA (10-14). For MWA there is no literature on this important topic. In case no cortical insulation exists for MWA, there is a high risk of damage to surrounding structures like the spinal cord in spine ablations.

Since spine is the most common location for bone metastases, knowledge on treatment options needs to be expanded. The aim of the current study was to determine whether MWA is a safe option for treatment in vertebral bodies and to form assumptions on the amount of cortical insulation in spine.

### **Tissue reaction to heat**

Instant cell death occurs at temperatures over 60 °C. Between 50-60 °C it takes 1-6 minutes to reach complete cell death (15-18). To ensure complete ablation, a target temperature of over 60 °C should be reached up to the very edge of the tumor. At temperatures over 100 °C vaporization of water (leading to desiccation of the cell) and carbonization occur, potentially limiting heat conduction (15-22). To prevent damage to surrounding structures in minimally invasive MWA, the temperature on the outside of the bone should not exceed the upper limit of 60°C (5-8).

## Method

### Safety of surrounding structures

For safety evaluation in spine, the spinal cord and nerve root are the most important structures. Weinstein, Boriani and Biagini divided the vertebral body in 12 zones (see figure 1). In this 'WBB-classification', zones 4, 5 and 6 are most important in safety evaluation. The spinal nerve originates from zone 4 (23). High surface temperature in this zone leads to nerve damage. The spine holds multiple potential heatsinks (i.e. thermal flow from areas with high temperature towards areas with lower temperature) that can influence the shape of the halo (i.e. area of ablated tissue) (24). Examples are the spinal arteries and the cerebral spinal fluid. Measurements at zone 5 (lateral/anterior) and zone 6 (anterior body) can be used to account for differences in halo shape.

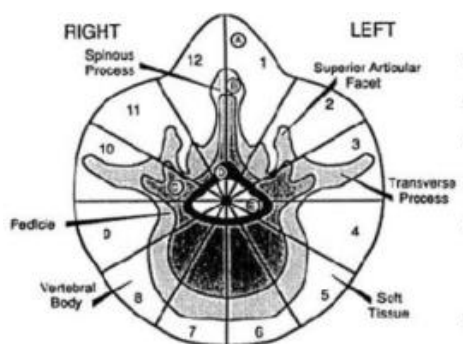


**Figure 1** Weinstein, Boriani, Biagini (WBB) classification for spine. The spinal nerve originates from zone 4 (23).

### Ablation procedure

All ablations were performed with a 2.45GHz Kang-You 2000 microwave ablation generator (Kang-You Medical, Nanjing, China) and internally cooled needles with a three cm active tip size. Needles are internally cooled to prevent temperatures over 45°C in the non-active part.

From clinical experience with RFA and pilot studies with MWA it was experienced that too rapid heating results in charring and loss of tissue conductivity, thereby resulting in ineffective ablation. Therefore, we developed a slow-cooking model in which temperature was slowly increased towards the aimed temperature. Every ablation started with 10W for one minute, followed by 20W for one minute (except the 10W ablations).

### **Ex-vivo experiments**

Fresh sheep bones were collected from the slaughterhouse on the day of experiments (within 2 hours after sacrifice). Bones were from sheep aged 1 – 1.5 years with an average weight of 50kg. MWA procedures were performed within 6-12 hours after the sheep were sacrificed to ensure good bone quality. First, the bones were put into 37 °C water (range 37-40 °C) for 20-30 minutes to mimic body temperature. Before ablation, inner bone temperature was measured to ensure it was between 36-39 °C. Access to the vertebral body was reached by drilling a tract through the pedicle towards the anterior cortex of the body.

#### *Safety of surrounding structures*

To determine safety of surrounding structures, temperature was measured ex-vivo at the posterior wall of the vertebral body (inside the spinal canal) and at zone 4, 5 and 6 (see figure 1). Ablations were carried out for six minutes at 10- and 20W and for ten minutes at 30-, 40- and 50W. For 10W only the temperature at the posterior wall and zone 4 was measured. Temperature was measured with handheld temperature probes on the exterior side of the cortex and noted every minute. In every ablation a maximum of two locations was measured at the same time to prevent errors as a result from shifting probes. To accurately position the probe at the posterior wall a tunnel was drilled through the lamina vertebralis. The set-up of an ablation with temperature probes at the posterior wall and zone 3 is depicted in figure 4. After the ablation samples were cut to examine the halo size.



**Figure 2** Set-up for the temperature measurement at zone 4 and the posterior wall. Left to right: zone 4 temperature probe, ablation needle, posterior wall temperature probe. The hole for the probe for the posterior wall is drilled through the lamina vertebralis.

### *Cortical insulation*

A separate tract with the same depth was drilled parallel to the tract of the ablation needle at five mm distance (see figure 3a). To determine cortical insulation, temperature at five mm from the needle was compared to temperature at the posterior wall. During ablation, temperature was live recorded (see figure 3b) and noted on a result sheet every minute. Ablation was carried out for six minutes at 20- and 30W and for ten minutes at 40- and 50W. A 3D-printed polyamid navigation tool (see figure 3c) was designed to standardize distance and needle direction.

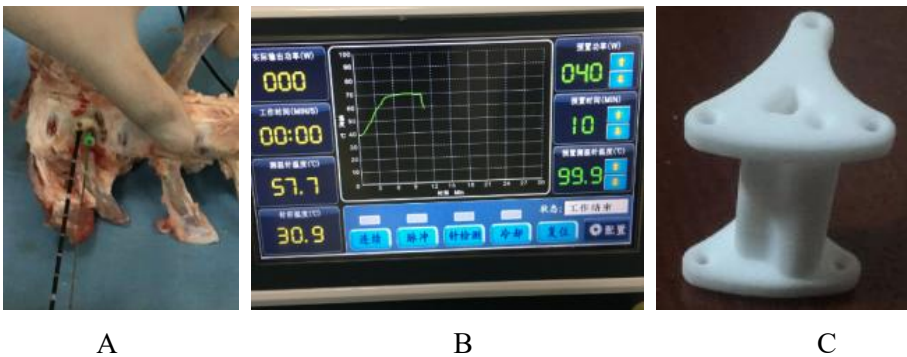


**Figure 3:** *A.* Ablation at L6 with temperature probe at 5mm. *B.* Live temperature tracking on the generator. *C.* The 3D-printed navigation tool.

### **In-vivo experiments**

Based on the results of the ex-vivo study an in-vivo model was designed. Ablations were carried out for four minutes with 20- and 30W and for six minutes at 20W. For every setting four animals were used. Image guidance was not available for this study. Therefore, location of the L5 vertebral body was determined by palpating the spinous process. Subsequently the vertebral body was manually approached from posteriorly by drilling a tract through the pedicle for the ablation probe. Another tract was drilled through the lamina for placement of the temperature probe. Procedures were performed by a specialized spine orthopedic surgeon (JZ).

Temperature at the posterior wall was measured with a temperature probe and noted every minute. Ablation was ended when temperature at the posterior wall reached 60 °C before the planned time interval. Before starting the procedure, the sheep were sedated by a veterinarian with an intramuscular injection of 5 ml Shutai (1 : 1 combination of Tiletamine 50mg/ml & Zolazepam hydrochloride 50mg/ml) (Virbac, France) and subsequently intubated. During the complete procedure inhaled isoflurane (1-5%) was used for general anesthesia and a maintenance dose up to 2.5ml Shutai was given in case deemed necessary by the veterinarian. Animals were sacrificed one week after the procedure to examine halo size and histologic changes at the posterior wall and other sensitive structures. For this in-vivo design permission was given by the Medical Ethical Committee of the HongHui hospital, Xi'an.

### **Data analysis**

A minimum of seven bones was included per setting for ex-vivo. Samples were excluded when sudden temperature drops occurred or temperature differed more than two standard deviations (SD) from the average value for at least three time intervals. Data was analyzed using SPSS v25 (IBM, Armonk, United States). Values for temperature were noted as mean ( $\pm$ SD). Data was examined using non-parametric tests



due to the relatively small group size and low amount of variance within the groups. Linear regression was used to predict the effect of time and wattage on temperature at surrounding structures. Temperatures at 5mm from the needle (from the heat distribution experiment) were compared to the temperatures at the posterior wall to get an indication of cortical insulation. These differences were tested using a mixed repeated measures ANOVA design. Sphericity and equality of differences were non-significant. Data was tested for time up to six minutes given the fact temperatures at time over six minutes remains stable and variance at these intervals is very limited. P-values of  $< .05$  were considered significant for all tests.

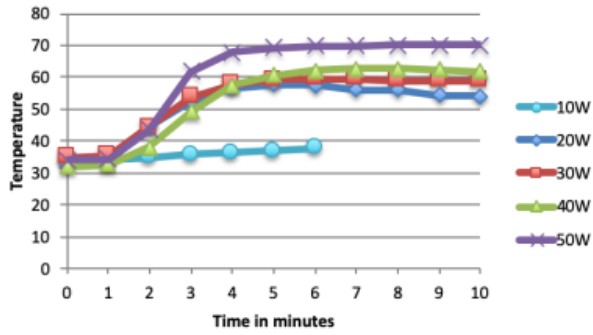
## **Results**

### **Ex-vivo safety of surrounding structures**

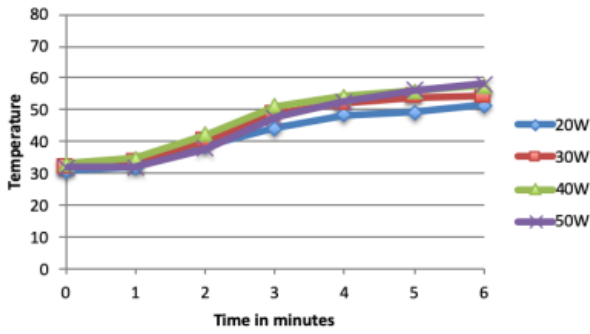
Temperatures at the posterior wall over time for the different wattage levels are depicted in figure 5. At three minutes, the first measurement after the slow cooking period, temperature at 40- and 50W exceeds 60° C. At 20- and 30W temperature reaches 60 °C after four- and five minutes respectively. At 10W temperature remains below 40 °C.

At zone 4 temperatures do not exceed 60 °C for the 10-, 20- and 30W ablations over the course of a ten-minute ablation. The 50 °C threshold is reached after three minutes for both levels. At 40W temperature reaches over 60 °C after five minutes, at 50W this is after three minutes. Temperatures at zone 5 and 6 do not exceed 60 °C for any wattage level during the course of a six minute ablation. Temperature over time at the posterior wall and zones 4-6 is plotted in figure 4. Temperature at the posterior wall and zone 4 mainly increases between two and four minutes and remains stable afterwards. At zone 5 and 6 the increase is more gradual and comparable between both zones.

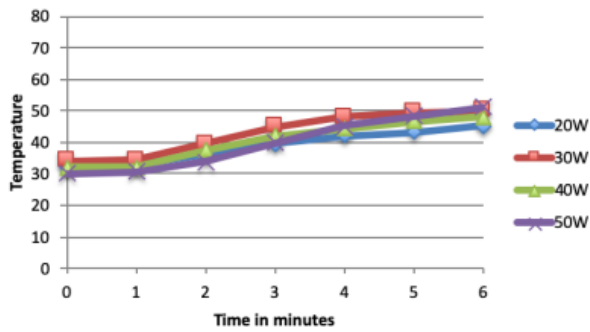
### Averages - Zone 4

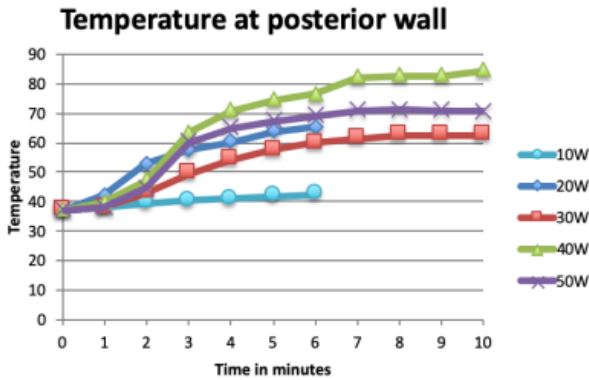


### Averages - Zone 5



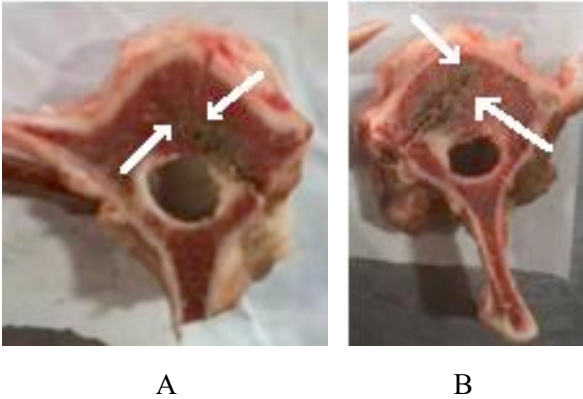
### Averages - Zone 6





**Figure 4** Average temperatures at zone 4, 5, 6 and the posterior wall (PW). At the PW the 60 °C threshold is reached within three minutes for 40- and 50W ablations. At 20- and 30W temperature reaches 60 °C after four- and five minutes respectively. At zone 4 only the 50W ablations reach over 60 °C within four minutes.

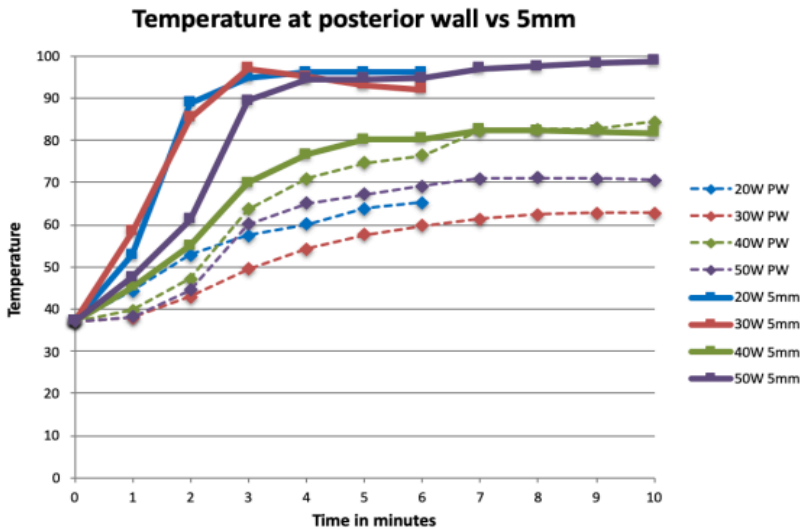
Since the curve for temperature in the 10W ablations is clearly different from the other wattage levels, measurements at 10W were not used for linear regression to prevent finding an effect only based on 10W. Temperature at zone 4 is dependent of both time ( $p < .001$ ) and wattage ( $p = .002$ ). Temperature at the posterior wall is dependent of time ( $p < .001$ ). In zones 5 and 6 temperature gradually increases with time ( $p < .001$ ), without a significant effect of wattage ( $p > .05$ ). Figure 5 depicts halo size at 10- and 20W. The halo is indicated by white arrows. Halo size of the 10W group was hardly larger than the size of the needle. The halo of the 20W samples was larger, however not reaching over the posterior wall.



**Figure 5** Halos after MWA in a vertebral body. **A.** 10W – 6 minutes **B.** 20W– 6 minutes.

#### *Cortical insulation*

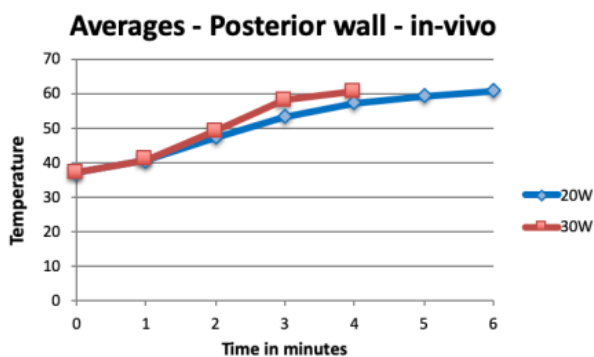
The average minimal distance between the active part of the needle and the posterior wall was 5.5mm. In figure 6 temperature at 5mm from the needle is compared to temperature at the posterior wall. Heat distribution at 5mm from the needle reached over 90 °C after three minutes for 20-, 30- and 50W. At the posterior wall temperature reached 50-60 °C after three minutes. Temperatures at the posterior wall were significantly lower compared to five mm for 20W ( $p < .01$ ), 30W ( $p < .01$ ) and 50W ( $p < .01$ ). For the 40W group temperatures were not different ( $p = .455$ ). This supports the literature on the effect of cortical insulation for lower wattages (10-14).



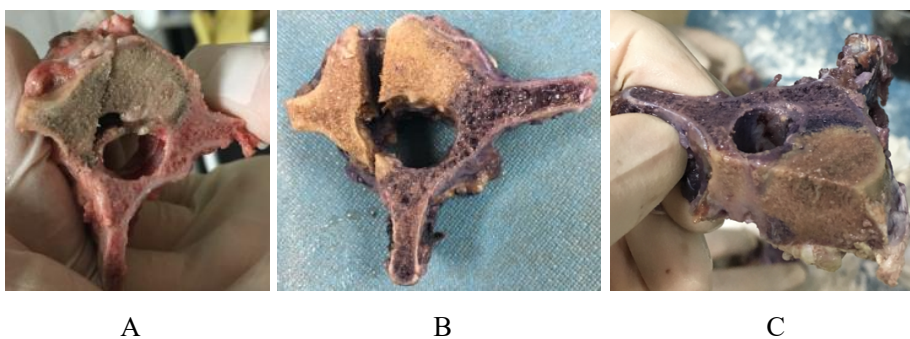
**Figure 6** Temperature at the posterior wall (PW) vs temperature at 5mm from the needle for 20-50W for ex-vivo ablations.

### In-vivo safety of surrounding structures

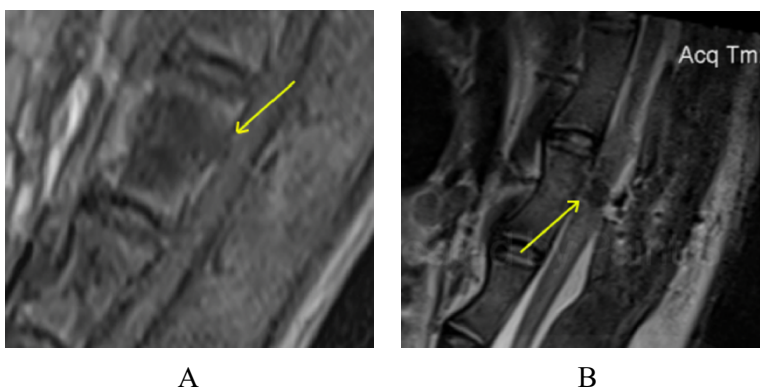
Temperatures over time at the posterior wall for the different wattage levels are depicted in figure 7. Temperature reached 60 °C after six minutes at 20W and after four minutes at 30W. Ablation was ended when temperature reached 60 °C. At inspection one day after ablation 10 out of 12 sheep showed signs of (partial) paralysis. They could not stand up and in half of the sheep no muscle reflexes could be objectivated. The two sheep without symptoms were both from the 20W, four minutes group. Based on these findings the in-vivo study was discontinued. All animals were sacrificed as planned and halo size was evaluated. As depicted in figures 8 and 9, halos reach over the posterior wall into the spinal canal for most samples. Figure 9c depicts the halo of one of the samples without paraplegia.

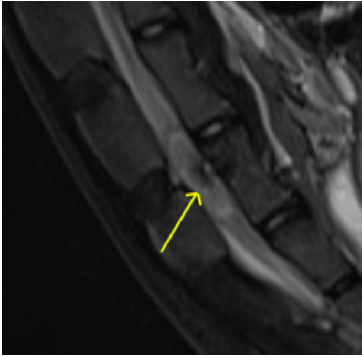


**Figure 8** *Temperature at the posterior wall for in-vivo ablations*



**Figure 8 A-B** *Halos for six minutes with 20W. A. Halo size before staining. B. Halo size after staining. The halo reaches into the spinal canal. C. Halo after staining for a four minute ablation with 20W. A large part of the vertebral body is ablated but the halo does not reach over the posterior wall.*





C

**Figure 9A.** MRI of a 20W, 4 minute ablation. The halo fills the complete vertebral body and reaches up to the posterior wall without causing damage to the spinal cord. **B.** MRI after a 20W, 6 minute ablation. The halo fills the complete body and reaches over the posterior wall. **C.** 20W, 4 minute ablation. Needle position was too posterior, the halo reaches over the (complete) spinal canal.

## Discussion

This study extends the knowledge on the properties of MWA in vertebral bodies. It is the first to evaluate safety for a range of settings. Temperature on the in- and outside of the bone rapidly increases in the first four minutes of ablation and subsequently stabilizes. Safety is mainly dependent on ablation time. However, severe complications already occur after short time intervals. Therefore, MWA in vertebral bodies should only be performed with great caution.

Wallace et al. described white matter necrosis on histology of the spinal cord after microwave- and cryoablation (14). However, ablations were not done directly next to the posterior wall and therefore the cortical insulation cannot be determined from this. Furthermore, they used MWA with 100W (for max 50 seconds). This is a very aggressive

approach, given the fact that in clinical application MWA for spine is only applied with 10-50W. Kastler et al. measured temperature next to the spinal cord with a thermocouple during clinical microwave ablations. When temperature exceeded 42 °C the cycle was aborted. They faced no complications and therefore concluded MWA to be a safe option for treatment of spinal metastases (8). They only reported the change in pain perception, not the resulting halo size. Khan et al. (9) also concluded MWA to be safe and effective in a clinical setting for treatment of spinal metastases. They used an average power of 13.3W ( $\pm 3.25$ ) for 3.0-10.5 minutes, which is smaller than the 20-30W used in our study. Since the effect of ablations with 10W were marginal in our ex-vivo experiments, it was decided to not use 10W for the in-vivo experiment.

### **Cortical insulation**

Dupuy et al. found temperature inside the body to increase with 25.7 °C ( $\pm 7.0$ ) during a 6-minute ablation with 94 °C. On the other side of the cortex this increase was only 11.2 °C ( $\pm 2.0$ ) (12). Zhang et al. found temperature next to the spinal cord for RFA on intact vertebral bodies to be 37.4 °C ( $\pm 4.43$ ) and 49.4 °C ( $\pm 3.34$ ) for bodies with a damaged posterior wall (13). Even though temperatures at the posterior wall reached 60 °C in short time, our data supports the assumption of cortical insulation as found in literature on RFA to exist for MWA as well. Temperature at 5mm from the needle was significantly higher compared to the posterior wall for ablations with 20-, 30- and 50W. However, for the 40W group no difference was seen. Since distance was not exactly the same, data does not depict the exact scope of insulation. However, given the large differences, cortical insulation is assumed to exist for (ex-vivo) MWA. Temperature differences found in the current data are larger than found in literature on RFA, indicating the cortical bone potentially functions as a stronger insulator for microwaves than for radiofrequency waves. More research is needed to confirm this finding.



### **Safety of surrounding structures**

In the ex-vivo experiment temperature at the posterior wall reached 60 °C after four to six minutes at 20- and 30W. For ablations with 40- and 50W temperature reached 60 °C after three minutes, the first measurement after the two-minute slow cooking period (with max 20W). This is in line with the results of Wallace et al. on MWA in spine (11). Therefore, it can be concluded that increasing the wattage to 40W and higher leads to instant damage to the spinal cord and should be avoided. At zone 4 temperature only reached 60°C for wattage levels of 40- or 50W (after five and three minutes respectively). With regard to possible damage to the nerve root, ablations over 40W should be avoided. At zone 5 and 6 temperature does not exceed 60 °C within six minutes of ablation for any wattage level. Therefore, risk of damage in that area is relatively low (15-18). Given the aggressive effect of 40- and 50W we concluded four to six minutes to be safe for in-vivo ablations with 20- to 30W. In addition, we hypothesized the ablation effect to be smaller in-vivo compared to ex-vivo as a result of cortical insulation, heat sinks by vascularity and the cerebral spinal fluid.

In-vivo, temperature at the posterior wall reached 60 °C after six minutes at 20W and after four minutes at 30W after which ablation was ended. The resulting halos clearly reached into the spinal canal. Therefore, it is hypothesized damage to the spinal cord already occurs at lower temperatures than hypothesized based on our model (figure 1). The effects of cortical insulation and heatsinks as predicted from the ex-vivo study appear to be limited. Since the ex-vivo vertebral bodies were fresh, no clear explanation for the large difference between in- and ex-vivo could be found. Based on these results we recommend great caution in performing MWA in a clinical setting.

Vertebral bodies in sheep are smaller compared to those in humans. Therefore, with ablations in the anterior part of the body and with small tip size, safety of MWA can be improved. However, given the high rate of paralyzed sheep in our in-vivo experiment a large risk exists. Less aggressive approaches like RFA are thought to be safer. When MWA

is used, continuous measurement of posterior wall temperature (for instance by MR thermometry) and nerve function is recommended. Even then, the risk of damage to the spinal cord is considered significant.

### **Strengths/weaknesses**

For all ex-vivo settings at least seven samples were included to ensure a reliable outcome. Distance between the needle and the temperature probe was standardized by using a navigation tool. With this tool we tried to ensure same direction as well to limit variation between samples as a result of human error. However, positioning of the drill was done by hand and without image-guidance. Therefore, small differences between the measurements cannot be ruled out. An example is that temperature at the posterior wall reaches 60 °C later at 30W than at 20W. Probably needle placement was more lateral in these samples. Given the irregular surface of the pedicle, placement of the tool was difficult for a number of samples.

Furthermore, we aimed to position the needle tip against the anterior cortex. Positioning could have been improved by use of image guidance. Unfortunately, for the current research this was not available. Finally, for the in-vivo experiment we hypothesized temperatures at the posterior wall up to 60 °C to be safe. Retrospectively it would have been better to stop the ablation at a temperature over 50 °C.

### **Conclusion**

MWA is an effective minimally invasive approach for local destruction of bone. It has an aggressive nature, which is beneficial for treatment of larger tumors. However, given low predictability and reproducibility of the technique, treatment in vertebral bodies is not recommended. When used, recommended maximum ablation settings are 10-20W for three minutes. Cortical insulation is insufficient to protect the spinal canal from excess heat leading to paraplegia.

## References

1. Coleman RE. Clinical features of metastatic bone disease and risk of skeletal morbidity. *Clin Cancer Res.* 2006;12(20 Pt 2):6243s-6249s.
2. Sayed D, Jacobs D, Sowder T, Haines D, Orr W. Spinal Radiofrequency Ablation Combined with Cement Augmentation for Painful Spinal Vertebral Metastasis: A Single-Center Prospective Study. *Pain Physician.* 2019;22(5):E441-E449.
3. Pennington Z, Ahmed AK, Molina CA, Ehresman J, Laufer I, Sciubba DM. Minimally invasive versus conventional spine surgery for vertebral metastases: a systematic review of the evidence. *Ann Transl Med.* 2018;6(6):103.
4. Hikata T, Isogai N, Shiono Y, et al. A Retrospective Cohort Study Comparing the Safety and Efficacy of Minimally Invasive Versus Open Surgical Techniques in the Treatment of Spinal Metastases. *Clin Spine Surg.* 2017;30(8):E1082-E1087.
5. Miscusi M, Polli FM, Forcato S, et al. Comparison of minimally invasive surgery with standard open surgery for vertebral thoracic metastases causing acute myelopathy in patients with short- or mid-term life expectancy: surgical technique and early clinical results. *J Neurosurg Spine.* 2015;22(5):518-525.
6. Hansen-Algenstaedt N, Kwan MK, Algenstaedt P, et al. Comparison Between Minimally Invasive Surgery and Conventional Open Surgery for Patients With Spinal Metastasis: A Prospective Propensity Score-Matched Study. *Spine (Phila Pa 1976)* 2017;42:789-97.
7. Huntoon K, Eltobgy M, Mohyeldin A, Elder JB. Lower Extremity Paralysis After Radiofrequency Ablation of Vertebral Metastases. *World Neurosurg.* 2020;133:178-184.
8. Kastler A, Alnassan H, Aubry S, Kastler B. Microwave thermal ablations of spinal metastatic bone tumors. *J vasc interv Radiol* 2014; 25:1470-1475
9. Khan MA, Deib G, Delbar B, Patel AM, Barr JS. Efficacy and Safety of Percutaneous Microwave Ablation and Cementoplasty in the Treatment of Painful Spinal Metastases and Myeloma. *AJNR Am J Neuroradiol.* 2018 Jul;39(7):1376-1383.
10. Rachbauer F, Mangat J, Bodner G, Eichberger P, Krismer M. Heat distribution and heat transport in bone during radiofrequency catheter ablation. *Arch Orthop Trauma Surg (2003)* 123 : 86–90.
11. Zhao W, Peng ZH, Chen JZ, Hu JH, Huang JQ, Jiang YN et al. Thermal

effect of percutaneous radiofrequency ablation with a clustered electrode for vertebral tumors: In vitro and vivo experiments and clinical application. *Journal of bone oncology* 12 (2018) 69-77.

12. Dupuy DE, Hong R, Oliver B, Goldberg SN. Radiofrequency ablation of spinal tumors: temperature distribution in the spinal canal. *AJR Am J Roentgenol* 2000; 175:1263-66

13. Zhang C, Han X, Douglas P, Dai Y, Wang G. Bipolar Radiofrequency Ablation of Spinal Tumors: The Effect of the Posterior Vertebral Cortex Defect on Temperature Distribution in the Spinal Canal. *AJNR Am J neuroradiol.* 2018 Jan; 39(1)

14. Wallace AN, Hillen TJ, Friedman MV, Zohny ZS, Stephens BH, Greco SC et al. Percutaneous spinal ablation in a sheep model: protective capacity of an intact cortex, correlation of ablation parameters with ablation zone size, and correlation of postablation MRI and pathologic findings (2017). *AJNR Am J Neuroradiology* 2017 Aug; 38(8): 1653-1659.

15. Eriksson AR, Albrektsson T: Temperature threshold levels for heat-induced bone tissue injury: A vital-microscopic study in the rabbit. *J Prosthet Dent.* 1983 Jul;50(1):101-7.

16. Eriksson A, Albrektsson T, Grane B, McQueen D. Thermal injury to bone. A vital microscopic description of heat effects. *Int J Oral Surg.* 1982 Apr;11(2):115-21.

17. Feldman L, Fuchshuber P, Jones DB. The SAGES Manual on the Fundamental Use of Surgical Energy (FUSE). Springer 2012.

18. Dewhirst MW, Viglianti BL, Lora-Michiels M, Hanson M, Hoopes PJ. Basic principles of thermal dosimetry and thermal thresholds for tissue damage from hyperthermia. *Int. J. Hyperth., vol. 19, no. 3, pp. 267–294, 2003.*

19. Brace CL. Thermal Tumor Ablation in Clinical Use. *IEEE Pulse* 2011;2(5):28-38.

20. Lavergne T, Sebag C, Ollitrault J, Chouari S, Copie X, Le Heuzey JY et al. Radiofrequency ablation: physical bases and principles. *Arch Mal Coeur Vaiss* 1996 Feb;89 Spec No 1: 57-63.

21. Issa ZF, Miller JM, Zipes DP. Clinical Arrhythmology and Electrophysiology. Chapter 7: Ablation energy sources. 2nd ed. Elsevier 1983.

22. Nijland H, Overbosch J, Ploegmakers JJW, Kwee TC, Jutte PC. Radiofrequency Ablation for Atypical Cartilaginous Tumors is safe and effective; analysis of 189 consecutive cases. *Open Access Journal of Oncology and Medicine* (2020).

23. Choi D, Crockard A, Bungler C, Harms J, Kawahara N, Mazel C et al. Review of metastatic spine tumour classification and indications for surgery: the consensus statement of the Global Spine Tumour Study Group. *Eur Spine J.* 2010 Feb;19(2):215-22.

24. Khan F, Rodriguez E, Finley DS, Skarecky DW, Ahlering TE. Spread of Thermal Energy and Heat Sinks: Implications for Nerve-Sparing Robotic Prostatectomy. *Journal of Endourology.*



# Chapter 9

General discussion

## Discussion

### **Part 1: looking back – how far are we in minimally invasive treatment?**

In the first part of this thesis, the use of minimally invasive treatment in the current practice of treating bone tumors was evaluated. As described in **chapter 2**, accuracy and precision of CT-guided (freehand) needle positioning are fairly good. No effect of lesion diameter was found for positioning. This implies that CT-guidance is a reliable tool for needle placement. At larger depths, both accuracy and precision appear to worsen. This, in combination with the absence of live tracking, leads to a larger risk of damage to surrounding structures. This is especially concerning for ablations close to sensitive structures like the spinal cord. For deeper lesions, it would be interesting to compare CT-guided positioning with live tracking, for instance by fluoroscopy, computer-assisted surgery (navigation), ultrasound fusion, or optical shape sensing. There is little research in this field, and more options for guidance are likely to enhance accuracy for deeper-seated lesions and thereby improve safety and efficacy.

In our study, only single-point ablations were performed. Another challenge comes with larger lesions, where multiple-point ablations are needed. For these procedures, the aim of needle placement is no longer in the center of the tumor. A combination of multiple overlapping halos needs to be used. However, there is insufficient knowledge on the predicted halo size for different ablation settings. Furthermore, the size of the ablation halo is dependent on several factors like tissue type, proximity to the cortex, and proximity to heat sinks. With more data, a model can be built on the expected halo size for different tumor characteristics and ablation settings. Considering safety margins and the range of error, a patient-specific approach can be planned before the procedure.



In **chapter 3**, a large cohort of RFA procedures for ACT was analyzed. With larger tumor diameter, ablation turned out to be less effective, given the loss of heat during distribution through the tissue. Larger tumors, therefore, require a multiple-point approach with overlapping halos. In this study, several multiple-point ablations were used, however, without exact knowledge of required needle positions. This is one of the main reasons why complete ablation was achieved in only 84.4% of cases, stressing the importance of a model for procedure planning as stated above.

An average ablation time of nine minutes was used per position. There is no literature on the increase of halo size with time in RFA. In **chapter 5**, it was shown that increasing time beyond six minutes did not result in a substantial increase in the size of the halo for MWA. It is likely that for RFA the same principle applies, but this has not been tested during the present research. The heat further from the needle is the result of heat conduction rather than heat generation by electricity and friction. It is, therefore, recommended not to extend ablation time beyond six minutes at target temperature per ablation position. In future research, it would be interesting to repeat the experiments on heat distribution at different distances from the needle as performed in **chapters 5 and 6** for RFA as well to confirm this. With extended data on heat distribution and halo size, better predictions can be made on the maximum halo size per single-point ablation. In case shorter intervals than the average nine minutes (as described above) can be used, thermal complications are less likely to occur. The main complications found in our RFA study were fractures (4.8% of patients) and avascular necrosis (2.1% of patients). The incidence of both of these complications could be decreased with less aggressive treatment (i.e shorter ablation times, lower temperature). Interestingly, from our results in **chapter 2**, no apparent association was found between mean ablation time per position and the number of complications.

Higher temperatures (80-90°C) led to more complete ablations without a higher risk of complications. Ablations at temperatures lower than 80°C led to more incomplete ablations. This indicates a quick loss of temperature further away from the needle, in case the model for tissue reaction to heat (as described in **chapter 2**) is correct. This would argue for more aggressive temperature settings. However, more factors need to be considered when developing a model for procedural planning. Heat conduction is influenced by the location in the bone (proximity to the cortex, proximity to heat sinks). In the literature, a so-called "oven effect" is described (1). The major portion of heat from RFA is hypothesized to be blocked by cortical bone. According to this hypothesis, ablation halos in diaphyseal bone will be elliptical and larger in diameter than halos further away from the cortex. There is only limited data in the current literature on cortical insulation in RFA (2). This makes aggressive treatment, especially close to sensitive structures, a hazardous option until more data are available. For MWA, this "oven effect" has not been described. The MRI data from **chapter 6** does not indicate such an effect for MWA. Halo size did not appear to be influenced by the cortex at all.

In **chapter 4**, long-term follow-up after RFA was described. The average halo volume was 3.7 times larger than the tumor volume. This indicates a large overshoot of ablation. With respect to decreasing the complication risk of surrounding tissues, the target halo should be closer around the tumor. To ensure complete ablation, a safety margin should be incorporated into the model (in our studies, a margin of two millimeters was used). The finding that the halo was 3.7 times larger than the tumor confirms that the exact settings required for ablation remain a topic for discussion and predictability is limited so far. It would be interesting to perform ablations under MRI with heat mapping, as has been the topic of recent research as well (3).

Follow-up demonstrated the halo volume to decrease over time, up to almost 50% after seven years. This is most likely the result of

regenerative processes in the body removing the ablated bone tissue and creating new bone. The original tumor tissue can still be visible but is considered avital. Since no tumor recurrence or other long-term complications were seen, RFA can be deemed safe and effective in the long term. Therefore, follow-up is unnecessary in case treatment is concluded effective on the first MRI control.

Concluding from the first part of this thesis, RFA is safe and effective for treating small, low-grade tumors like ACT. However, given the limited number of symptoms and low rate of metastases in ACT, the question arises whether surgical treatment is always required. In recent literature, a wait-and-see policy has been advocated for (4). Minimally invasive treatment has a lot of advantages compared to more invasive alternatives like curettage surgery and wide resection, but still comes with more complications and higher costs than no surgery at all. For symptomatic lesions or lesions with progressive growth, RFA is an excellent treatment option.

For higher-grade tumors, a wait-and-see policy obviously is no option. Given the finding that complete ablation was lower than 100% in our ACT cases, the question arises whether this type of treatment has potential for higher-grade tumors, where complete ablation is of paramount importance with regard to tumor spill and continued tumor growth with incomplete ablation. Before RFA can be used as treatment for this type of tumors, predictability needs to be improved. Recommendations to improve this predictability are better needle placement, for instance by direct guidance (e.g., with fluoroscopy), computer-assisted surgery or temperature-guided MRI. Furthermore, a model based on data of experiments with different settings for ablation time and temperature, measurement of heat distribution, and adjustment for tumor location (e.g. proximity of cortex/heat sinks) and tissue characteristics (e.g., H<sub>2</sub>O content) should be built. Regardless of the current limitations, RFA has the potential to become the main technique for a major part of bone tumor treatment. A major limitation for larger

tumors, however, is the relatively small halo size per single-point ablation, requiring multiple needle positions.

Finally, RFA is also a good option for the treatment of metastases with insufficient response to radiation therapy (5-6). Pain from bone metastases is likely due to periosteal nociceptors and pressure by tumor mass (6). Ablation of tumor tissue destroys these nociceptors and reduces tumor bulk, thereby reducing pain. Even though incomplete ablation could lead to tumor spill and continued growth of tumor tissue, it will likely lead to pain relief given the reduction in tumor bulk. Given the palliative character of treatment in osseous metastases, relief of symptoms is the main aim of treatment. Secondary to RFA, vertebral augmentation (e.g., with bone cement) is recommended to prevent vertebral body collapse and stabilizing fractured trabeculae (6). The combination of these therapies can be performed with a relatively short hospitalization and can be followed by direct mobilization.

## **Part 2: looking ahead towards safe, reliable and effective treatment**

In the second part of this thesis, the basic principles of MWA in bone were evaluated to assess whether it can be a good alternative to RFA in the field of minimally invasive treatment for bone tumors. MWA is used on a large scale for treatment in liver, kidney, and lung tumors. However, experience in bone is very limited and very likely different from soft tissue. Therefore, several experimental studies to the basic effect of the technique in bone were conducted for this thesis. In **chapter 5**, the goal was to obtain better insight into the actual effect of MWA in bone by examining different parameters and settings.

There was a significant difference in both heat distribution as well as resulting halo size between ex-vivo and in-vivo samples. The heat

distribution was smaller for the in-vivo samples. This is likely the result of heat sinks (e.g. vessels). It, however, complicates translation from ex- to in-vivo and therefore makes it harder to study outcomes of MWA in the lab (since these heat sinks cannot easily be added to ex-vivo experiments). Interestingly, the resulting halo size was larger for in-vivo samples. There might be an effect of late-apoptosis, for instance, by reactive oxygen species, however, the amount of difference as found in our experiments appears too large for that. Another possible explanation for this is the higher H<sub>2</sub>O content of in-vivo tissue. Conduction of microwaves is hypothesized to be better with higher H<sub>2</sub>O content and could therefore be an explanation for the difference in halo size.

Finally, there was a difference in (surrounding) temperature for the specimens between the in- and ex-vivo experiments. For the in-vivo samples, the body constantly keeps temperature around 37°C. Before starting the ablations, bones in the ex-vivo experiment were heated in a 37°C bath to mimic body circumstances. After the procedure, the bones cooled down quickly as a result of a room temperature of 20°C. An option for future research would be to keep the bones warm after the procedure as well for a certain amount of time.

Another interesting finding was that neither a longer ablation time (12- vs. 6 minutes) nor a higher wattage level (80W vs. 65W) led to larger halos. It appears MWA is already effective after only a few minutes, thereby being more aggressive than RFA. Therefore, experiments measuring halo size for shorter time intervals would be of interest. In tissue where temperature reaches over 60°C, instant cell death as a result of protein denaturation is hypothesized to occur. As depicted in Figure 6 of **chapter 5**, in-vivo heat distribution at 10mm reaches this 60°C threshold after four minutes. This suggests four minutes to be enough within that range. In **chapter 6**, however, it was found that at six weeks follow-up halos were actually larger for longer ablation time. A possible explanation for this difference is that the tissue at the edge

of the halo could be reactive/damaged after six minutes but not necrotic and has potential to regenerate. It is subject to discussion if such a process would also apply to tumor tissue instead of bone.

Another point to support the aggressive character of MWA was the finding that a gradual increase in wattage towards the aimed maximal wattage eventually led to higher temperatures at both 10mm and 15mm from the ablation needle. This implicates a process of desiccation around the needle tip when too much heat is produced in little time, limiting the conduction of heat ( $H_2O$  increases conduction). Eventually, even tissue charring can occur.

In **chapter 6**, the results of our in-vivo study on MWA were described. Currently, MWA in bone is being used in a clinical setting in a few centers already. As described in the only systematic review published so far, a wide range of wattage levels is used and recommendations vary between safe and hazardous (7). Our data advocate against MWA to replace the already existing alternatives, based on the apparent risk of collateral damage. Ablation results were not consistent enough, and complication rates were relatively high.

There appears to be a certain regenerative potential of tissue after MWA in bone, which corresponds to literature on MWA in other types of tissue. For MWA in breast tissue, full regenerative capacity was found, leaving no lesion one year after treatment (8). However, this effect was not seen for the higher wattage levels. Given the good regeneration capacity of bone tissue, such a reaction can be expected to occur. In literature, regenerative potential of bone was already reported after high-intensity focused ultrasound ablation (HIFU) (9-10). In our follow-up study as described in **chapter 3**, a similar image was seen for RFA. It would be interesting to perform a similar study for the halo after MWA over time.

Halo shape was (almost perfectly) round on MR images. This implicates there was no effect of cortical insulation, and an "oven effect" as described in RFA does not seem to apply for MWA. Since most bone tumors occur in the ends of long bones, close to sensitive structures like cartilage, this is a direct contra-indication to the therapy. In our study, 12.5% of sheep had (thermally) induced damage to the cartilage.

In **chapter 7**, the effects of MWA on biomechanical properties were examined. From our results, it appeared MWA only decreases bone strength to a small extent (and mainly for the more aggressive settings). The bones remain strong enough to carry a patient's body mass. Therefore, it is considered safe to directly start mobilizing. This is in line with results for other therapies like HIFU and RFA (9, 11-12). This is a major advantage compared to more invasive forms of therapy like curettage surgery and resection, which lead to a (long) period of immobilization. Given the patient group with primary bone tumors consists of a lot of young people, direct remobilization is of large importance given the impact of immobilization on personal life. Also for the group of bone metastases direct remobilization is important with regard to preserving quality of life. Given that mechanical strength is preserved after ablation a more invasive form of MWA could be considered as well when quick remobilization is required. When performing MWA in an open setting, better cooling could be performed on the bone, reducing the risk of thermal complications and still guaranteeing quick remobilization and preservation of quality of life.

In the final part of this thesis, **chapter 8**, experiments with MWA in the spine were performed. Bone tumors in the spine are in the majority of cases metastases. The aim of treatment is no longer curative but aimed at relief of symptoms, mainly pain. Unfortunately, like in long bone we found large halos for only short ablation times and at relatively low wattage levels. There did not appear to be an effect of cortical insulation. This leads to a large risk of severe complications like

damage to the spinal cord. The implications of such complications do not match the potential benefit on symptom relief. Therefore, MWA should only be used in the spine when continuous monitoring of temperature near relevant neural structures is possible, and great caution should be taken not to cause irreversible paralysis. Another issue is positioning of the needle. In our study, this was done manually. Given the very small margin of error allowed in spinal application, this should always be done with continuous guidance of position and monitoring of temperature in areas at risk.

For future developments, two lines of research could be embarked on. First, it would be interesting to repeat our MWA experiments under continuous monitoring of needle location and temperature around the needle, for instance by MR-based thermometry (13). Given the large halos, it is very likely that MWA can play a role in treatment of larger bone tumors, especially with regard to the small halos reached by alternatives like RFA. However, this only applies under the condition that safety can be guaranteed.

Secondly, in our experiments we performed MWA in healthy bone. Given that conductance of heat will likely be higher in tumor tissue, even smaller amounts of wattage and time could be sufficient (14). Ex-vivo research would include reliable model development including relevant characterization of tissue properties of the tumor types and regular tissues, including effects of vascularization, heat conduction, and heat sink. For in-vivo studies it would require laboratory animals with bone cancer like dogs with osteosarcoma. Experiments with different settings for time and wattage in human patients can only be performed with sufficient understanding and reliable models developed in ex- and in-vivo applications. It would be interesting to examine whether there is a fixed ratio between tumor tissue and bone tissue that could be included in a formula to predict resulting halo size.



Concluding from this second part of the thesis, MWA does not (yet) have the potential that other techniques like RFA and HIFU demonstrate. However, not all is negative on MWA. It does have potential for larger tumors given its high effectiveness. It clearly has the potential of initiating cell death. Using MWA as a minimally invasive treatment, as was the focus in this thesis, is unsafe just yet. Potential implications for the technique could be as adjuvant therapy in an open setting next to curettage surgery or as monotherapy with sufficient cooling to the structures surrounding the ablation area. The advantages of minimally invasive therapy as mentioned before do however no longer apply and therefore the question arises whether there is a benefit of MWA compared to open therapies (e.g. curettage surgery) for which a large body of experience exists.

## References

1. Liu Z, Ahmed M, Weinstein Y, Yi M, Mahajan RL, Goldberg SN. Characterization of the RF ablation-induced 'oven effect': the importance of background tissue thermal conductivity on tissue heating. *Int J Hyperthermia*. 2006 Jun;22(4):327-42.
2. Irastorza RM, Trujillo M, Martel Villagrán J, Berjano E. Computer modelling of RF ablation in cortical osteoid osteoma: Assessment of the insulating effect of the reactive zone. *Int J Hyperthermia*. 2016 May;32(3):221-30.
3. Zhang Z, Michaelis T, Frahm J. Towards MRI temperature mapping in real time-the proton resonance frequency method with undersampled radial MRI and nonlinear inverse reconstruction. *Quant Imaging Med Surg*. 2017 Apr;7(2):251-258.
4. Scholte CHJ, Dorleijn DMJ, Krijvenaar DT, van de Sande MAJ, van Langevelde K. Wait-and-scan: an alternative for curettage in atypical cartilaginous tumours of the long bones. *Bone Joint J*. 2024 Jan 1;106-B(1):86-92.
5. Wallace AN, Greenwood TJ, Jennings JW. Radiofrequency ablation and vertebral augmentation for palliation of painful spinal metastases. *J Neurooncol*. 2015 Aug;124(1):111-8.
6. Lane MD, Le HB, Lee S, Young C, Heran MK, Badii M, Clarkson PW, Munk PL (2011) Combination radiofrequency ablation and cementoplasty for palliative treatment of painful neoplastic bone metastasis: experience with 53 treated lesions in 36 patients. *Skeletal Radiol* 40:25–32
7. Cazzato RL, de Rubeis G, de Marini P, Dalili D, Koch G, Auloge P, Garnon J, Gangi A. Percutaneous microwave ablation of bone tumors: a systematic review. *Eur Radiol*. 2021 May;31(5):3530-3541.
8. Zhang W, Li JM, He W, et al. Ultrasound-guided percutaneous microwave ablation for benign breast lesions: evaluated by contrast-enhanced ultrasound combined with magnetic resonance imaging. *J Thorac Dis*. 2017;9(11):4767-4773.
9. Bucknor MD, Rieke V, Seo Y, Horvai AE, Hawkins RA, Majumdar S et al. Bone remodeling after MR imaging-guided high-intensity focused ultrasound ablation: evaluation with MR imaging, CT, Na(18)F-PET, and histopathologic examination in a swine model. *Radiology*. 2015;274(2):387-394.

10. Bucknor MD, Goel H, Pasco C, Horvai AE, Kazakia GJ. Bone remodeling following MR-guided focused ultrasound: Evaluation with HR-pQCT and FTIR. *Bone*. 2019;120:347-353.
11. Herman A, Avivi E, Brosh T, Schwartz I, Liberman B. Biomechanical properties of bone treated by magnetic resonance-guided focused ultrasound - an in vivo porcine model study. *Bone*. 2013;57(1):92-97.
12. Yamamoto S, Kaminou T, Ono Y, et al. Thermal influence of radiofrequency ablation for bone: an experimental study in normal rabbit bone. *SkeletalRadiol*.2014;43(4):459-465.
13. Zhu M, Sun Z, Ng CK. Image-guided thermal ablation with MR-based thermometry. *Quant Imaging Med Surg*. 2017 Jun;7(3):356-368.
14. Haemmerich D, Schutt DJ, Wright AW, Webster JG, Mahvi DM. Electrical conductivity measurement of excised human metastatic liver tumours before and after thermal ablation. *Physiol Meas*. 2009 May;30(5):459-66.



# Chapter 10

English summary  
Nederlandse samenvatting

## **English summary**

Orthopedic oncology is the medical field dedicated to the diagnosis and treatment of tumors in bones and soft tissues. Significant progress has been made in recent decades. A possible next step towards effective, safe, and patient-friendly treatment is minimally invasive therapy.

This dissertation is divided into two parts. The first part focuses on the outcomes and follow-up of treating bone tumors using radiofrequency ablation (RFA). The second part is from a more experimental nature, examining effectiveness and reliability of microwave ablation (MWA).

**Chapter 1** provides a general introduction to the topic of minimally invasive treatment for bone tumors. It offers an overview of the different types of bone tumors and traditional treatment options. The concepts of minimally invasive treatment and hyperthermia are then explained. Finally, the rationale and objectives of this dissertation are outlined.

### **Part 1: looking back – how far are we in minimally invasive treatment?**

**Chapter 2** explores the accuracy and precision of manually positioning the ablation probe during RFA procedures for the treatment of osteoid osteomas. These parameters are essential for safe and predictable procedures. The position of the ablation probe in relation to the tumor was determined using CT imaging. A complete ablation was achieved in 79% of the 86 procedures. The accuracy (measured as the distance between the tip of the ablation probe and the center (nidus) of the tumor) averaged 2.8 mm. The precision (defined as the degree of agreement of this distance between different patients, measured as the standard deviation of the accuracy) was 2.9 mm. In deeper lesions, both accuracy and precision decreased.

**Chapter 3** describes our study on the results of treating atypical cartilaginous tumors (ACT) with RFA at the University Medical Center Groningen. The effectiveness and safety of 189 procedures (performed between 2007 and 2018) were analyzed. Effectiveness was categorized as R0 (complete ablation of the lesion with a planned safety margin of 2 mm), R1 (complete ablation without the safety margin), and R2 (incomplete ablation). A complete ablation was achieved in 84.4 % of the procedures, with 66.7 % being R0 and 17.7 % R1. Factors significantly influencing ablation effectiveness included longer ablation time, smaller tumor size (higher effectiveness with smaller tumors), and higher temperature. Complications occurred in 15 procedures (7.9 %), with fractures being the most common (9 cases).

**Chapter 4** examines the follow-up after RFA procedures for ACT. For the procedures discussed in Chapter 3, the ablation halo (area of ablated tissue) was measured at various time intervals after treatment using follow-up MRI scans. Follow-up occurred at 3 months, 1 year, and 2 years, with some patients also having follow-up scans at 5 and 7 years. The halo size decreased by an average of 21.5 % during the first year. Over the following years, a slow further reduction was observed, reaching nearly 50 % after 7 years. This decrease suggests revitalization of bone tissue over time. No recurrences were observed during follow-up. Based on these results, frequent monitoring after an RFA procedure for a low-grade bone tumor is considered not necessary.

## **Part 2: looking ahead - towards safe, reliable and effective treatment**

**Chapter 5** presents the results of MWA in sheep bone. First, ex-vivo experiments were used to create a model of expected ablation halos for different settings of ablation time and wattage. An in-vivo study was then conducted. The distribution of heat through the bone at 10 mm and 15 mm from the ablation probe was measured. The in-vivo study

showed that the size of the ablation halo was up to six times larger than in the ex-vivo model with the same settings. Measured temperatures at 10 mm and 15 mm from the ablation probe were higher in the ex-vivo studies than in-vivo. Halo growth occurred mostly within the first six minutes. There was no difference between ablation at 65 W and 80 W. Compared to RFA, MWA led to a larger variability between individual ablations, resulting in insufficient reliability. More research and improvements in technique are necessary before MWA can be accepted as a standard treatment for treating bone tumors.

**Chapter 6** describes an in-vivo study on the treatment of sheep bone with MWA. Sheep were randomly divided into two groups. In the first group sheep were sacrificed after one week and in the other group after six weeks. Prior to this, an MRI scan was performed, and the bones were harvested and sectioned. Lactate dehydrogenase (LDH) staining was performed, and halo size was measured. There was significant variability in halo size between samples with the same ablation settings. No significant differences in halo size were found between the different time intervals, suggesting that most halo formation occurs in the early phase of the ablation. Complications occurred in 40 % of the sheep, with most being thermally related. The results argue against replacing existing techniques with (minimally invasive) MWA for the treatment of bone tumors.

**Chapter 7** examines the effects of ablation on the mechanical strength of sheep bone. Given that one of the main benefits of minimally invasive treatment is early mobilization, it is important to know if there is an increased risk of fractures after treatment. The force required to break the tibia mid-diaphysis was measured after in-vivo ablation. Half of the sheep were sacrificed after one week, the other half after six weeks. There was a decrease in mechanical strength six weeks after ablation. This decrease was not observed in the group sacrificed after one week. Despite the reduction in mechanical strength, the force remained sufficient for early mobilization.



**Chapter 8** discusses the application of MWA in vertebral bodies. The spine is a common site for bone metastases, and ablation could be a good option for rapid, minimally invasive treatment. In this study, MWA was applied in in-vivo bone of 12 sheep. There appears to be an effect of cortical insulation, however insufficient to protect the spinal cord from heat-induced damage. The predictability of halo size was low, and the risk of complications was high. Despite using low wattages (20-30 W) and continuous monitoring of temperature around the ablation probe and near the spinal canal, 10/12 sheep developed paralysis after treatment. Based on these results, the use of MWA in vertebral bodies is not recommended.

**Chapter 9** provides a general discussion of the dissertation. The results from the various chapters are reviewed and integrated into conclusions. Clinical implications and future perspectives are discussed.

## **Nederlandse samenvatting**

De orthopedische oncologie is het medische vakgebied dat zich bezighoudt met de diagnostiek en behandeling van tumoren in bot en de omliggende weke delen. In de afgelopen decennia is er al veel vooruitgang geboekt. Een mogelijke volgende stap in effectieve, veilige en patiëntvriendelijke behandeling is minimaal invasieve behandeling.

Dit proefschrift is opgedeeld in twee delen. In het eerste gedeelte wordt er gekeken naar de uitkomsten en follow-up van de behandeling van bottumoren middels radiofrequente ablatie (RFA). Het tweede gedeelte is meer experimenteel van aard. Hierin worden de effectiviteit en betrouwbaarheid van microwave ablatie (MWA) beschreven.

**Hoofdstuk 1** is een algemene inleiding op het onderwerp minimaal invasief behandelen van bottumoren. Hierin wordt er een overzicht gegeven van de verschillende typen bottumoren en de traditionele behandelopties. Vervolgens worden de concepten minimaal invasief behandelen en hyperthermie toegelicht. Tenslotte worden de aanleiding en het doel van dit proefschrift uiteengezet.

### **Deel 1: hoever zijn we in de minimaal invasieve behandeling van bottumoren?**

In **hoofdstuk 2** is er gekeken naar de nauwkeurigheid en precisie van handmatig positioneren van de ablatie probe tijdens RFA-procedures voor de behandeling van osteoïd osteomen. Deze waarden zijn van belang voor veilige, voorspelbare procedures. De positionering van de ablatieprobe ten opzichte van de tumor werd bepaald middels CT-beelden. In 79 % van de in totaal 86 procedures bleek een complete ablatie te zijn bereikt. De nauwkeurigheid (beschreven als de afstand tussen het uiteinde van de ablatieprobe en het centrum (=nidus) van de tumor) was gemiddeld 2.8 mm. De precisie (beschreven als de mate van

overeenkomst van deze afstand tussen verschillende patiënten en gemeten als de standaarddeviatie van de nauwkeurigheid) bleek 2.9 mm. Bij dieper gelegen laesies namen zowel de nauwkeurigheid als de precisie af.

**Hoofdstuk 3** beschrijft de studie naar de resultaten van de behandeling van atypische cartilagineuze tumoren (ACT) middels RFA in het Universitair Medisch Centrum Groningen. Van de 189 procedures (verricht tussen 2007-2018) werden zowel de effectiviteit als de veiligheid geanalyseerd. Voor de effectiviteit werd een onderscheid gemaakt tussen R0 (volledige ablatie van de laesie inclusief een geplande veiligheidsmarge van 2 mm rondom), R1 (volledige ablatie, echter zonder de veiligheidsmarge) en R2 (incomplete ablatie). In 84.4 % van de procedures bleek complete ablatie te zijn bereikt. Hiervan was 66.7 % R0 en 17.7 % R1. Factoren met significante invloed op effectiviteit van de ablatie waren langere ablatietijd, tumorgrootte (hogere effectiviteit bij kleinere tumor) en hogere temperatuur. In 15 procedures (7.9 %) ontstond een complicatie. Hierbij was een fractuur de meest voorkomende complicatie (9 maal beschreven).

In **hoofdstuk 4** is er gekeken naar de follow-up na RFA-procedures voor ACT. Voor de procedures uit hoofdstuk 3 werd op follow-up MRI-scans de resulterende ablatiehalo (gebied van geableerd weefsel) op meerdere tijdsintervallen na behandeling gemeten. Hierbij was er voor alle patiënten na 3 maanden, 1 jaar en 2 jaar een controle. Voor de patiënten waar ook een follow-up MRI scan na 5- en 7 jaar beschikbaar was werd deze ook meegenomen. De grootte van de halo nam in het eerste jaar gemiddeld met 21.5% af. Over de daaropvolgende jaren werd een langzame verdere afname gezien, tot bijna 50% na 7 jaar. Deze afname impliceert revitalisatie van botweefsel. Er werden geen recidieven gezien gedurende follow-up. Op basis van deze resultaten blijkt frequente controle na een RFA-procedure voor een laaggradige bottumor niet nodig te zijn.

## **Deel 2: verder ontwikkelen van veilige, betrouwbare en effectieve toepassing van minimaal invasieve behandeling van bottumoren.**

In **hoofdstuk 5** zijn de resultaten van MWA in schapenbot beschreven. Hierbij is er eerst middels ex-vivo experimenten een model gemaakt van te verwachten ablatie halo's voor verschillende instellingen voor ablatietijd en wattage. Vervolgens werd een in-vivo studie uitgevoerd. De verspreiding van warmte door het bot op 10- en 15 mm van de ablatieprobe werden gemeten. Er bleek dat de grootte van de ablatie halo bij de in-vivo studie tot zesmaal groter werd dan ex-vivo met dezelfde instellingen. De gemeten temperaturen op 10- en 15 mm van de ablatieprobe bleken juist ex-vivo hoger dan in-vivo. De groei van de halo vond met name plaats in de eerste zes minuten. Er was geen verschil tussen ablatie met 65 W en 80 W. In vergelijking met RFA bleek er bij MWA een veel grotere variatie te bestaan tussen de individuele ablaties. Hierdoor is de betrouwbaarheid onvoldoende. Meer onderzoek en verbetering van de techniek lijkt benodigd voordat MWA standaardbehandeling kan worden.

**Hoofdstuk 6** beschrijft de in-vivo studie naar de behandeling van schapenbotten met MWA. Schapen werden random verdeeld in twee groepen waarvan de ene groep na een week werd opgeofferd en de andere groep na zes weken. Hieraan voorafgaand werd een MRI-scan gemaakt. De botten werden geogst en tot samples gezaagd. Er werd een kleuring middels lactaathydrogenase (LDH) verricht en de halogrootte werd gemeten. Er bleek veel variatie te zijn in grootte van deze halo tussen samples met dezelfde instellingen voor ablatie. Er werd geen significant verschil in halogrootte gevonden voor de verschillende tijdsintervallen. Derhalve lijkt het grootste gedeelte al in de beginfase van de ablatie gevormd te worden. In 40 % van de schapen ontstond een complicatie. Het grootste deel hiervan was thermisch gerelateerd. De resultaten pleiten tegen het vervangen van de al bestaande technieken door (minimaal invasieve) MWA voor de behandeling van bottumoren.

In **hoofdstuk 7** is er gekeken naar de effecten van ablatie op de mechanische sterkte van schapenbot. Gezien directe mobilisatie na behandeling een van de grootste voordelen is van minimaal invasieve behandeling, is het van belang te weten of er een verhoogd fractuurrisico bestaat. De hoeveelheid kracht die benodigd was om de tibia mid-diafysair te breken werd gemeten na in-vivo ablaties. Hierbij werd de helft van de schapen na een week geofferd, de andere helft na zes weken. Mid-diafysair bleek er een afname van mechanische kracht te zijn zes weken na ablatie. Deze afname van kracht was in de groep die na een week werd geofferd niet te zien. Ondanks de afname van de mechanische kracht bleef de kracht voldoende voor directe mobilisatie.

**Hoofdstuk 8** beschrijft de toepassing van MWA in wervellichamen. De wervelkolom is een frequente locatie voor botmetastasen. Voor snelle, minimaal invasieve behandeling zou ablatie een goede optie kunnen zijn. In de huidige studie werd MWA toegepast in in-vivo schapenbot bij 12 schapen. Er bleek een warmte absorberende functie te zijn van de cortex, echter onvoldoende om het ruggenmerg te beschermen tegen hitte geïnduceerde schade. De voorspelbaarheid van halogrootte bleek laag en het risico op complicaties hoog. Ondanks gebruik van lage wattages (20-30 W) en continue monitoring van temperatuur rondom de ablatieprobe en naast het spinale kanaal, bleek er na behandeling bij 10/12 schapen een paralyse te zijn ontstaan. Derhalve wordt op basis van deze resultaten het gebruik van MWA in wervellichamen afgeraden.

**Hoofdstuk 9** is een algemene discussie op het proefschrift. De resultaten van de verschillende hoofdstukken worden besproken en samengevoegd tot conclusies. Tevens worden de klinische implicaties en toekomstperspectieven beschreven.



# Appendices

Dankwoord  
List of lectures  
Curriculum Vitae

## Dankwoord

Promoveren doe je niet alleen. Het is het resultaat van jarenlang samenwerken. Dit boekje had ik dan ook niet kunnen afronden zonder de hulp van mijn promotieteam, vrienden en familie.

Te beginnen met Paul Jutte, als promotor ben jij vanaf het begin betrokken geweest. We kennen elkaar inmiddels bijna 10 jaar. Ik weet nog goed dat we in mijn derde jaar van de bachelor Geneeskunde spraken over de opties om onderzoek te doen binnen de Orthopedie. Hieruit kwam al snel een eerste project via de JSM. Dat dit uiteindelijk zou leiden tot dit proefschrift kon ik toen nog niet vermoeden. Je hebt mij altijd gemotiveerd verder te blijven gaan en de schouders er onder te blijven zetten. Ook toen het besluit kwam om mijn carrière te vervolgen richting de acute Geneeskunde in plaats van de Orthopedie, verloor jij me niet uit het oog. Verder gaf je me de kans om in China 7 maanden lang onder supervisie experimenten uit te voeren. Een tijd die ik niet snel zal vergeten.

Ten tweede Thomas Kwee. Toen jij in de tweede fase van mijn PhD-traject instapte kwam de trein steeds beter op gang. Het project dat door carrièrekeuzes steeds meer naar de achtergrond leek te verdwijnen, kreeg nieuw leven. Jouw manier van denken en schrijven heeft me veel geleerd en geholpen om de lading aan onderzoeksdata vanuit de ‘Chinese experimenten’ om te zetten in overzichtelijke wetenschappelijke stukken. Je reageerde altijd snel op mijn vragen en hielp me weer op weg wanneer ik door de bomen het bos niet meer zag. Zonder jouw inzet was dit proefschrift er nu niet geweest.

Verder wil ik graag de beoordelingscommissie, prof. dr. R.A.J.O. Diercx, prof. dr. J.J. Fütterer en prof. dr. S. Misra, hartelijk danken voor de interesse en het beoordelen van mijn proefschrift.



Dan door naar China. In China heb ik dankzij de begeleiding van Prof. Hao 7 maanden lang experimenten kunnen uitvoeren in Xi'an. In een land waar over het algemeen de deuren gesloten blijven voor Westerlingen bleken de mogelijkheden ongekend. Binnen het ziekenhuis werden zowel labruimte als personeel vrijgemaakt wanneer ik het maar vroeg. Het hoogtepunt hiervan was het compleet vrijstellen van Jinwen van zijn klinische werkzaamheden als orthopeed, zodat hij fulltime mee kon werken aan de experimenten.

Jinwen, heerlijke chaoot, altijd druk, altijd in de weer. Soms meer dan 80 uur in de week. Je zette je klinische werk als orthopeed voor 7 maanden vrijwel volledig aan de kant om met mij te werken aan de experimenten. Zowel je ideeën als technische skills hebben me een stuk verder geholpen en zonder jou was het afronden van de experimenten niet gelukt. Maar ook buiten het lab om was je er altijd voor me. Wat hebben we een hoop gezellige momenten beleefd samen. Je nam me mee naar het Chinese platteland, stelde me voor aan je lieve familie en organiseerde karaokeavonden met collega's uit het ziekenhuis. Ook onze gesprekken over verschillen tussen elkaars culturen en gebruiken en met name de verbazing hierover, zal ik niet snel vergeten.

Na de onderzoeksperiode in China kwam de lastigste periode van mijn PhD onderzoek. Het analyseren van de data heeft vele uren gekost, maar met name het omzetten hiervan in overzichtelijke papers leek bij vlagen uitzichtloos. Dankzij de motiverende rol van familie en vrienden kreeg ik gelukkig de nodige duwtjes in de rug om toch verder te gaan. Jullie bleven maar vragen wanneer dat boekje nou eindelijk eens klaar zou zijn. Soms zorgde dit voor jeuk van mijn kant omdat ik weer geen steek verder was, maar zeker in het afgelopen jaar kon ik steeds vaker melden dat een volgende stap gezet was. En nu ligt hier een compleet boekje.

Op de eerste plaats komt (ook) hier natuurlijk mijn familie. Mijn ouders, Jan en Geesje, altijd daar wanneer er iets is. Niets is onmogelijk,

altijd daar met een helpende hand. In jullie schuur heb ik urenlang staan boren en branden in botten uit het slachthuis. Tussendoor kwamen jullie dan even polshoogte nemen. Met de nodige verbazing werd dan gekeken tot wat voor slachthuis de schuur weer was omgebouwd, maar altijd bleef jullie deur openstaan. Verder wil ik hier mijn zusjes Ellis en Ine en zwagers Nicolaas en Gerhardus bedanken. Met zijn allen zijn we de laatste jaren tot een grote familie gegroeid. Inmiddels is er zelfs een kleine spruit bij de familie gekomen. Pieter Nicolaas: hierbij je eerste vermelding in een academisch stuk. Laten we hopen dat er nog velen zullen volgen.

De afgelopen jaren is er in het Oosten van het land een tweede familie bijgekomen. Steeds vaker zijn we in Enschede op bezoek. Ook hier werd de voortgang van dit boekje met grote interesse gevolgd. Uit de ervaringen van het promotietraject van Lyset leerde ik dat promoveren voor iedereen een grote uitdaging is en tegenslagen er eenmaal bij horen.

Ook de vriendengroepen vanuit Groningen wil ik graag benoemen, zowel de jongens van de studie Geneeskunde als wel de jongens van het zeilen. Sommigen van jullie zullen wellicht niet meer verwacht hebben dat dit proefschrift succesvol afgerond zou worden. Toch bleven jullie ernaar vragen. En hier ligt het!

Tenslotte wil ik Anouk noemen. We zijn inmiddels ruim 3 jaar samen en hebben in Nijmegen ons nieuwe thuis gevonden. Ik kijk er heel erg naar uit om samen met jou over 2 maanden in ons eerste koophuis in Lent te gaan wonen en daar aan een toekomst te bouwen. Jij bent de grootste motivator geweest om mijn proefschrift tot een goed einde te brengen. Ook al dacht je volgens mij vaak dat ik alleen maar boos en geïrriteerd werd van jouw vragen over de voortgang, stiekem motiveerde dit me juist om door te blijven gaan. Je drukt en drukte me met de neus op de feiten en helpt me altijd te relativieren wanneer ik weer eens doorsla. Dankjewel!

## List of lectures

### 2019

32nd annual meeting of the EMSOS – May 15-17 – Florence (Italy) - *Radiofrequency Ablation for Atypical Cartilaginous Tumors (ACT); analysis of 189 consecutive cases.*

Oral presentation

Xi'an International Orthopaedic congress – October 11-13 – Xi'an (China) - *Local tumor ablation in Musculoskeletal Tumors (RFA & MWA).*

Oral presentation

### 2021

32nd annual meeting of the EMSOS – December 1-3 – Graz (Austria) - *Evaluation of efficacy of microwave ablation in sheep long bone.*

Oral presentation

32nd annual meeting of the EMSOS – December 1-3 – Graz (Austria)- *Evaluation of safety and efficacy of microwave ablation in sheep spine.*

Oral presentation

## Curriculum vitae

Hendricus Nijland was born on September 26, 1992, in Waalre, the Netherlands. He attended the Gymnasium at Aletta Jacobs College in Hoogezand-Sappemeer. After graduating from high school, he began studying Human Movement Studies at the University of Groningen in 2010. In 2012 he began studying Medicine as well. After completing both bachelor's degrees in 2015, he entered his master's phase. During this time he became involved in research projects in orthopedic oncology at the University Medical Center Groningen, which eventually led to a PhD track on minimally invasive treatment of bone tumors.



Upon completing his Medical training in 2020, he began working as a resident orthopedic surgery not in training at Deventer Hospital and later at MST Enschede. In 2022, he shifted his career focus towards Emergency Medicine, working in the Emergency Departments at ZGT Almelo and Canisius Wilhelmina Hospital Nijmegen, as well as in the Intensive Care Unit at the latter. In 2025, he started his residency in Emergency Medicine at Radboud University Medical Center in Nijmegen. Throughout his work as a resident not in training, he continued his scientific career, which ultimately culminated in the completion of his doctoral thesis.

In his free time, he enjoys spending time outdoors and has a passion for travel, particularly to countries that are often overlooked by most travelers. To date, he has visited 74 countries.